UNIVERSITY OF CALIFORNIA
RIVERSIDE

Lipids, Lungs, and Livestock: An Exploration of How Omega-3 Fatty Acid-Derived Mediators Impact Airway Inflammation and Carcinogenesis

A Dissertation submitted in partial satisfaction
of the requirements for the degree of

Doctor of Philosophy

in

Environmental Toxicology

by

Edward C. Dominguez

March 2022

Dissertation Committee:
Dr. Prue Talbot, Chairperson
Dr. Tara Nordgren
Dr. Nicholas DiPatrizio
Dr. Ying-Hsuan Lin

The Dissertation of Edward C. Dominguez is approved:

_____

_____

_____

_____

Committee Chairperson

University of California, Riverside

Acknowledgements

I would like to acknowledge the individuals who have provided me with support, inspiration, and confidence to achieve all that I have during my doctoral studies at UC Riverside. First and foremost, I would like to express my deepest gratitude to my dissertation committee members Dr. Prue Talbot, Dr. Tara Nordgren, Dr. Nicholas DiPatrizio, and Dr. Ying-Hsuan Lin for their time and guidance during my doctoral journey. I am appreciative of each of you for your willingness to serve on my committee and encouraging feedback during each of our annual meetings. I would also like to give special appreciation to my advisors Dr. Prue Talbot and Dr. Tara Nordgren. Dr. Talbot, thank you for providing thoughtful insight to my experiments and bringing me into your lab as one of your own. I am grateful for all that you have done for me during my time at UCR. Dr. Nordgren, thank you for always pushing me to think harder, teaching me to trust in my work (the data are, what the data are!), and believing in my abilities as a scientist. Your support of my ambitious projects allowed me to reach higher and dream bigger, and I am forever thankful to have had worked under your guidance during my time at UCR. I would also like to thank all the Nordgren and Talbot lab members for their assistance with experiments, feedback into data analysis, project design, and constant support in my endeavors. Lastly, I would like to express thankfulness for my friends and family who have supported my academic and professional ventures during my doctoral studies. To my wife Valeria, thank you for always motivating, inspiring, and showing me that I can accomplish anything I set my mind to. All that I have achieved is a reflection of

the strong support system I have behind me, and I am grateful to each of you all for allowing this to be possible.

Chapter 1: The text and figures of this chapter are a reprint of the material as it appears in *Nutrients* 2020, 12(8), 2334; https://doi.org/10.3390/nu12082334. We are very grateful for the support from the National Institutes of Health, National Institute of Environmental Health Sciences for funding and would like to thank We would like to thank NanoString support members for their assistance with using the nSolver analysis features to analyze and interpret the gene expression data in this study.

Chapter 2: The text and figures of this chapter were submitted for review to *Cancers*. We are very grateful for the support from the NIEHS and NHLBI for funding and would like to thank Dr. Rachel Behar and the UC Riverside Stem Cell Core for allowing to use the BioStation CT incubator and analysis software, Dr. Anil Bhatia and the UC Riverside Metabolomics Core for their assistance in processing and analyzing the oxylipin analysis data, NanoString support for their assistance with data processing, the UCI tissue path core for processing our lung tissue samples, Dr. Stefane Thibault for his evaluation of our murine lung pathology for carcinogenic outcomes of interest, and Dr. Debra Romberger for providing us with the swine dust.

ABSTRACT OF THE DISSERTATION

Lipids, Lungs, and Livestock: An Exploration of How Omega-3 Fatty Acid-Derived Mediators Impact Airway Inflammation and Carcinogenesis

by

Edward C. Dominguez

Doctor of Philosophy, Graduate Program in Environmental Toxicology
University of California, Riverside, March 2022
Dr. Prue Talbot, Chairperson

Exposure to agricultural organic dusts have been well-documented to increase the risk of acute and chronic lung disease among individuals working in the farming and livestock industries. Particulates in organic dust, as well as gaseous compounds in some environments, are what contribute to the lung inflammation elicited upon exposure. As individuals in these industries are exposed to longer durations of agricultural organic dust, the risk increases for the development of chronic lung diseases, such as bronchitis, COPD, and cancer. In addition, these food deserts face restricted access to healthier dietary selections which can be directly correlated to their occupation and lower socioeconomic status. Although the farming industries have access to personal protective equipment, such as masks and ventilators to protect against exposures to dust, they are not always used and as such, additional intervention strategies to protect against these exposures are needed. Omega-3 polyunsaturated fatty acids, such as docosahexaenoic

acid (DHA), and their corresponding bioactive-lipid mediators, including resolvin D1 (RvD1), have been shown in the literature to elicit anti-inflammatory and pro-resolving properties making them a unique choice as a therapeutic strategy. The work presented in this dissertation identified the use of a DHA-rich diet as an effective intervention strategy to preemptively dampen a single dust-induced intranasal challenge in mice, providing evidence that dietary supplementation with omega-3 fatty acids is efficient for mitigating the acute inflammatory effects associated with agricultural organic dust exposure. Furthermore, we present data supporting the hypothesis that chronic exposure to agricultural organic dust enhances lung carcinogenesis in mice as well as promotes metastatic properties including epithelial to mesenchymal transition within human lung adenocarcinoma cells. Moreover, this project provides evidence for the therapeutic use of RvD1's synthetic epimer, aspirin-triggered resolvin D1, for mitigating chronic lung inflammatory responses induced by organic dust. These outcomes are evidenced by reduced leukocyte recruitment, altered oxylipin levels in the lungs, and dampened lung tissue histopathology. Overall, the data presented in this dissertation support the use of omega-3 fatty acid dietary supplementation and administration of their bioactive lipid mediators as potential therapeutic intervention strategies for alleviating the negative acute and chronic lung inflammatory effects of agricultural organic dust exposure among livestock and other farming occupations.

Table of Contents

List of Figures

List of Tables

INTRODUCTION

Occupational Dust Exposure

Environmental and occupational exposures in livestock and farming industries induce a multitude of lung inflammatory responses elicited from inorganic and organic agents circulating in these environments such as chemicals, aerosols, and dusts [1-3]. The USDA reports that in 2020, agriculture and related industries accounted for approximately 10.3% of employment or 19.7 million full- and part-time jobs in the U.S. [4]. Additionally, it has been reported that in 2019 roughly 50% of individuals worldwide were employed within the agriculture industry, and related occupations [5]. Agricultural organic dust exposure has been strongly correlated with adverse risk for the development of acute and chronic lung inflammatory diseases such as asthma, bronchitis, and chronic obstructive pulmonary disease (COPD) [1,6-8].

Epidemiological studies have shown that livestock and other farm workers are among the occupational groups most associated with these exposures and face increased risk for the development of negative respiratory symptoms and diseases [9-12]. Swine, poultry, cattle, and cotton textile industry workers are among those most negatively impacted by organic dust exposure within their respective industries [13-16]. Although there is not a single agent responsible for stimulating the inflammatory effects these populations endure, the literature has established organic dust as a major component of the negative respiratory effects seen in exposed workers [7,17-19].

Epidemiological studies have identified strong correlations between lower socioeconomic status (SES), minority populations, and increased risk of lung inflammatory diseases (including lung cancer) following repeated exposure to particulate matter, which includes organic dust [20-23]. The negative respiratory health consequences that workers in these industries experience can be lessened with the use of personal protective equipment (PPE) and proper preventative measures such as the use of respirators, masks, and indoor ventilation [24,25]. Nonetheless, proper PPE is not always attainable or adopted by these industries, especially those working in lower income areas [23-25]. Without effective precautionary or intervention measures in place to protect against these exposures, the risk for developing acute and chronic lung inflammatory diseases rises.

Acute and Chronic Inflammation

Inflammation is the body's natural immune response to injury or foreign pathogen invasion such as bacterial, viral, and toxin exposure. Upon initial contact to these external invaders, our bodies respond by inducing the five cardinal signs of inflammation: pain, swelling, redness, fever, and loss of tissue function. The induction of these signs is facilitated through the release of chemical and endogenous mediators [26]. These mediators work in tandem to rid the body of the foreign antigens, repair any tissue damage, and eventually return our bodies back to homeostasis [26-28]. The biological and molecular effects of these mediators include increased vasodilation to allow for the recruitment of leukocytes including

macrophages and polymorphonuclear cells (PMNs), such as neutrophils, to the site of inflammation [29,30]. These mediators drive the secretion of pro-inflammatory cytokines such as the neutrophil chemoattractant interleukin-8 (IL-8) to assist with eliminating the foreign pathogen from our systems [31,32]. Cytokines such as tumor necrosis factor-alpha (TNF-α) and transforming growth factor beta-1 (TGFβ-1) are also secreted to promote both immune activation as well as tissue repair following injury [33,34]. The collection of these biological mechanisms and responses creates the acute inflammatory cascade, all of which can be a beneficial aspect of our bodies' innate immune response if undergone in a complete and time efficient manner [35,36]. Despite the benefits of our systems' natural responses, acute lung injury can result in negative respiratory symptoms and disorders including coughing, pneumonia, acute bronchitis, and acute respiratory distress syndrome (ARDS) [18,37]. After the acute inflammatory response is resolved, our bodies can go back to their original state; however, if inflammation is unresolved, the responses can worsen and become chronic.

Chronic inflammation is an unresolved or persistent immunological process that includes failed resolution of the acute inflammatory response. Properties of chronic inflammation include prolonged neutrophil recruitment, persistent (or aggravated) tissue damage, reduced clearance of apoptotic cells, and altered macrophage polarization from the classically activated (M1) to the alternatively activated (M2) phenotype [18,38]. In a chronic setting, an overabundance of either macrophage type can drive overactive biological responses such as pro-inflammatory cytokine

secretion and tissue-repair pathogenesis that could be avoided if the system was able to resolve the acute inflammatory response [39]. Chronic lung inflammation can promote increased risk for the development of chronic lung diseases including asthma, bronchitis, fibrosis, COPD, and cancer [40,41]. Development of pulmonary fibrosis stems from the lengthened chronic inflammatory process after failing to resolve the initial inflammatory response. Biological mechanisms for the development of fibrosis include increased fibrocyte recruitment, which promotes elevated collagen deposition and tissue thickening, persistent neutrophil recruitment, and activation of M2 macrophages [42,43]. Prolonged neutrophil recruitment can lead to eventual release of ROS and other chemical molecules that may cause further tissue damage and injury [42,43]. Overactivation of M2 macrophages, which secrete anti-inflammatory cytokines and growth factors, can result in tissue over-remodeling and subsequent fibrotic pathogenesis [42,43]. Environmental occupational groups such as livestock and other farm workers face increased risk for the development of the mentioned chronic lung diseases due to their everyday or repeated exposures to organic dust. But what parts of the dust are potent enough to elicit the acute and possible chronic inflammatory lung diseases mentioned previously? An important facet to understanding how exposure to organic dusts elicits inflammation and possible acute and chronic respiratory diseases requires a comprehensive examination of the inflammatory components in agricultural dust.

Agricultural Organic Dust

It has been reported that a variety of inorganic and organic components exit within agricultural dusts such as trace metals, fungi, bacteria, and gaseous compounds [2,3,44]. A previous in-depth assessment of dust from indoor swine feeding facility operations classified bacteria, archaebacteria, fungi, and viral components to exist within these dust—all of which can contribute to the lung inflammatory responses elicited upon exposure [44,45]. Detailed examination of these inflammatory components identified proteases, endotoxin, which comprises the outer membrane of gram-negative bacteria, and peptidoglycan, which is a major cell wall component of gram-positive bacteria, as causative agents for the lung inflammatory effects of the dust [45,46]. Proteases in agricultural organic dust have been identified to be one of the more significant contributors to the lung inflammatory responses elicited following exposure, including inflammatory cytokine and chemokine production and airway inflammation [47]. The pro-inflammatory effects of proteases are induced via protease-activated receptors (PARs), and in the case of swine dust exposure, PAR-1 and PAR-2 are the main receptors for proteolytic activation [47]. Endotoxins are made up of a combination of lipids, proteins, and lipopolysaccharides (LPS) which are released into the environment following bacterial cell lysing and are deposited into the airways of our respiratory tracts during inhalation exposure [48,49]. LPS, more specifically, the lipid A portion of LPS, are hydrophilic and heat-stable molecules that are biologically responsible for the potent inflammatory and toxicological effects of endotoxin following exposure [48,50,51]. Mechanistically,

these negative health effects are initiated when LPS binds to LPS binding proteins (LBP), which are prominent in the fluid of the airway surface, to form a complex that is transported to the CD14 activation site expressed on lung macrophages, as seen below in **Figure 1** [49]. Following activation, the LPS-LBP complex is transferred to toll-like receptor 4 (TLR4) via the MD2 accessory protein, initiating a cascade of innate immune responses including the downstream activation of NF-κB, and subsequent release of pro-inflammatory cytokines, such as IL-6, IL-8, and TNF-α [45,49,52]. These cytokines can promote further recruitment of PMNs and macrophages to the site of inflammation, continuing the inflammatory response.

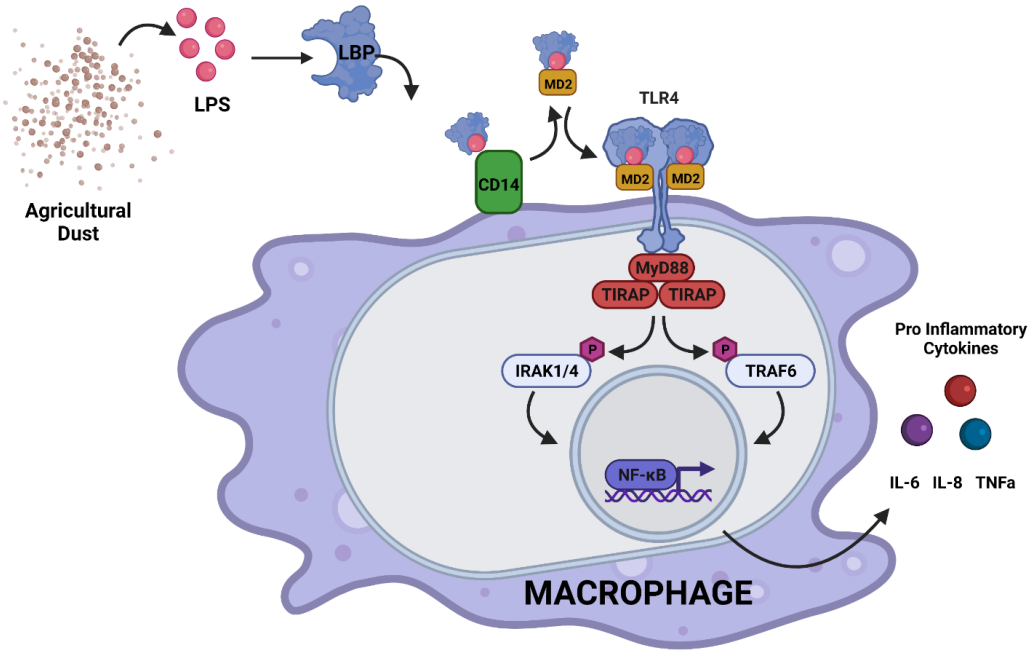

Figure 1. Mechanism for The Release of Pro-Inflammatory Mediators Following Exposure to Endotoxin. Agricultural organic dust contains LPS which are components of the gram-negative bacteria endotoxin. LPS forms a complex with LBP and is transported to the macrophage surface receptor CD14 which becomes activated and initiates the transfer of the LPS-LBP complex to TLR4 via the accessory protein MD2. Activation of TLR4 initiates the eventual activation of NF-κB and subsequent release of pro-inflammatory cytokines.

Several epidemiological studies have evaluated the contents of organic dusts from a variety of occupational environments and have characterized LPS as one of the minor components that contribute to the inflammatory and systemic effects elicited from the dust exposures, whereas other components such as proteases are of the more prominent factors contributing to lung inflammation [14,45-47,53]. It is important to note that previous examinations of the lung inflammatory effects of swine dust exposure are not solely linked to LPS, but a combination of peptidoglycans, bacterial proteases, fungal components, and LPS—all of which provide a synergistic role for eliciting an inflammatory response [45,47,54]. Despite the vast amount of research examining the negative effects induced by LPS exposure, there is still a gap in the literature regarding how LPS alters lung carcinogenesis, with some studies suggesting it provides a protective role against lung tumorigenesis and others an enhancement effect [48,49,55,56].

Endotoxin Hypothesis

The inflammatory responses elicited from endotoxin exposure have been well established in the literature; however, the consensus on the carcinogenic effects following acute or chronic exposure have far more disparities. Several epidemiological studies examining health outcomes associated with endotoxin exposure among agricultural workers reported both deleterious and protective health effects [48,56-58]. These disparaging effects can best be explained by first outlining the “hygiene hypothesis.” This theory suggests that those who are exposed to a clean

environment with minimal environmental or inflammatory agents exhibit a greater shift to T-helper 2 (Th2) cell activation, whereas those who experience elevated exposure to environmental agents such as endotoxin may experience an increased shift to T-helper 1 (Th1) cells [59-61]. Activation of Th1 cells results in increased production of pro-inflammatory cytokines, including TNF-α and interferon-gamma (IFN-γ), that help initiate the acute inflammatory response needed to rid the body of the infection or foreign invaders [60]. Th2 cells regulate eosinophilic cell activation, immunoglobulin E (IgE) production, interleukin-4 (IL-4), interleukin-5 (IL-5), and interleukin-13 (IL-13) secretion, all of which contribute to an increased allergic response [49,59]. It has been speculated that increased exposure to antigenic determinants (including pathogen-associated molecular patterns such as LPS) promotes an immunostimulatory Th1 response that may result in reduced risk for the development of allergic disorders [57,62,63]. Support of this theory has been seen in epidemiological studies of younger children and adults that experienced a lower prevalence of asthma after being raised in farming environments, which support the proposed beneficial immunostimulatory effects of endotoxin [49,64]. Moreover, epidemiological studies assessing the impact of endotoxin exposure found that following chronic inhalation, individuals experienced several negative respiratory health effects including coughing, wheezing, nasal and throat irritation, and shortness of breath suggesting there can still be negative effects associated with endotoxin exposure [49,65,66].

As mentioned above, there are numerous studies in the literature outlining the health effects of endotoxin exposure in relation to inflammatory-related outcomes. However, research on the effects of endotoxin exposure and cancer have been conflicting. An epidemiological study examining populations exposed to organic dust over a 20-year monitoring period found that exposure to occupational organic dusts containing endotoxins or LPS was associated with increased risk for the development of lung cancer [56]. In a mouse model of lung tumorigenesis, chronic exposure to LPS significantly increased lung tumorigenesis compared to non-LPS treated mice, further supporting the idea that chronic LPS or endotoxin exposure promotes an increased risk for the development of lung cancer [67]. Conversely, other epidemiological studies have identified that among individuals in agricultural industries, such as dairy farming, reduced odds ratios for lung cancer were observed [55,63]. The exact explanation for this proposed mechanistic reduction of lung cancer is not known, however, one possible reason is that LPS induces a more Th1 phenotype which will increase the activation of immune cells such as macrophages, which secrete the pro-inflammatory cytokine TNF-α. TNF-α can activate anti-tumorigenic effects including the activation of cytotoxic T-cells or tumor infiltrating macrophages which will promote immunomodulatory effects that suppress tumorigenesis [68]. There is a clear gap of understanding for the definitive role of endotoxin exposure on carcinogenesis that needs to be addressed. Further human epidemiological and long-term animal exposure studies are needed to better understand the biological and mechanistic abilities for endotoxin to alter

carcinogenesis following chronic exposure, especially since cancer is one of the leading causes of mortality worldwide [69].

Lung Cancer

The CDC reports that cancer is the second leading cause of deaths in the United States, with lung cancer being the leading cause of cancer-related deaths worldwide [70]. Non-small cell lung cancer (NSCLC) is the most prevalent form of lung cancer with adenocarcinomas occupying roughly 85% of NSCLCs while squamous cell carcinoma and large cell lung cancer make up the other 15% of lung cancers [69,70]. There are a multitude of factors that contribute to increased cancer risk including diet, physical activity, environmental factors, age, sex, genetics, and tobacco smoking [71,72]. Cigarette smoking is the number one risk factor for lung cancer and has been linked to approximately 80% to 90% of lung cancer-related deaths [69,70]. Tobacco smoke has over 7000 different toxic and carcinogenic chemicals, including the tobacco-specific nitrosamine Methyl[4-oxo-4-(pyridin-3-yl)butyl]nitrous amide (NNK).

NNK is present in unburned tobacco, in cigarette smoke, and is formed during the tobacco curing, fermenting, and aging processes when nicotine undergoes nitrosation to form NNK [73-75]. It is also present in secondhand tobacco smoke, which also increases the risk for developing lung cancer [70,76]. Due to a high incidence of smoke-associated lung cancers, and the recognized role of NNK as a carcinogen, numerous rodent models use NNK as a model of cigarette smoke-associated lung

carcinogenesis [67,77,78]In rodents, NNK is enzymatically activated by cytochrome p450 (CYP450) via α-methylene hydroxylation, which results in the formation of O6-mGu DNA adducts causing G to A transitions in codon 12 of the oncogene KRAS [79-81]. NNK can also promote pyridyloxobutylation of DNA, which inhibits the DNA repair enzyme O6-alkylguanine-DNA-alkyltransferase (AGT) resulting in even greater levels of O6-mGu adducts in the lungs [82,83]. These processes result in eventual lung tumor formation since the lung contains an abundance of CYP450 enzymes within the peripheral and bronchial epithelia, making it a perfect target organ for NNK to be bioactivated [80]. A single 100 mg/kg of NNK administered via intraperitoneal injection (i.p.) into A/J mice, which contain a polymorphism in intron 2 of KRAS, allows for the mice to be sensitized to NNK and lung tumor formation—making it an effective animal model for investigating lung tumorigenesis [84-86]. This single dose of NNK is more than enough to induce lung tumorigenesis in mice resulting in lung adenomas after 21 weeks and possible adenocarcinomas formed 50 or more weeks post-injection [77,80]. The consistency and reproducibility of this dosing strategy allows for it to be an effective animal model to screen chemical and chemo preventative agents such as NNK. Alveolar type II cells, which secrete surfactant to reduce alveolar collapse, metabolize xenobiotics, and partake in the regeneration of the alveolar epithelium following any damage or injury that it endures, are known to be the site of origin for mouse lung adenoma formation [87]. About 25-50% of human adenocarcinomas possess mutations in codon 12 of KRAS and are more likely to exist among smokers and former smokers than in non-smokers

[88,89]. Likewise, the comparisons that can be made between this mouse model of lung carcinogenesis and human adenocarcinomas provides further evidence for why this model can be used to effectively investigate lung carcinogenic mechanisms, including tumor metastasis.

EMT and Metastasis

Cancer is best defined as the uncontrolled growth of abnormal cells that lead to malignancies in the body. The spread of cancer cells from the localized or primary tumor to surrounding tissues and other organs utilizes the invasive process known as cancer metastasis [90]. This biological process accounts for approximately 90% of cancer-related deaths and can be induced by a variety of system-wide responses including epithelial to mesenchymal transition (EMT) [90-92]. EMT, a hallmark of cancer metastasis, is the process in which an epithelial cell transforms into an elongated-shaped mesenchymal cell that can more easily invade other tissues and organs [91,93]. In the context of cancer specifically, EMT is a multi-step biological process where cuboidal epithelial tumor cells detach from the primary tumor and undergo a physiological change into a more elongated or stretched shaped mesenchymal cell that has the ability to invade and inhabit other tissues or organs, **Figure 2** [90-92].

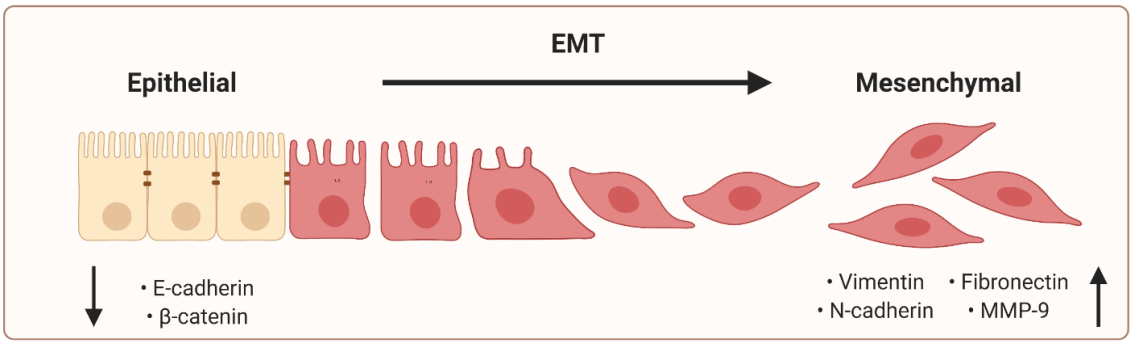

Figure 2. Changes Exhibited During Epithelial to Mesenchymal Transition. During EMT, cells undergo morphological changes including loss of tight junctions and exhibit increased motility and extracellular matrix dissociation.

Although EMT is a hallmark of cancer metastasis, it can also be a beneficial process that is involved with tissue remodeling, embryonic development, and wound healing [93].

During EMT-driven metastasis, epithelial tumor cells lose their basement membrane and cell to cell junctions, such as tight junctions, gap junctions, and adherens junctions, are dissociated— all of which leads to a loss of epithelial structure [92]. These junctions, including the tight-junction protein e-cadherin, are what help provide the cell its cuboidal epithelial structure. Dissociation or loss of e-cadherin results in the subsequent breakdown of other cell junctions which releases β-catenin, a transcriptional activator of target genes that promote cell proliferation and differentiation [92,94]. Loss of tight junction proteins such as e-cadherin, also allows for the cell to become less rigid and more easily detach from the primary tumor and adjacent tumor cells [92,93]. The reduction of tight junctions also increases the degradation of the extracellular matrix (ECM) and increases the filamentous

structures shaping the cell, which allow for greater movement and flexibility [90-92]. Notable markers expressed by mesenchymal cells that are responsible for these physiological properties of the cell can be seen in **Figure 2** and include fibronectin, vimentin, MMP-9 and n-cadherin [90-92]. This increase in structural fluidity allows for the cell to permeate the lymphatic system more easily, which increases the likelihood the cancerous cell will migrate and invade other tissues or organs [92,93]. One of the most notable inducers of EMT is the growth factor TGFβ-1, as it plays a role in enhancing angiogenesis, while also triggering the series of biological processes that are responsible for driving a more invasive mesenchymal phenotype [95,96]. These processes occur as TGFβ-1 induces the activation of Smad2 and Smad3, which become phosphorylated and form a complex with Smad4 that then moves into the nucleus [93,96]. The Smad complex then regulates the activation of the transcription factors ZEB1, TWIST1, and SNAI1, all of which promote alterations in the EMT biomarkers seen in **Figure 2** [93,96]. EMT is a hallmark of cancer metastasis, and a thorough understanding of this mechanistic process is important for the development of new therapeutic or intervention strategies that may protect against or dampen carcinogenesis.

Polyunsaturated Fatty Acids

It has generally been accepted that omega-3 polyunsaturated fatty acids (PUFA) are anti-inflammatory, whereas omega-6 PUFA are pro-inflammatory. Eicosapentaenoic acid (EPA) and docosahexaenoic acid (DHA) are long-chain

essential omega-3 PUFA that are naturally occurring in aquatic environments and are rich in foods that we eat including plants such as seaweed, fish, nuts, and seeds [97,98]. The omega-6 PUFA, arachidonic acid (AA), is also an essential fatty acid that exists in foods such as wheat, corn, and fried foods [97,99]. The human body is not capable of self-producing the fatty acids linoleic acid (LA), which is the precursor to AA, and alpha-linolenic acid (ALA), which serves as the precursor to EPA and DHA [97,100]. It is necessary for these essential fatty acids to be incorporated into our systems through dietary consumption, to serve a substrates for AA, EPA, and DHA. Due to the typical western diet, which is about a 15:1 omega-6 to omega-3 fatty acid ratio as opposed to the ideal 1:1, the average person's tissues are at an omega-3 PUFA deficit—thus providing a potential intervention target for modulating inflammation [97,100]. During the initial inflammatory response, LA is cleaved from the phospholipid bilayer by the Ca2+-dependent cytosolic phospholipase A2 (cPLA2) enzyme, which subsequently produces AA that can then be metabolized by the body **Figure 3** [101,102]. AA is enzymatically activated by cyclooxygenase (COX-1 and COX-2) as well as 5-lipoxygenase (5-LOX) following acute injury or infection to produce the pro-inflammatory eicosanoids prostaglandins, thromboxanes, and leukotrienes, **Figure 3** [28,103]. These lipid mediators function to promote the acute inflammatory response needed to rid the body of the foreign pathogen(s) by increasing vasodilation, elevating platelet activation, and increasing neutrophil chemotaxis, respectively [28]. This promotes increased vascular permeability and the recruitment of PMNs such as neutrophils, to site of inflammation from the bone

marrow [29,104]. Neutrophils fight infection by engulfing foreign antigens through phagocytosis and releasing pro-inflammatory cytokines including TNF-α, which continues the recruitment process of leukocytes to induce inflammation [28,105]. Following the acute phase inflammatory response, there is a lipid mediator class switching mechanism where omega-3 PUFAs such as EPA and DHA begin to get cleaved from the lipid membrane by cPLA2 and Ca2+-independent phospholipase A2 (iPLA2) enzymes, respectively, creating a competitive inhibition of AA cleavage by phospholipase A2, **Figure 3** [102,106,107]. The complete mechanistic understanding of the lipid mediator switching process, is not entirely understood.

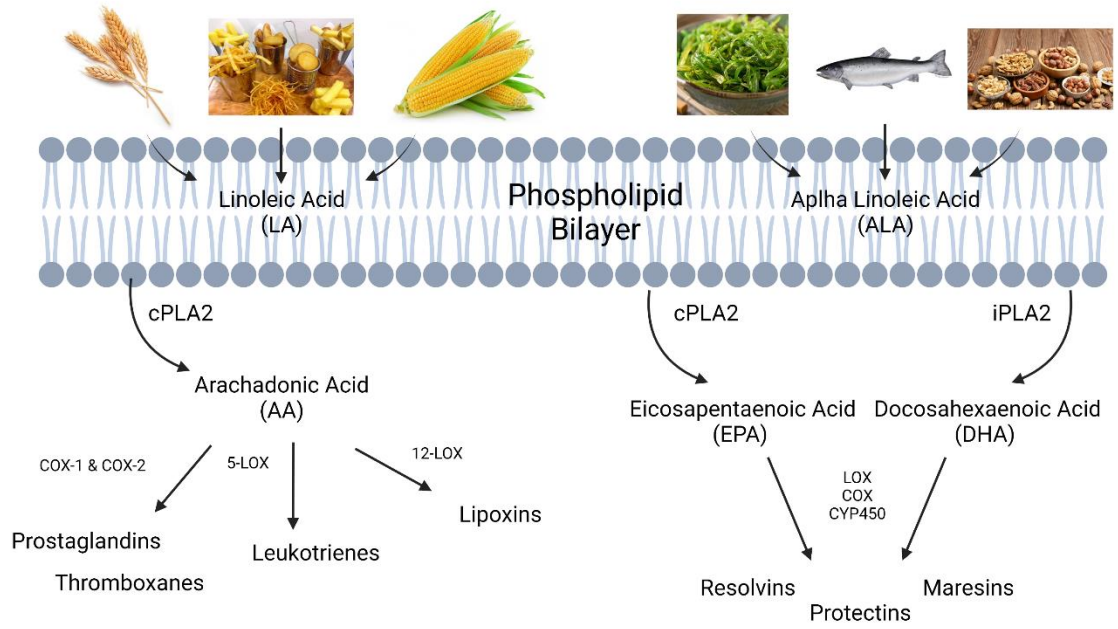

Figure 3. Cleavage of Arachidonic acid, EPA, and DHA from the phospholipid bilayer. Upon the initial inflammatory response, arachidonic acid is cleaved from the phospholipid bilayer by cPLA2 until a lipid mediator class switching mechanism occurs, wherein EPA and DHA begin to get cleaved from the lipid bilayer by cPLA2 and iPLA2, respectively.

Upon the increase in omega-3 PUFA synthesis, AA undergoes a lipid mediator class switch mechanism and is enzymatically activated by 12-LOX which produce lipoxins, the omega-6 PUFA-derived specialized pro-resolving lipid mediator (SPM) class, Figure 3 [28,35]. SPMs function as biological anti-inflammatory lipid mediators that promote the resolution of inflammation and return our systems back to homeostasis [28,35]. Newly synthesized EPA and DHA undergo enzymatic activation themselves via LOX, COX, and CYP450 into the SPMs resolvins, protectins, and maresins, **Figure 3** [29,108-110]. SPMs have been well established in the literature to exhibit their anti-inflammatory and pro-resolving effects by reducing neutrophil chemotaxis, increasing macrophage phagocytosis and efferocytosis, and promoting the repair of damaged tissue through the secretion of growth factors, such as TGFβ-1 [35,105,111]. Neutrophils undergo apoptosis following phagocytosis and begin to express membrane antigens that signal for macrophages to be recruited to the site of inflammation, which remove the apoptotic PMNs via phagocytosis [29,33,112]. This process promotes further recruitment of macrophages to the site of inflammation and reduces the production of pro-inflammatory cytokines while increasing production of growth factors [28,35,36]. If uninterrupted, the resolution of the acute inflammatory response will occur, and our bodies will return to their initial state. It is clear from the literature that diet plays a key role in modulating the inflammatory response, and dietary intervention strategies may be utilized to protect against acute or chronic injury following exposure to inflammatory agents such as agricultural organic dust.

PUFA Therapeutic Strategies

Fish oil is a widely popular dietary supplement used by individuals as they are rich in omega-3 PUFAs such as EPA and DHA. As previously stated, the typical western diet is at a significant omega-3 to omega-6 PUFA ratio deficit, which may increase the risk for development of inflammatory diseases among individuals who endure exposure to inflammatory agents, such as agricultural dust [97,100]. Dietary intervention studies have examined the beneficial protective effects of omega-3 PUFA. Several in vivo studies have examined the protective effects of administering a DHA-rich diet prior to exposing mice to agricultural dust extracts from swine confinement feeding facilities [98,113,114]. These studies showed that a DHA-rich diet reduces total cell infiltration in the lungs of exposed mice, reduces production of pro-inflammatory cytokines and chemokines, reduces neutrophil infiltration in the lung airways, and increases production of SPMs, such as resolvin D1 (RvD1) in the lungs of DHA-treated mice [98,113,114]. Overall, the literature has well-documented the immunomodulatory effects of elevating omega-3 PUFA intake prior to exposing mice to environmental inflammatory agents, suggesting dietary supplementation to be an effective strategy for dampening inflammation.

Additionally, dietary intervention studies assessing the beneficial effects of omega-3 PUFAs have examined the protective effects of fish oil supplementation against carcinogenesis in a mouse model of lung tumorigenesis [115]. A/J mice were administered a fish oil-rich diet 3 weeks prior to receiving a single 100 mg/kg of NNK and were sacrificed 17 weeks post-injection [115]. Although mice still developed tumors

following the NNK injection, mean tumor counts were significantly lower than all other dietary groups (soybean, corn oil, and control diet), suggesting that an omega-3 PUFA-rich diet can serve as a preventative intervention strategy for mitigating lung tumorigenesis [115]. From the data reported in the literature, it is evident that increasing omega-3 PUFA dietary intake can serve as increased substrate for the production of SPMs that can reduce inflammation and, in some instances, carcinogenesis. In addition to dietary intervention strategies, therapeutic treatment using SPMs themselves have shown promise for alleviating acute and chronic lung inflammation.

SPM Treatment

Hsiao et. al reported that long-term exposure to cigarette smoke-induced emphysema in mice, increased neutrophil recruitment in the lungs, elevated levels of pro-inflammatory cytokines, and severe alveolar airspace depletion in the lungs [116,117]. Mice were exposed to cigarette smoke for 1 hr, twice per day, for 3 consecutive days [116]. Following exposures, cigarette smoke-exposed mice were then treated with the SPM RvD1 for 3 consecutive days which significantly reduced the aforementioned inflammatory outcomes compared to the control mice administered only cigarette smoke [116]. To determine if the synthetic epimer version of RvD1, aspirin-triggered resolvin D1 (AT-RvD1) would display even greater dampening effects, Hsiao et. Al treated mice twice per week for 12 weeks with this epimer [117]. AT-RvD1 is formed endogenously when DHA undergoes enzymatic activation via COX-1 or CYP450 in the presence of aspirin [118,119]. This synthetic epimer has the same receptor binding and pro-resolving

effects as RvD1, however, possesses an approximate one log order of increased potency and is more resistant to rapid inactivation by eicosanoid oxidoreductase (EOR) than RvD1, allowing it to carry out its effects for a longer duration [118,119]. Long-term treatment with AT-RvD1 reduced cigarette smoke-induced emphysema, inhibited airspace enlargement, reduced oxidative stress and cell death, and did not promote tissue fibrosis [117]. Additional long-term studies examining the beneficial effects of AT-RvD1 on aerosol allergen-challenged mice were performed and identified similar protective outcomes including reduced inflammatory markers, increased macrophage phagocytosis of allergens, and reduced alveolar and bronchial inflammation [120]. In addition to alleviating inflammatory outcomes, treatment with RvD1 and AT-RvD1 have also been shown to inhibit TGFβ-1-induced EMT in human lung adenocarcinoma cells, suggesting a possible protective effect against cancer metastasis [121,122]. Therapeutic effects of other SPMs, such as maresin-1 (MaR1), have also been examined in the literature [123-125] for their anti-inflammatory, pro-resolving, and anti-tumorigenic effects. MaR1 has been shown to reduce neutrophil influx and release of pro-inflammatory cytokines in mice, following a single or repetitive exposure to organic agricultural dust [123]. In vitro, MaR1 has been shown to significantly reduce organic dust-induced pro-inflammatory cytokine release in bronchial epithelial cells, as well as inhibit TGFβ-1-induced EMT in alveolar epithelial cells [124,125]. Overall, the immunomodulatory effects of SPM treatment are well-documented and provide strong evidence that could suggest the therapeutic use of these SPMs for alleviating inflammation and carcinogenesis.

Rationale of Dissertation Work

The research presented in this dissertation examines the potential therapeutic effects of omega-3 fatty acids and their derived bioactive lipid mediators for alleviating acute and chronic lung inflammation. Chapter 1 discusses the proposed use of dietary supplementation using a DHA-rich diet, prior to administering a single intranasal challenge of hog dust extract (HDE), to protect against acute lung inflammation. We hypothesized that pre-treating mice with a high DHA diet 4-weeks before administering a single intranasal challenge of HDE, would significantly dampen the dust-induced inflammatory response. Through our investigations, we determined that a DHA-rich diet can serve as an increased substrate for the biosynthesis of SPMs during the resolution phase of inflammation, which may help dampen the acute lung inflammation elicited from the agricultural dust exposure. These findings were evidenced by the increase in RvD1 levels found in the BALF and reduced AA levels in the blood of DHA+HDE-exposed mice, compared to the dust-exposed mice fed a control diet. This study provided new questions to be answered including how protective can direct use of SPMs be in mitigating dust-induced inflammation.

As mentioned, Chapter 1 demonstrates the acute lung inflammatory effects in mice following a single intranasal challenge of hog dust extract (HDE). Other studies have even explored the acute inflammatory effects of repetitive dust exposure; however, the chronic inflammatory and carcinogenic effects of the dust had not been investigated. Chapter 2 addresses this gap of knowledge and explores the chronic inflammatory and carcinogenic effects of 24 weeks of HDE exposure in A/J mice. The research provided in

Chapter 2 also explore the use of AT-RvD1 as a possible therapeutic strategy for alleviating dust-induced chronic inflammation and protecting against dust-enhanced lung tumorigenesis. Lastly, Chapter 2 also provides evidence to suggest that chronic exposure to agricultural organic dust can induce epithelial to mesenchymal transition in the tumor microenvironment, a hallmark of tumor metastasis. Overall, these studies address large gaps in the literature and provide convincing evidence for the therapeutic use of omega-3 fatty acids and their derived bioactive lipid mediators for dampening acute and chronic lung inflammatory effects elicited by agricultural organic dust exposure, which can benefit the livestock and farming industries.

References

1. Bailey, K.L.; Meza, J.L.; Smith, L.M.; Von Essen, S.G.; Romberger, D.J. Agricultural exposures in patients with COPD in health systems serving rural areas. J Agromedicine 2007, 12, 71-76, doi:10.1300/J096v12n02_10.

2. Von Essen, S.; Romberger, D. The respiratory inflammatory response to the swine confinement building environment: the adaptation to respiratory exposures in the chronically exposed worker. J Agric Saf Health 2003, 9, 185-196, doi:10.13031/2013.13684.

3. Nordgren, T.M.; Bailey, K.L. Pulmonary health effects of agriculture. Curr Opin Pulm Med 2016, 22, 144-149, doi:10.1097/MCP.0000000000000247.

4. (USDA), U.S.D.o.A. Farming and Farm Income. Availabe online: https://www.ers.usda.gov/data-products/ag-and-food-statistics-charting-the-essentials/farming-and-farm-income/ (accessed on

5. Roser, M. Employment in agriculture. Our world in data 2013.

6. Szczyrek, M.; Krawczyk, P.; Milanowski, J.; Jastrzebska, I.; Zwolak, A.; Daniluk, J. Chronic obstructive pulmonary disease in farmers and agricultural workers - an overview. Ann Agric Environ Med 2011, 18, 310-313.

7. Kirkhorn, S.R.; Garry, V.F. Agricultural lung diseases. Environmental health perspectives 2000, 108 Suppl 4, 705-712, doi:10.1289/ehp.00108s4705.

8. Monso, E.; Riu, E.; Radon, K.; Magarolas, R.; Danuser, B.; Iversen, M.; Morera, J.; Nowak, D. Chronic obstructive pulmonary disease in never-smoking animal farmers working inside confinement buildings. Am J Ind Med 2004, 46, 357-362, doi:10.1002/ajim.20077.

9. Von Essen, S.; Donham, K. Illness and injury in animal confinement workers. Occup Med 1999, 14, 337-350.

10. Von Essen, S.; Fryzek, J.; Nowakowski, B.; Wampler, M. Respiratory symptoms and farming practices in farmers associated with an acute febrile illness after organic dust exposure. Chest 1999, 116, 1452-1458.

11. Guillien, A.; Puyraveau, M.; Soumagne, T.; Guillot, S.; Rannou, F.; Marquette, D.; Berger, P.; Jouneau, S.; Monnet, E.; Mauny, F., et al. Prevalence and risk factors for COPD in farmers: a cross-sectional controlled study. European Respiratory Journal 2016, 47, 95-103, doi:10.1183/13993003.00153-2015.

12. Linaker, C.; Smedley, J. Respiratory illness in agricultural workers. Occupational Medicine 2002, 52, 451-459, doi:10.1093/occmed/52.8.451.

13. Bongers, P.; Houthuijs, D.; Remijn, B.; Brouwer, R.; Biersteker, K. Lung function and respiratory symptoms in pig farmers. Br J Ind Med 1987, 44, 819-823, doi:10.1136/oem.44.12.819.

14. Charavaryamath, C.; Singh, B. Pulmonary effects of exposure to pig barn air. J Occup Med Toxicol 2006, 1, 10-10, doi:10.1186/1745-6673-1-10.

15. Cole, D.; Todd, L.; Wing, S. Concentrated swine feeding operations and public health: a review of occupational and community health effects. Environmental health perspectives 2000, 108, 685-699, doi:10.1289/ehp.00108685.

16. May, S.; Romberger, D.J.; Poole, J.A. Respiratory health effects of large animal farming environments. J Toxicol Environ Health B Crit Rev 2012, 15, 524-541, doi:10.1080/10937404.2012.744288.

17. Respiratory Health Hazards in Agriculture. American Journal of Respiratory and Critical Care Medicine 1998, 158, S1-S76, doi:10.1164/ajrccm.158.supplement_1.rccm1585s1.

18. Aghasafari, P.; George, U.; Pidaparti, R. A review of inflammatory mechanism in airway diseases. Inflammation Research 2019, 68, 59-74, doi:10.1007/s00011-018-1191-2.

19. Crook, B.; Robertson, J.F.; Glass, S.A.; Botheroyd, E.M.; Lacey, J.; Topping, M.D. Airborne dust, ammonia, microorganisms, and antigens in pig confinement houses and the respiratory health of exposed farm workers. Am Ind Hyg Assoc J 1991, 52, 271-279, doi:10.1080/15298669191364721.

20. Aldrich, M.C.; Selvin, S.; Wrensch, M.R.; Sison, J.D.; Hansen, H.M.; Quesenberry, C.P., Jr.; Seldin, M.F.; Barcellos, L.F.; Buffler, P.A.; Wiencke, J.K. Socioeconomic status and lung cancer: unraveling the contribution of genetic admixture. Am J Public Health 2013, 103, e73-80, doi:10.2105/ajph.2013.301370.

21. Forastiere, F.; Stafoggia, M.; Tasco, C.; Picciotto, S.; Agabiti, N.; Cesaroni, G.; Perucci, C.A. Socioeconomic status, particulate air pollution, and daily mortality: differential exposure or differential susceptibility. Am J Ind Med 2007, 50, 208-216, doi:10.1002/ajim.20368.

22. Hajat, A.; Hsia, C.; O'Neill, M.S. Socioeconomic Disparities and Air Pollution Exposure: a Global Review. Curr Environ Health Rep 2015, 2, 440-450, doi:10.1007/s40572-015-0069-5.

23. Mines, R. Findings from the National Agricultural Workers Survey (NAWS) 1990. A Demographic and Employment Profile of Perishable Crop Farm Workers. Research Report No. 1. 1991.

24. Mitchell, D.C.; Schenker, M.B. Protection against breathing dust: behavior over time in Californian farmers. J Agric Saf Health 2008, 14, 189-203, doi:10.13031/2013.24350.

25. Schenker, M.B.; Orenstein, M.R.; Samuels, S.J. Use of protective equipment among California farmers. American Journal of Industrial Medicine 2002, 42, 455-464, doi:10.1002/ajim.10134.

26. Hannoodee, S.; Nasuruddin, D.N. Acute inflammatory response. StatPearls [Internet] 2020.

27. Sansbury, B.E.; Spite, M. Resolution of Acute Inflammation and the Role of Resolvins in Immunity, Thrombosis, and Vascular Biology. Circ Res 2016, 119, 113-130, doi:10.1161/CIRCRESAHA.116.307308.

28. Levy, B.D.; Clish, C.B.; Schmidt, B.; Gronert, K.; Serhan, C.N. Lipid mediator class switching during acute inflammation: signals in resolution. Nature Immunology 2001, 2, 612-619, doi:10.1038/89759.

29. Serhan, C.N.; Savill, J. Resolution of inflammation: the beginning programs the end. Nature Immunology 2005, 6, 1191-1197, doi:10.1038/ni1276.

30. Von Essen, S.G.; O'Neill, D.P.; Olenchok, S.A.; Robbins, R.A.; Rennard, S.I. Grain dusts and grain plant components vary in their ability to recruit neutrophils. J Toxicol Environ Health 1995, 46, 425-441, doi:10.1080/15287399509532047.

31. Romberger, D.J.; Bodlak, V.; Essen, S.G.V.; Mathisen, T.; Wyatt, T.A. Hog barn dust extract stimulates IL-8 and IL-6 release in human bronchial epithelial cells via PKC activation. Journal of Applied Physiology 2002, 93, 289-296, doi:10.1152/japplphysiol.00815.2001.

32. Tanaka, T.; Narazaki, M.; Kishimoto, T. IL-6 in inflammation, immunity, and disease. Cold Spring Harb Perspect Biol 2014, 6, a016295-a016295, doi:10.1101/cshperspect.a016295.

33. Oishi, Y.; Manabe, I. Macrophages in inflammation, repair and regeneration. International Immunology 2018, 30, 511-528, doi:10.1093/intimm/dxy054.

34. Serhan, C.N.; Dalli, J.; Karamnov, S.; Choi, A.; Park, C.-K.; Xu, Z.-Z.; Ji, R.-R.; Zhu, M.; Petasis, N.A. Macrophage proresolving mediator maresin 1 stimulates tissue regeneration and controls pain. FASEB J 2012, 26, 1755-1765, doi:10.1096/fj.11-201442.

35. Levy, B.D.; Serhan, C.N. Resolution of acute inflammation in the lung. Annu Rev Physiol 2014, 76, 467-492, doi:10.1146/annurev-physiol-021113-170408.

36. Serhan, C.N.; Chiang, N.; Van Dyke, T.E. Resolving inflammation: dual anti-inflammatory and pro-resolution lipid mediators. Nature Reviews Immunology 2008, 8, 349-361, doi:10.1038/nri2294.

37. Ward, P.A. Acute lung injury: how the lung inflammatory response works. Eur Respir J Suppl 2003, 44, 22s-23s, doi:10.1183/09031936.03.00000703a.

38. Chazaud, B. Macrophages: Supportive cells for tissue repair and regeneration. Immunobiology 2014, 219, 172-178, doi:https://doi.org/10.1016/j.imbio.2013.09.001.

39. Murthy, S.; Larson-Casey, J.L.; Ryan, A.J.; He, C.; Kobzik, L.; Carter, A.B. Alternative activation of macrophages and pulmonary fibrosis are modulated by scavenger receptor, macrophage receptor with collagenous structure. The FASEB Journal 2015, 29, 3527-3536, doi:10.1096/fj.15-271304.

40. Parris, B.A.; O'Farrell, H.E.; Fong, K.M.; Yang, I.A. Chronic obstructive pulmonary disease (COPD) and lung cancer: common pathways for pathogenesis. J Thorac Dis 2019, 11, S2155-S2172, doi:10.21037/jtd.2019.10.54.

41. Raposo, T.P.; Beirão, B.C.B.; Pang, L.Y.; Queiroga, F.L.; Argyle, D.J. Inflammation and cancer: Till death tears them apart. The Veterinary Journal 2015, 205, 161-174, doi:https://doi.org/10.1016/j.tvjl.2015.04.015.

42. Phillips, R.J.; Burdick, M.D.; Hong, K.; Lutz, M.A.; Murray, L.A.; Xue, Y.Y.; Belperio, J.A.; Keane, M.P.; Strieter, R.M. Circulating fibrocytes traffic to the lungs in response to CXCL12 and mediate fibrosis. J Clin Invest 2004, 114, 438-446, doi:10.1172/jci20997.

43. Sun, L.; Louie, M.C.; Vannella, K.M.; Wilke, C.A.; LeVine, A.M.; Moore, B.B.; Shanley, T.P. New concepts of IL-10-induced lung fibrosis: fibrocyte recruitment and M2 activation in a CCL2/CCR2 axis. American journal of physiology. Lung cellular and molecular physiology 2011, 300, L341-L353, doi:10.1152/ajplung.00122.2010.

44. Boissy, R.J.; Romberger, D.J.; Roughead, W.A.; Weissenburger-Moser, L.; Poole, J.A.; LeVan, T.D. Shotgun pyrosequencing metagenomic analyses of dusts from swine confinement and grain facilities. PLoS One 2014, 9, e95578-e95578, doi:10.1371/journal.pone.0095578.

45. Poole, J.A.; Dooley, G.P.; Saito, R.; Burrell, A.M.; Bailey, K.L.; Romberger, D.J.; Mehaffy, J.; Reynolds, S.J. Muramic acid, endotoxin, 3-hydroxy fatty acids, and ergosterol content explain monocyte and epithelial cell inflammatory responses to agricultural dusts. J Toxicol Environ Health A 2010, 73, 684-700, doi:10.1080/15287390903578539.

46. Roque, K.; Shin, K.M.; Jo, J.H.; Lim, G.D.; Song, E.S.; Shin, S.J.; Gautam, R.; Lee, J.H.; Kim, Y.G.; Cho, A.R., et al. Association between endotoxin levels in dust from indoor swine housing environments and the immune responses of pigs. J Vet Sci 2018, 19, 331-338, doi:10.4142/jvs.2018.19.3.331.

47. Romberger, D.J.; Heires, A.J.; Nordgren, T.M.; Souder, C.P.; West, W.; Liu, X.-d.; Poole, J.A.; Toews, M.L.; Wyatt, T.A. Proteases in agricultural dust induce lung inflammation through PAR-1 and PAR-2 activation. American journal of physiology. Lung cellular and molecular physiology 2015, 309, L388-L399, doi:10.1152/ajplung.00025.2015.

48. Lundin, J.I.; Checkoway, H. Endotoxin and cancer. Environ Health Perspect 2009, 117, 1344-1350, doi:10.1289/ehp.0800439.

49. Liebers, V.; Raulf-Heimsoth, M.; Bruning, T. Health effects due to endotoxin inhalation (review). Arch Toxicol 2008, 82, 203-210, doi:10.1007/s00204-008-0290-1.

50. Hodgson, J.C. Endotoxin and Mammalian Host Responses During Experimental Disease. Journal of Comparative Pathology 2006, 135, 157-175, doi:https://doi.org/10.1016/j.jcpa.2006.09.001.

51. Reisser, D.; Pance, A.; Jeannin, J.F. Mechanisms of the antitumoral effect of lipid A. Bioessays 2002, 24, 284-289, doi:10.1002/bies.10053.

52. Behzad Kasravi, F.; Lee, D.H.; Weisgraber, K.; Harris, H.W. Lipoprotein-bound endotoxin exerts an immunomodulatory effect on hepatocytes through the lipid A domain of LPS. Journal of Endotoxin Research 2005, 11, 19-24, doi:10.1177/09680519050110010601.

53. Poole, J.A.; Thiele, G.M.; Alexis, N.E.; Burrell, A.M.; Parks, C.; Romberger, D.J. Organic dust exposure alters monocyte-derived dendritic cell differentiation and maturation. American journal of physiology. Lung cellular and molecular physiology 2009, 297, L767-L776, doi:10.1152/ajplung.00107.2009.

54. Poole, J.A.; Romberger, D.J. Immunological and inflammatory responses to organic dust in agriculture. Curr Opin Allergy Clin Immunol 2012, 12, 126-132, doi:10.1097/ACI.0b013e3283511d0e.

55. Lange, J.H. Reduced cancer rates in agricultural workers: a benefit of environmental and occupational endotoxin exposure. Medical Hypotheses 2000, 55, 383-385, doi:https://doi.org/10.1054/mehy.2000.1072.

56. Peters, S.; Kromhout, H.; Olsson, A.C.; Wichmann, H.-E.; Brüske, I.; Consonni, D.; Landi, M.T.; Caporaso, N.; Siemiatycki, J.; Richiardi, L., et al. Occupational exposure to organic dust increases lung cancer risk in the general population. Thorax 2012, 67, 111-116, doi:10.1136/thoraxjnl-2011-200716.

57. Liebers, V.; Brüning, T.; Raulf-Heimsoth, M. Occupational endotoxin-exposure and possible health effects on humans (review). American Journal of Industrial Medicine 2006, 49, 474-491, doi:https://doi.org/10.1002/ajim.20310.

58. Mastrangelo, G.; Marzia, V.; Marcer, G. Reduced lung cancer mortality in dairy farmers: Is endotoxin exposure the key factor? American Journal of Industrial Medicine 1996, 30, 601-609, doi:10.1002/(SICI)1097-0274(199611)30:5<601::AID-AJIM8>3.0.CO;2-V.

59. Lange, J.H.; Rylander, R.; Fedeli, U.; Mastrangelo, G. Extension of the “hygiene hypothesis” to the association of occupational endotoxin exposure with lower lung cancer risk. Journal of allergy and clinical immunology 2003, 112, 219-220.

60. Liu, A.H. Endotoxin exposure in allergy and asthma: Reconciling a paradox. Journal of Allergy and Clinical Immunology 2002, 109, 379-392, doi:https://doi.org/10.1067/mai.2002.122157.

61. Okada, H.; Kuhn, C.; Feillet, H.; Bach, J.F. The 'hygiene hypothesis' for autoimmune and allergic diseases: an update. Clin Exp Immunol 2010, 160, 1-9, doi:10.1111/j.1365-2249.2010.04139.x.

62. Eduard, W.; Pearce, N.; Douwes, J. Chronic bronchitis, COPD, and lung function in farmers: the role of biological agents. Chest 2009, 136, 716-725, doi:10.1378/chest.08-2192.

63. Mastrangelo, G.; Grange, J.M.; Fadda, E.; Fedeli, U.; Buja, A.; Lange, J.H. Lung Cancer Risk: Effect of Dairy Farming and the Consequence of Removing that Occupational Exposure. American Journal of Epidemiology 2005, 161, 1037-1046, doi:10.1093/aje/kwi138.

64. Wong, G.W.; Chow, C.M. Childhood asthma epidemiology: insights from comparative studies of rural and urban populations. Pediatr Pulmonol 2008, 43, 107-116, doi:10.1002/ppul.20755.

65. Bakirci, N.; Kalaca, S.; Francis, H.; Fletcher, A.M.; Pickering, C.A.C.; Tumerdem, N.; Cali, S.; Oldham, L.; Niven, R. Natural history and risk factors of early respiratory responses to exposure to cotton dust in newly exposed workers. J Occup Environ Med 2007, 49, 853-861, doi:10.1097/jom.0b013e3180dca598.

66. Heederik, D.; Douwes, J. Towards an occupational exposure limit for endotoxins. Annals of Agricultural and Environmental Medicine 1997, 4.

67. Melkamu, T.; Qian, X.; Upadhyaya, P.; O'Sullivan, M.G.; Kassie, F. Lipopolysaccharide enhances mouse lung tumorigenesis: a model for inflammation-driven lung cancer. Vet Pathol 2013, 50, 895-902, doi:10.1177/0300985813476061.

68. Wang, X.; Lin, Y. Tumor necrosis factor and cancer, buddies or foes? Acta Pharmacol Sin 2008, 29, 1275-1288, doi:10.1111/j.1745-7254.2008.00889.x.

69. Torre, L.A.; Siegel, R.L.; Jemal, A. Lung Cancer Statistics. In Lung Cancer and Personalized Medicine: Current Knowledge and Therapies, Ahmad, A., Gadgeel, S., Eds. Springer International Publishing: Cham, 2016; 10.1007/978-3-319-24223-1_1pp. 1-19.

70. (CDC), C.f.D.C.a.P. An Update on Cancer Deaths in the United States. Availabe online: (accessed on

71. Hanahan, D.; Weinberg, R.A. The Hallmarks of Cancer. Cell 2000, 100, 57-70, doi:10.1016/S0092-8674(00)81683-9.

72. Hanahan, D.; Weinberg, Robert A. Hallmarks of Cancer: The Next Generation. Cell 2011, 144, 646-674, doi:10.1016/j.cell.2011.02.013.

73. Humans, I.W.G.o.t.E.o.C.R.t. Tobacco smoke and involuntary smoking. IARC Monogr Eval Carcinog Risks Hum 2004, 83, 1-1438.

74. Humans, I.W.G.o.t.E.o.C.R.t.; Organization, W.H.; Cancer, I.A.f.R.o. Smokeless tobacco and some tobacco-specific N-nitrosamines; World Health Organization: 2007; Vol. 89.

75. Konstantinou, E.; Fotopoulou, F.; Drosos, A.; Dimakopoulou, N.; Zagoriti, Z.; Niarchos, A.; Makrynioti, D.; Kouretas, D.; Farsalinos, K.; Lagoumintzis, G., et al. Tobacco-specific nitrosamines: A literature review. Food Chem Toxicol 2018, 118, 198-203, doi:10.1016/j.fct.2018.05.008.

76. Xue, J.; Yang, S.; Seng, S. Mechanisms of Cancer Induction by Tobacco-Specific NNK and NNN. Cancers (Basel) 2014, 6, 1138-1156, doi:10.3390/cancers6021138.

77. Vikis, H.G.; Rymaszewski, A.L.; Tichelaar, J.W. Mouse models of chemically-induced lung carcinogenesis. Front Biosci (Elite Ed) 2013, 5, 939-946.

78. Hecht, S.S.; Isaacs, S.; Trushin, N. Lung tumor induction in A/J mice by the tobacco smoke carcinogens 4-(methylnitrosamino)-l-(3-pyridyl)-l-butanone and benzo[a]pyrene: a potentially useful model for evaluation of chemopreventive agents. Carcinogenesis 1994, 15, 2721-2725, doi:10.1093/carcin/15.12.2721.

79. Hecht, S.S. Cigarette smoking and lung cancer: chemical mechanisms and approaches to prevention. The Lancet Oncology 2002, 3, 461-469, doi:https://doi.org/10.1016/S1470-2045(02)00815-X.

80. Hecht, S.S. Biochemistry, Biology, and Carcinogenicity of Tobacco-Specific N-Nitrosamines. Chemical Research in Toxicology 1998, 11, 559-603, doi:10.1021/tx980005y.

81. Hecht, S.S. Tobacco Smoke Carcinogens and Lung Cancer. JNCI: Journal of the National Cancer Institute 1999, 91, 1194-1210, doi:10.1093/jnci/91.14.1194.

82. Peterson, L.A.; Hecht, S.S. O6-methylguanine is a critical determinant of 4-(methylnitrosamino)-1-(3-pyridyl)-1-butanone tumorigenesis in A/J mouse lung. Cancer Res 1991, 51, 5557-5564.

83. Peterson, L.A.; Liu, X.-K.; Hecht, S.S. Pyridyloxobutyl DNA Adducts Inhibit the Repair of O⁶-Methylguanine. Cancer Research 1993, 53, 2780-2785.

84. Hecht, S.S. Tobacco carcinogens, their biomarkers and tobacco-induced cancer. Nat Rev Cancer 2003, 3, 733-744, doi:10.1038/nrc1190.

85. Hecht, S.S.; Morse, M.A.; Amin, S.; Stoner, G.D.; Jordan, K.G.; Choi, C.-I.; Chung, F.-L. Rapid single-dose model for lung tumor induction in A/J mice by 4-(methylnitrosainino)-1-(3-pyridyl)-1-butanone and the effect of diet. Carcinogenesis 1989, 10, 1901-1904, doi:10.1093/carcin/10.10.1901.

86. Ge, G.-Z.; Xu, T.-R.; Chen, C. Tobacco carcinogen NNK-induced lung cancer animal models and associated carcinogenic mechanisms. Acta Biochimica et Biophysica Sinica 2015, 47, 477-487, doi:10.1093/abbs/gmv041.

87. Castranova, V.; Rabovsky, J.; Tucker, J.H.; Miles, P.R. The alveolar type II epithelial cell: a multifunctional pneumocyte. Toxicol Appl Pharmacol 1988, 93, 472-483, doi:10.1016/0041-008x(88)90051-8.

88. Westcott, P.M.K.; To, M.D. The genetics and biology of KRAS in lung cancer. Chin J Cancer 2013, 32, 63-70, doi:10.5732/cjc.012.10098.

89. Yamakawa, K.; Yokohira, M.; Nakano, Y.; Kishi, S.; Kanie, S.; Imaida, K. Activation of MEK1/2-ERK1/2 signaling during NNK-induced lung carcinogenesis in female A/J mice. Cancer Med 2016, 5, 903-913, doi:10.1002/cam4.652.

90. Seyfried, T.N.; Huysentruyt, L.C. On the origin of cancer metastasis. Crit Rev Oncog 2013, 18, 43-73, doi:10.1615/critrevoncog.v18.i1-2.40.

91. Brabletz, T.; Kalluri, R.; Nieto, M.A.; Weinberg, R.A. EMT in cancer. Nature Reviews Cancer 2018, 18, 128-134, doi:10.1038/nrc.2017.118.

92. Loh, C.-Y.; Chai, J.Y.; Tang, T.F.; Wong, W.F.; Sethi, G.; Shanmugam, M.K.; Chong, P.P.; Looi, C.Y. The E-Cadherin and N-Cadherin Switch in Epithelial-to-Mesenchymal Transition: Signaling, Therapeutic Implications, and Challenges. Cells 2019, 8, 1118, doi:10.3390/cells8101118.

93. Barriere, G.; Fici, P.; Gallerani, G.; Fabbri, F.; Rigaud, M. Epithelial Mesenchymal Transition: a double-edged sword. Clin Transl Med 2015, 4, 14-14, doi:10.1186/s40169-015-0055-4.

94. Couffinhal, T.; Dufourcq, P.; Duplàa, C. β-Catenin Nuclear Activation. Circ Res 2006, 99, 1287-1289, doi:doi:10.1161/01.RES.0000253139.82251.31.

95. Derynck, R.; Akhurst, R.J.; Balmain, A. TGF-beta signaling in tumor suppression and cancer progression. Nat Genet 2001, 29, 117-129, doi:10.1038/ng1001-117.

96. Xu, J.; Lamouille, S.; Derynck, R. TGF-β-induced epithelial to mesenchymal transition. Cell research 2009, 19, 156-172.

97. Simopoulos, A.P. The importance of the ratio of omega-6/omega-3 essential fatty acids. Biomed Pharmacother 2002, 56, 365-379, doi:10.1016/s0753-3322(02)00253-6.

98. Dominguez, E.C.; Heires, A.J.; Pavlik, J.; Larsen, T.D.; Guardado, S.; Sisson, J.H.; Baack, M.L.; Romberger, D.J.; Nordgren, T.M. A High Docosahexaenoic Acid Diet Alters the Lung Inflammatory Response to Acute Dust Exposure. Nutrients 2020, 12, 2334.

99. Nordgren, T.M.; Friemel, T.D.; Heires, A.J.; Poole, J.A.; Wyatt, T.A.; Romberger, D.J. The Omega-3 Fatty Acid Docosahexaenoic Acid Attenuates Organic Dust-Induced Airway Inflammation. Nutrients 2014, 6, 5434-5452.

100. Simopoulos, A.P. The importance of the omega-6/omega-3 fatty acid ratio in cardiovascular disease and other chronic diseases. Exp Biol Med (Maywood) 2008, 233, 674-688, doi:10.3181/0711-mr-311.

101. Dyall, S.C. Long-chain omega-3 fatty acids and the brain: a review of the independent and shared effects of EPA, DPA and DHA. Front Aging Neurosci 2015, 7, 52-52, doi:10.3389/fnagi.2015.00052.

102. Hayashi, D.; Mouchlis, V.D.; Dennis, E.A. Omega-3 versus Omega-6 fatty acid availability is controlled by hydrophobic site geometries of phospholipase A(2)s. J Lipid Res 2021, 62, 100113-100113, doi:10.1016/j.jlr.2021.100113.

103. Giudetti, A.M.; Cagnazzo, R. Beneficial effects of n-3 PUFA on chronic airway inflammatory diseases. Prostaglandins Other Lipid Mediat 2012, 99, 57-67, doi:10.1016/j.prostaglandins.2012.09.006.

104. Crooks, S.W.; Stockley, R.A. Leukotriene B4. The International Journal of Biochemistry & Cell Biology 1998, 30, 173-178, doi:https://doi.org/10.1016/S1357-2725(97)00123-4.

105. Buckley, C.D.; Gilroy, D.W.; Serhan, C.N. Proresolving lipid mediators and mechanisms in the resolution of acute inflammation. Immunity 2014, 40, 315-327, doi:10.1016/j.immuni.2014.02.009.

106. Strokin, M.; Sergeeva, M.; Reiser, G. Role of Ca2+-independent phospholipase A2 and n−3 polyunsaturated fatty acid docosahexaenoic acid in prostanoid production in brain: perspectives for protection in neuroinflammation. International Journal of Developmental Neuroscience 2004, 22, 551-557, doi:https://doi.org/10.1016/j.ijdevneu.2004.07.002.

107. Strokin, M.; Sergeeva, M.; Reiser, G. Docosahexaenoic acid and arachidonic acid release in rat brain astrocytes is mediated by two separate isoforms of phospholipase A2 and is differently regulated by cyclic AMP and Ca2+. Br J Pharmacol 2003, 139, 1014-1022, doi:10.1038/sj.bjp.0705326.

108. Haworth, O.; Levy, B.D. Lipoxins, resolvins and protectins: new leads for the treatment of asthma. Expert Opinion on Drug Discovery 2008, 3, 1209-1222, doi:10.1517/17460441.3.10.1209.

109. Levy, B. Resolvin D1 and Resolvin E1 Promote the Resolution of Allergic Airway Inflammation via Shared and Distinct Molecular Counter-Regulatory Pathways. Front Immunol 2012, 3, doi:10.3389/fimmu.2012.00390.

110. Serhan, C.N.; Petasis, N.A. Resolvins and protectins in inflammation resolution. Chemical reviews 2011, 111, 5922-5943.

111. Ramirez, H.; Patel, S.B.; Pastar, I. The role of TGFβ signaling in wound epithelialization. Advances in wound care 2014, 3, 482-491.

112. Fadok, V.A.; Bratton, D.L.; Konowal, A.; Freed, P.W.; Westcott, J.Y.; Henson, P.M. Macrophages that have ingested apoptotic cells in vitro inhibit proinflammatory cytokine production through autocrine/paracrine mechanisms involving TGF-beta, PGE2, and PAF. J Clin Invest 1998, 101, 890-898.

113. Nordgren, T.M.; Heires, A.J.; Bailey, K.L.; Katafiasz, D.M.; Toews, M.L.; Wichman, C.S.; Romberger, D.J. Docosahexaenoic acid enhances amphiregulin-mediated bronchial epithelial cell repair processes following organic dust exposure. Am J Physiol Lung Cell Mol Physiol 2018, 314, L421-l431, doi:10.1152/ajplung.00273.2017.

114. Ulu, A.; Burr, A.; Heires, A.J.; Pavlik, J.; Larsen, T.; Perez, P.A.; Bravo, C.; DiPatrizio, N.V.; Baack, M.; Romberger, D.J., et al. A high docosahexaenoic acid diet alters lung inflammation and recovery following repetitive exposure to aqueous organic dust extracts. The Journal of Nutritional Biochemistry 2021, 97, 108797, doi:https://doi.org/10.1016/j.jnutbio.2021.108797.

115. Mernitz, H.; Lian, F.; Smith, D.E.; Meydani, S.N.; Wang, X.-D. Fish Oil Supplementation Inhibits NNK-Induced Lung Carcinogenesis in the A/J Mouse. Nutrition and Cancer 2009, 61, 663-669, doi:10.1080/01635580902825589.

116. Hsiao, H.-M.; Sapinoro, R.E.; Thatcher, T.H.; Croasdell, A.; Levy, E.P.; Fulton, R.A.; Olsen, K.C.; Pollock, S.J.; Serhan, C.N.; Phipps, R.P., et al. A novel anti-inflammatory and pro-resolving role for resolvin D1 in acute cigarette smoke-induced lung inflammation. PLoS One 2013, 8, e58258-e58258, doi:10.1371/journal.pone.0058258.

117. Hsiao, H.-M.; Thatcher, T.H.; Colas, R.A.; Serhan, C.N.; Phipps, R.P.; Sime, P.J. Resolvin D1 Reduces Emphysema and Chronic Inflammation. The American journal of pathology 2015, 185, 3189-3201, doi:10.1016/j.ajpath.2015.08.008.

118. Serhan, C.N.; Hong, S.; Gronert, K.; Colgan, S.P.; Devchand, P.R.; Mirick, G.; Moussignac, R.-L. Resolvins : A Family of Bioactive Products of Omega-3 Fatty Acid Transformation Circuits Initiated by Aspirin Treatment that Counter Proinflammation Signals. Journal of Experimental Medicine 2002, 196, 1025-1037, doi:10.1084/jem.20020760.

119. Sun, Y.-P.; Oh, S.F.; Uddin, J.; Yang, R.; Gotlinger, K.; Campbell, E.; Colgan, S.P.; Petasis, N.A.; Serhan, C.N. Resolvin D1 and its aspirin-triggered 17R epimer

stereochemical assignments, anti-inflammatory properties, and enzymatic inactivation. Journal of Biological Chemistry 2007, 282, 9323-9334.

120. Rogerio, A.P.; Haworth, O.; Croze, R.; Oh, S.F.; Uddin, M.; Carlo, T.; Pfeffer, M.A.; Priluck, R.; Serhan, C.N.; Levy, B.D. Resolvin D1 and aspirin-triggered resolvin D1 promote resolution of allergic airways responses. Journal of immunology (Baltimore, Md. : 1950) 2012, 189, 1983-1991, doi:10.4049/jimmunol.1101665.

121. Lee, H.J.; Park, M.K.; Lee, E.J.; Lee, C.H. Resolvin D1 inhibits TGF-β1-induced epithelial mesenchymal transition of A549 lung cancer cells via lipoxin A4 receptor/formyl peptide receptor 2 and GPR32. Int J Biochem Cell Biol 2013, 45, 2801-2807, doi:10.1016/j.biocel.2013.09.018.

122. Liu, Y.; Yuan, X.; Li, W.; Cao, Q.; Shu, Y. Aspirin-triggered resolvin D1 inhibits TGF-β1-induced EMT through the inhibition of the mTOR pathway by reducing the expression of PKM2 and is closely linked to oxidative stress. International journal of molecular medicine 2016, 38, 1235-1242.

123. Nordgren, T.M.; Bauer, C.D.; Heires, A.J.; Poole, J.A.; Wyatt, T.A.; West, W.W.; Romberger, D.J. Maresin-1 reduces airway inflammation associated with acute and repetitive exposures to organic dust. Translational Research 2015, 166, 57-69, doi:https://doi.org/10.1016/j.trsl.2015.01.001.

124. Nordgren, T.M.; Heires, A.J.; Wyatt, T.A.; Poole, J.A.; LeVan, T.D.; Cerutis, D.R.; Romberger, D.J. Maresin-1 reduces the pro-inflammatory response of bronchial epithelial cells to organic dust. Respir Res 2013, 14, 51, doi:10.1186/1465-9921-14-51.

125. Wang, Y.; Li, R.; Chen, L.; Tan, W.; Sun, Z.; Xia, H.; Li, B.; Yu, Y.; Gong, J.; Tang, M., et al. Maresin 1 Inhibits Epithelial-to-Mesenchymal Transition in Vitro and Attenuates Bleomycin Induced Lung Fibrosis in Vivo. Shock 2015, 44, 496-502, doi:10.1097/shk.0000000000000446.

Chapter 1

A High Docosahexaenoic Acid Diet Alters the Lung Inflammatory Response to Acute Dust Exposure

Edward C. Dominguez, Art J. Heires, Jacqueline Pavlik, Tricia D. Larsen, Stephanie Guardado, Joseph H. Sisson, Michelle L. Baack, Debra J. Romberger, and Tara M. Nordgren

Nutrients 2020, 12(8), 2334; https://doi.org/10.3390/nu12082334

Abstract: Agricultural workers are at risk for the development of acute and chronic lung diseases due to their exposure to organic agricultural dusts. A diet intervention using the omega-3 fatty acid docosahexaenoic acid (DHA) has been shown to be an effective therapeutic approach for alleviating a dust-induced inflammatory response. We thus hypothesized a high-DHA diet would alter the dust-induced inflammatory response through the increased production of specialized pro-resolving mediators (SPMs). Mice were pre-treated with a DHA-rich diet 4 weeks before being intranasally challenged with a single dose of an extract made from dust collected from a concentrated swine feeding operation (HDE). This omega-3-fatty-acid-rich diet led to reduced arachidonic acid levels in the blood, enhanced macrophage recruitment, and increased the production of the DHA-derived SPM Resolvin D1 (RvD1) in the lung following HDE exposure. An assessment of transcript-level changes in the immune response demonstrated significant differences in immune pathway activation and alterations of numerous macrophage-associated genes among HDE-challenged mice fed a high DHA diet. Our data indicate that consuming a DHA-rich diet leads to the enhanced production of SPMs during an acute inflammatory challenge to dust, supporting a role for dietary DHA supplementation as a potential therapeutic strategy for reducing dust-induced lung inflammation.

1. Introduction

Exposure to agricultural organic dusts can lead to the development of acute and chronic lung diseases including asthma, bronchitis, and chronic obstructive pulmonary disease (COPD) in exposed individuals [1,2,3,4]. Agricultural workers regularly exposed to these environmental pollutants are at increased risk of developing respiratory diseases [5,6,7,8]. Organic dusts from animal confinement facilities have previously been reported to contain a large variety of bacterial components, proteases, and particulates that induce a pro-inflammatory response following exposure [9,10,11]. Specifically, acute dust exposure from swine confinement facilities has been shown to stimulate the release of pro-inflammatory cytokines such as TNF-α and IL-6 [11,12]. There are several well-established preventative approaches to help minimize the exposure risk for these individuals, including the use of respirators or ventilator masks. Unfortunately, compliance with the prescribed use of personal protective equipment is not routinely followed by the farming community [13,14].

A multitude of proteins, mediators, and biological processes aid in the resolution of the inflammatory process, including the metabolism of omega-3 polyunsaturated fatty acids (omega-3 PUFAs) into specialized pro-resolving mediators (SPMs) [15,16]. Research has shown that a traditional Western diet is comprised of about 15:1 omega-6 to omega-3 fatty acids as opposed to the ideal 1:1 ratio [17]. Both omega-3 and omega-6 PUFAs are metabolized by the same enzymes to form bioactive lipids that are primarily SPMs or pro-inflammatory lipid mediators, respectively [18,19,20,21,22]. The omega-3

PUFA docosahexaenoic acid (DHA) is metabolized by lipoxygenase, cyclooxygenase, and epoxygenase enzymes into various SPMs, such as resolvins and maresins, which reduce inflammation in the lung [19,23,24,25,26]. During the inflammatory process, these SPMs function as anti-inflammatory and pro-resolving mediators by regulating various processes including neutrophil and macrophage influx into the lung, and promoting tissue repair and immunity [27,28]. Our previous investigations have examined the effectiveness of short-term 7-day DHA supplementation in altering the lung inflammatory response to organic dust exposure, where we identified DHA-mediated reductions in the lung inflammatory response and specific alterations to the airway epithelium following acute exposure to extracts of organic agricultural dusts collected from hog confinement facilities (HDE) [29]. No significant alterations in the DHA-derived SPM resolvin D1 (RvD1) were found upon the lavage of DHA-supplemented mice. To build on this study, we sought to test whether increasing the duration of dietary DHA treatment would lead to alterations in endogenous SPM production during an acute inflammatory challenge with environmental dust. Specifically, we tested whether a 4-week DHA-supplemented diet regimen prior to exposing mice to agricultural dust collected from a hog confinement facility would promote the enhanced production of SPM and an altered inflammatory response of dust-induced inflammation. To do so, we used a well-established mouse model using HDE to induce acute lung inflammation [10,30,31,32]. Following exposure, we assessed the lung's immune response to dust exposure, including the NanoString gene expression profiling of 561 genes related to the immune response, in addition to assessing alterations in SPM production in DHA-diet-

versus control (no DHA)-diet-fed mice. Overall, our findings demonstrate that a high DHA diet can enhance the biosynthesis of SPM during acute lung inflammation caused by organic dust exposure and alter the transcript-level gene expression changes of pro-/anti-inflammatory genes.

2. Materials and Methods

2.1. Reagents

Murine tumor necrosis factor-α (TNF-α), interleukin-6 (IL-6), chemokine C-X-C motif ligand 1 (CXCL1), amphiregulin (AREG), granulocyte-macrophage colony-stimulating factor (GM-CSF), myeloperoxidase (MPO), monocyte chemoattractant protein-1 (MCP-1), and macrophage migration inhibitory factor (MIF), Duoset ELISA kits were purchased from R&D Systems (Minneapolis, MN, USA). RvD1 and RvD2 murine ELISA kits were purchased from Cayman Chemicals (Ann Arbor, MI, USA). DHA and standard mouse chow diets were prepared by Envigo (Madison, WI, USA) as previously described [30].

2.2. Preparation of Organic Dust Extract

Organic agricultural dusts collected from hog confinement facilities were prepared into extracts (HDE) as previously described [30]. In short, settled dusts from swine confinement facilities were collected from surfaces 1 m above the ground and suspended in Hank's Balanced Salt Solution at a 100 mg/mL concentration. The mixture was centrifuged and filtered at 0.22 μm to form the 100% HDE extract, which was stored at −20 °C for future use and later diluted to a 12.5% HDE (vol/vol) concentration for animal studies, using sterile phosphate-buffered saline (PBS). The characterization of the bacterial components in the dust has been previously documented [9].

2.3. Animal Care

Male wildtype C57BL/6J mice at 5–8 weeks of age were obtained from The Jackson Laboratory (Bar Harbor, ME, USA) and housed in the University of Nebraska Medical Center (UNMC) Comparative Medicine Facilities. The mice were allowed free access to food and water and housed in micro-isolator cages (five per cage). The food was changed weekly by the investigators, while the water was changed by UNMC animal care staff. Each mouse was weighed weekly (see Figure S1 for initial and final weights) and examined for any signs of distress. All related experiments and procedures were approved by the UNMC Institutional Animal Care and Use Committee.

2.4. In Vivo Model of Dust Exposure

We employed a previously established murine model that utilizes an intranasal exposure to HDE to induce airway inflammation for our in vivo investigations [30,31]. The studies were performed as 3 independent experimental sets, for total of 8 mice for the saline-treated groups and 12 mice for the HDE-treated groups. The mice were lightly anesthetized by isoflurane inhalation prior to receiving a single intranasal challenge of 50 μL of sterile saline (PBS) or 12.5% HDE. Four weeks prior to receiving the intranasal instillation, the mice were initiated on either a DHA-rich diet or control diet containing no DHA. The animal chow diets were prepared by Envigo (Madison, WI, USA) using a base AIN-93G diet. The DHA diet preparation was the same as that previously described [30,33]. Briefly, to prepare the DHA-rich diet, soybean oil from the AIN-93G base diet was replaced with DHASCO oil (DSM Nutritional Products, Kingstree, SC, USA), a

DHA-based oil containing 39.2% DHA and high-oleic safflower oil. The control diet, containing no DHA, modified the same AIN-93G diet by replacing soybean oil with high-oleic safflower oil. The newly formulated DHA-rich diet provides the mice with approximately 1.4% of their total caloric intake strictly from DHA. Five hours following the single HDE intranasal challenge, the mice were euthanized. Blood was collected, bronchoalveolar lavage fluid (BALF) retrieval was performed using three 1 mL washes with sterile PBS, and the left lungs were collected and stored in RNAlater (Thermo Fisher, Waltham, MA, USA). BALF from the first lavage was stored and used to measure cytokine and chemokine levels by ELISA. Total cell counts from the BALF were obtained, and differential cell counts were determined microscopically on cytocentrifuge slides (Cytopro, ELITechGroup, Logan, UT, USA), which were stained using DiffQuick (Siemens, Newark, DE, USA).

2.5. Neutrophil Extracellular Trap (NET) Scoring

Cytospins were prepared from the BALF of each mouse following the administration of the diets and exposures. The neutrophil extracellular trap (NET) scoring of the BALF cytospins stained with the Diffquick Hema 3 Stat Pack (Fisherbrand, Pittsburg, PA) was performed as previously described [34]. In short, the entire periphery of each cytospin was divided into twenty-seven regions as this is where NETs are concentrated, and each region was assigned a NET score of 0 (no NETs), 1 (rare NETs), 2 (moderate NETs), or 3 (widely distributed NETs). All 40 cytospins from the mice used across the three separate experiments were assessed for NETs.

2.6. Analysis of Cytokines and Chemokines

Cytokine and chemokine levels were measured from the cell-free BALF of the first PBS wash using murine-specific ELISAs. We examined the levels of TNF-α, IL-6, CXCL1, AREG, GM-CSF, MPO, MCP-1, and MIF using commercially available kits (Duoset ELISA development kits, R&D Systems) as well as RvD1 and RvD2 (Cayman Chemical) according to the manufacturer's instructions.

2.7. Fatty Acid Blood Levels

Whole blood was collected from the axillary artery and placed in BD Microtainer Tubes (Becton Dickinson, Franklin Lakes, NJK). Fatty acid analysis was performed by direct transesterification using 14% boron-trifluoride methanol and hexane solution with an internal standard (17:0 heptadecanoic acid) at 100 °C for 60 min. After cooling, HPLC-grade water was added and the sample was vortexed and centrifuged for phase separation. Fatty acid methyl-esters in the hexane phase were analyzed by capillary gas chromatography (GC) on an Agilent 7890A GC (Agilent Technologies, Santa Clara, CA, USA) equipped with an Agilent CP7489 Capillary Column (100 m length × 0.25 mm internal diameter × 0.36 mm outer diameter, 0.20 μm film thickness). Hydrogen was the carrier gas. Fatty acids of carbon length 10 to 24 were detected with a flame ionization detector and recorded using the ChemStation interface system (Agilent Technologies, Santa Clara, CA, USA). Peaks were identified using the Open LAB Chromatography Data System and corresponding authentic standard, 37 FAME mix (Sigma Aldrich, St. Louis, MO, USA). The whole blood composition (wt/wt% of the sample) is reported for

individual FAs. The individuals performing the analyses were blinded to the study groups.

2.8. NanoString Gene Expression

Randomly selected left lung tissues (n = 24) out of the possible 40 mice, representing tissues collected across three unique experimental trials, were homogenized and RNA was extracted using the PureLink RNA Mini Kit (Invitrogen, Carlsbad, California, USA). RNA sample quality was quantified using the NanoDrop ND-100 (NanoDrop Technologies, Inc, Wilmington, DE, USA) and an Agilent 2100 Bioanalyzer (UC Riverside Core Facilities, Agilent Technologies, Santa Clara, CA, USA). The assessment of transcript-level gene expression changes was performed using the NanoString mouse Immunology Panel (NanoString Technologies, Seattle, WA, USA), a codeset designed to target 561 genes related to inflammation and the immune response. Fifty to one hundred nanograms of total RNA was mixed with the codeset and reporter probes and hybridized for 16 h to form a purified target–probe complex that was then imaged and quantified with a nCounter Sprint profiler. Gene expression data analysis was performed using the nCounter Analysis System, nSolver 4.0 software. The expression data were normalized by using the geometric mean of 4 housekeeping genes: OAZ1, PPIA, RPL19, and EEF1G. Following normalization, 20 of the samples passed normalization and were viable to use for the subsequent analyses, including 4 control diet + saline, 6 control diet + HDE, 3 DHA diet + saline, and 7 DHA + HDE samples. Raw and normalized NanoString data are deposited at

https://www.ncbi.nlm.nih.gov/geo/query/acc.cgi?acc=GSE155539. Following initial gene expression analysis, the STRING database was used to evaluate protein–protein interactions amongst high- or low-expressing genes.

2.9. Statistical Analyses

Statistical analysis and graphing were performed using the Prism Software by GraphPad (San Diego, CA, USA). All reported data are presented as the mean ± standard error. Statistical calculations were performed using two-way ANOVA with Tukey's post hoc test for multiple comparisons within the groups, and significance was set at $p \leq 0.05$. For graphical presentation, the # symbol is used to indicate significant differences in post hoc comparisons between the DHA and control diet groups. The * symbol is used to indicate significant differences in the post hoc comparisons between saline- and HDE-treated mice within diet groups. The + symbol is used to indicate significant interactions between diet and treatment groups.

Sample quality control for the NanoString gene expression dataset was performed manually by eliminating probes with fewer than 82 counts from the data set. This was executed by performing a background subtraction (mean +/− two standard deviations of negative controls) to more efficiently differentiate between biological or technical variation amongst the samples. Raw p-values from the differential expression analyses were used to assess gene expression data. All heat maps and data cluster sets were produced using the nCounter Analysis and Advanced Analysis packages in nSolver 4.0 (NanoString Technologies, Seattle, WA, USA).

3. Results

3.1. A High-DHA Diet Alters Blood Omega-3 and Omega-6 PUFA Levels

Following euthanasia at 5 h post-HDE challenge, whole blood was isolated and used to assess the levels of various medium- and long-chain fatty acids (C10–24). Mice that were given a high-DHA diet showed significantly increased levels of the omega-3 PUFAs DHA (Figure 1A, $p < 0.0001$), eicosapentaenoic acid (EPA; Figure 1B, $p = 0.006$), and docosapentaenoic acid (DPA; Figure 1C, $p = 0.0009$). Conversely, DHA-diet-fed mice exhibited significantly decreased levels of the omega-6 PUFA arachidonic acid (ARA; Figure 1E, $p < 0.0001$). There was no significant main effect for either the omega-3 PUFA alpha linolenic acid (ALA; Figure 1D, $p = 0.067$) or omega-6 PUFA linoleic acid (LA; Figure 1F, $p = 0.076$), as both slightly missed significance. There was, however, a significant difference in the LA levels for the control-diet- versus DHA-diet-fed mice challenged with HDE (LA; Figure 1F).

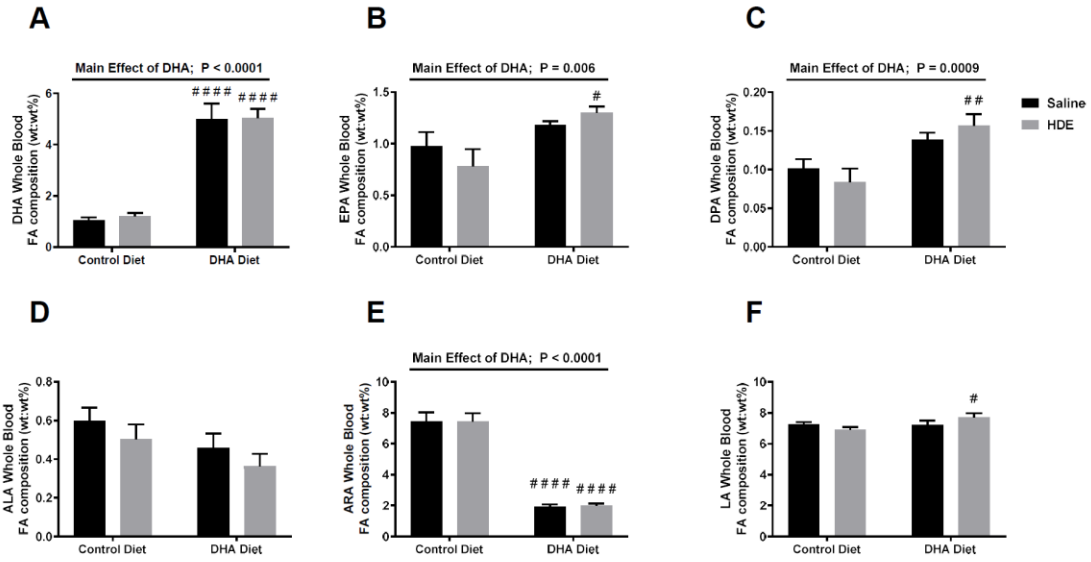

Figure 1. Fatty acid blood levels collected from the docosahexaenoic acid (DHA)- and control-diet-fed mice 5 h after the instillation of HDE or saline. Fatty acid blood levels of n-3 PUFA DHA (A), eicosapentaenoic acid (EPA) (B), docosapentaenoic acid (DPA) (C), alpha-linolenic acid (ALA) (D) and n-6 PUFA arachidonic acid (ARA) (E) and linoleic acid (LA) (F), measured in mice following administration of a diet and exposure. Significance for the main effect of the DHA diet is shown with the p-values and significance bars on top of the DHA, EPA, DPA, and ARA graphs. Tukey post hoc comparisons between the DHA- and control-diet-treated conditions are annotated with the # symbol. (# $p < 0.05$; ## $p < 0.01$; #### $p < 0.0001$).

The sums of the omega-6 PUFAs (ARA and LA) and omega-3 PUFAs (EPA, DPA, DHA, and ALA) were calculated to identify the ratio of omega-6 to omega-3 PUFAs for the mice that were fed a control diet compared to the DHA diet, as shown in Table 1. Mice fed a DHA-rich diet had an approximately 2.3:1 ratio of omega-6 PUFAs (ARA and LA) to omega-3 PUFA (EPA, DPA, DHA, and ALA), compared to those fed a control diet, which had an approximately 6.8:1 ratio.

Table 1. Mean ratio of omega-6 polyunsaturated fatty acids (PUFAs) to omega-3 PUFAs in blood of mice fed a high-DHA diet or control (no DHA) diet for 4 weeks and challenged with saline or HDE.

Experimental Group	Omega-6 PUFA/Omega-3 PUFA Ratio (95% CI)	*p*-Value*
Control Diet, Saline	6.20: 1 (3.58:1–8.82:1)	--
Control Diet, HDE	7.38:1 (4.91:1–9.85:1)	0.79
DHA Diet, Saline	2.34:1 (1.15:1–3.52:1)	0.039
DHA Diet, HDE	2.36:1 (1.40:1–3.31:1)	0.021

CI: Confidence interval; * p-values based on 2-way ANOVA with Tukey's multiple comparisons post hoc analysis. Main effect of diet, $p < 0.0001$.

3.2. A High-DHA Diet Impacts Overall Lung Cellular Influx in Mice Following Acute HDE Exposure

In our 7-day DHA oral gavage study, we reported that an acute (single) HDE challenge elicited a potent lung inflammatory response [29]. Additionally, we identified that a 7-day daily-gavage DHA pre-treatment prior to acute HDE challenge was effective in reducing the inflammatory effects of HDE [29,30]. To build on these initial findings, we opted to administer a DHA-rich diet to C57BL/6J mice 4 weeks prior to a single 50 µL intranasal challenge of 12.5% HDE to determine if a dietary intervention was similarly effective in reducing overall acute HDE-induced inflammation. Through these investigations, we identified that HDE exposure as a main effect was associated with significant increases in total BALF cellularity (Figure 2A), corresponding with significant increases in neutrophils (Figure 2C) and lymphocytes (Figure 2D).

Of interest, we identified that HDE-exposed mice that were fed a DHA-rich diet displayed changes in the types of cells recruited; in DHA diet-fed mice, we identified a significant elevation of BALF macrophages following HDE exposure (Figure 2B) that was not evident in the control-diet-fed mice. Furthermore, we identified that neutrophil

influx was decreased in DHA-diet-fed HDE-challenged mice compared to in control-diet-fed mice given HDE, although this missed statistical significance ($p = 0.070$; Figure 2C). We also identified a significant interaction (Figure 2B; $p = 0.021$) between diet and dust exposure for macrophage recruitment into the lung.

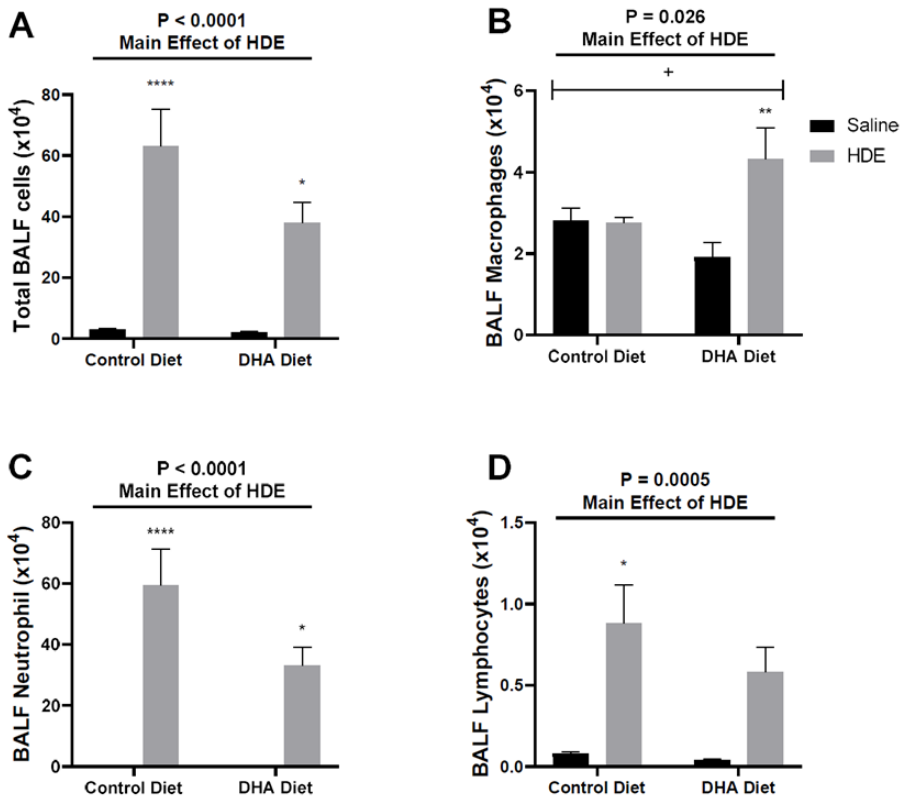

Figure 2. Effects of a high-DHA diet on total and immune cell lung influx after HDE instillation. Control- or DHA-diet-fed mice were challenged with a single intranasal HDE exposure. Five hours following exposure, bronchoalveolar lavage fluid (BALF) was collected and assessed for cellular influx including total BALF cells (A), BALF macrophages (B), BALF neutrophils (C), and BALF lymphocytes (D). The main effects of HDE vs. saline are indicated by the top lines with corresponding p-values. The * symbol above the HDE bars represents the statistical significance of the difference between the HDE- and saline-treated conditions within the same diet group (* $p < 0.05$; ** $p < 0.01$; **** $p < 0.0001$). Significant interactions between diet and exposure are depicted by the + symbol (+ $p < 0.05$).

3.3. A DHA-Rich Diet Alters HDE-Induced Changes in Pro-Inflammatory Cytokine/Chemokine Release

Acute HDE exposure leads to the production of pro-inflammatory cytokines and chemokines [12,29,30,35]. In our current investigation, we identified that acute HDE exposure led to increased levels of TNF-α, IL-6, CXCL1, AREG, GM-CSF, MPO, and MCP-1 (Figure 3) within the BALF, when compared to saline treatment. Mice that were administered a DHA-rich diet and exposed to HDE had significantly decreased levels of BALF AREG (Figure 3D, $p = 0.017$) and increased MPO levels (Figure 3F, $p = 0.016$) compared to HDE-instilled mice fed the control diet. There was also a significant interaction (Figure 3D; $p = 0.021$) between diet and dust exposure for AREG levels, with MPO missing significance (Figure 3F, $p = 0.057$) for this interaction. When assessing NET formation, we identified a significant major effect of HDE exposure on NET formation (Figure 3I) that was not impacted by diet.

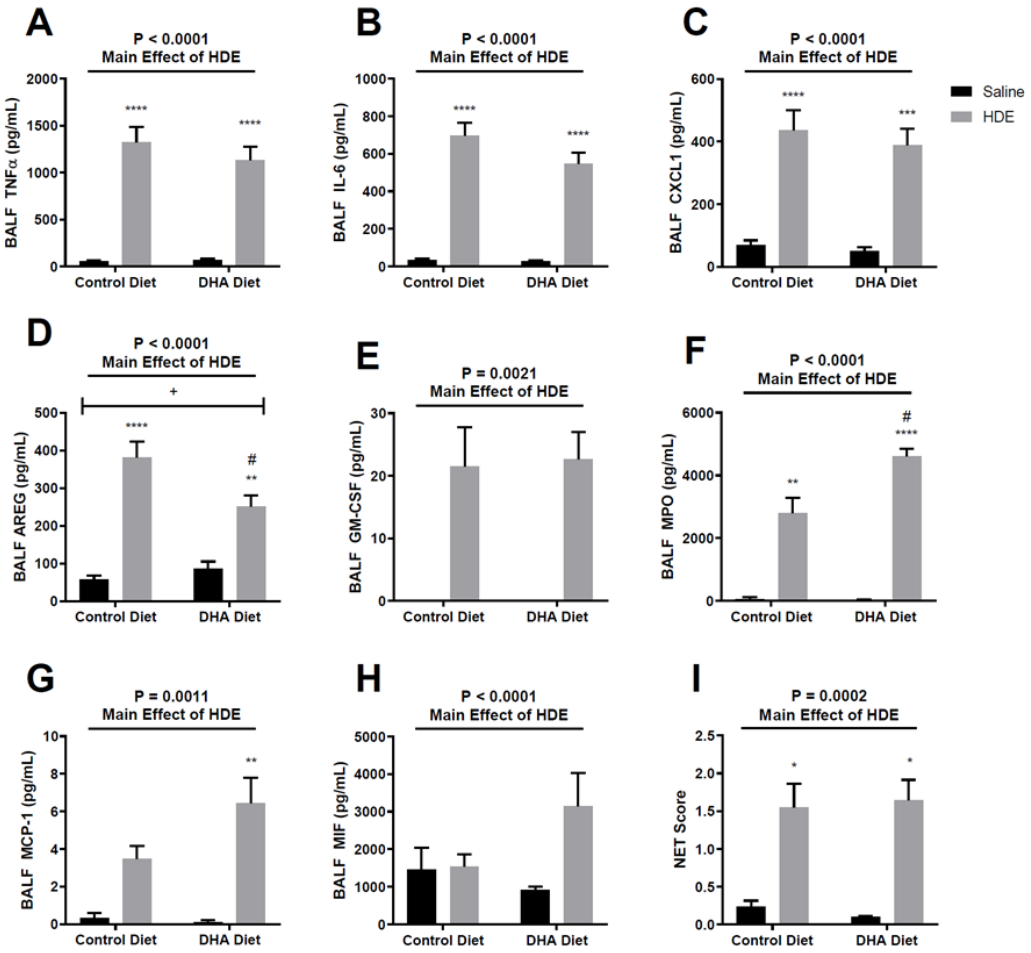

Figure 3. Effects of a DHA-rich diet on inflammatory mediator release and neutrophil extracellular trap (NET) formation following acute exposure to HDE. (A–H) BALF was collected from mice and screened for various cytokines and chemokines via ELISAs. (I) NET formation was assessed by scoring the BALF cytospins across all three experimental trials. The top line represents the main effect of HDE vs. saline with significance represented by p-values. Tukey post hoc comparisons are provided for DHA- vs. control-diet-treated conditions and are annotated by the # symbol (# $p < 0.05$). Significant differences between HDE- and saline-treated conditions within diet groups are represented by the * symbol above the HDE bars (* $p < 0.05$; ** $p < 0.01$; *** $p < 0.001$; **** $p < 0.0001$). Any significant interactions between diet and exposure are depicted by the + symbol (+ $p < 0.05$).

3.4. A High-DHA Diet Is Associated with Increased Production of Resolvin D1

To assess the impact of a longer-term DHA-rich diet on endogenous SPM production, we analyzed the BALF levels of DHA-derived resolvin D1 (RvD1) and Resolvin D2 (RvD2). DHA had an overall significant major effect on RvD1 production (Figure 4A), while RvD2 production slightly missed significance (Figure 4B). Here, DHA-diet-fed mice challenged with HDE exhibited significantly increased levels of the DHA-derived SPM RvD1 (Figure 4A, $p = 0.011$) in the BALF when compared to the control-diet-fed mice, with RvD2 levels also trending upward in the DHA-diet-fed mice but failing to reach significance (Figure 4B). Of note, RvD1 levels in DHA-diet-fed mice that were administered a saline intranasal challenge were also higher than those in control-diet-fed mice (Figure 4A, $p = 0.027$).

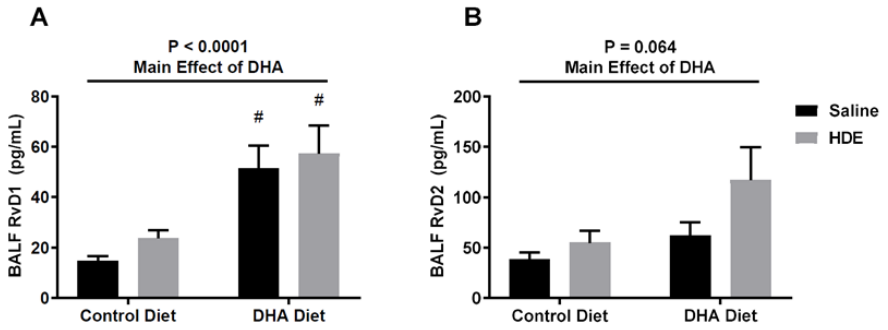

Figure 4. A high-DHA diet increases the production of Resolvin D1 in the lung following a single intranasal challenge with HDE. BALF levels of the specialized pro-resolving mediators (SPMs) Resolvin D1 (RvD1) (A) and Resolvin D2 (RvD2) (B) were assessed via ELISA following euthanasia. The main significance bars and p-values on the top represent the main effects of DHA on SPM production. Tukey post hoc comparisons for significant differences between the DHA- and control-diet-treated conditions are depicted by the # symbol (# $p < 0.05$).

3.5. In Vivo Gene Expression Changes in DHA-Diet-Fed Mice Following Exposure to HDE

To assess the transcript-level gene expression changes in the lungs of HDE-challenged mice fed a DHA-rich diet, a NanoString Mouse Immunology gene expression panel was used. Two separate advanced analyses were performed, one assessing the full 20-sample data set, and the other analysis assessing the 13 DHA vs. control-diet samples with exposure to HDE. All 20 NanoString samples were selected at random (see Materials and Methods), with 13 of them being HDE-exposed and seven, saline-exposed. Of the 13 HDE samples, six were control-diet-fed and seven were DHA-diet-fed. The full 20-sample data set showed expression changes for both the DHA diet and dust exposure, compared to the controls. After sample normalization, we performed the principal component analysis (PCA) of all 20 samples, which showed a clear clustering of exposure groups (Figure 5A). Corresponding with the PCA, the differential expression for the HDE vs. saline samples provided the greatest number of significantly altered genes of all the analysis sets (Figure 5B)

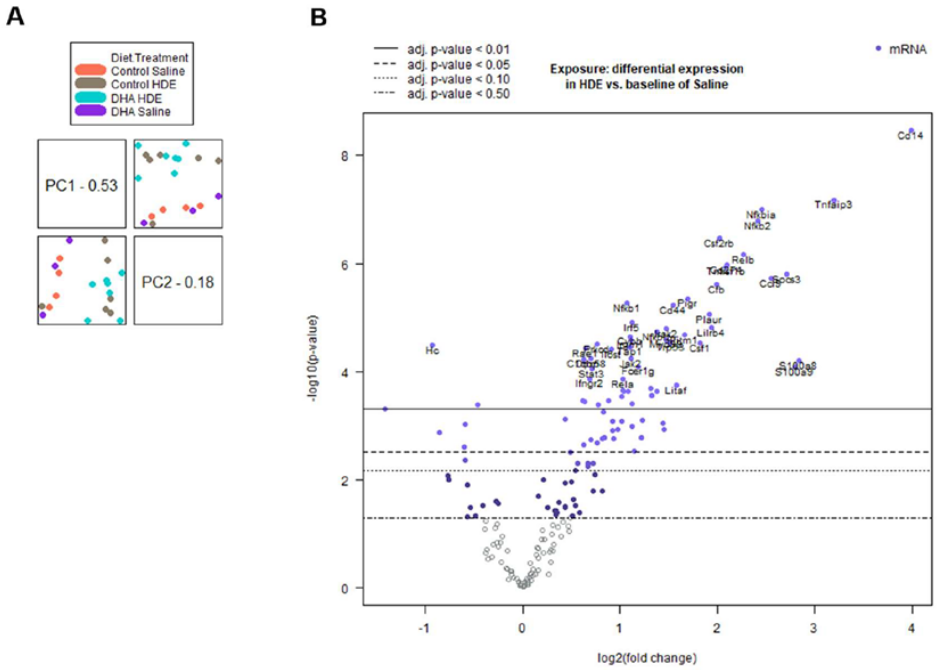

Figure 5. Principal component analysis and volcano plot of all 20 normalized samples. (A) Principal component analysis (PCA) and PCA scores displaying an overall strong clustering of related biological sample replicates for all 20 samples. (B) Volcano plot of expressed genes for the interaction between HDE and saline exposure among all 20 samples. p-value for volcano plot displayed as adjusted p-value.

The numbers of statistically significant ($p \leq 0.05$) genes that were differentially regulated of the 561 possible genes expressed are summarized in Table 2. As mentioned in the methods, genes below the 82-count threshold were removed from the analyses.

Table 2. Breakdown of differential expression for statistically significant genes from each experimental group.

Experimental Group	Number of Samples per Group	Differentially Regulated Genes		Total Number of Differentially Regulated Genes
		Up	*Down*	
DHA vs. Control Diet	20	3	3	6
HDE vs. Saline	20	94	16	110
DHA vs. Control Diet Exposed to HDE	13	6	1	7

Among the 20 DHA vs. control diet samples, *ITGAX*, *PIGR*, and *TGFBI* were significantly up-regulated, while *CXCL12*, *ITGA6*, and *STAT5B* were down-regulated (Figure 6A). Of the 110 significantly altered genes for the HDE vs. saline samples, we focused on the 20 most differentially expressed genes based on statistical significance ($p \leq 0.05$). These 20 significantly altered genes were input into the STRING database and produced a significant protein–protein interaction ($p < 1.0 \times 10{-}16$). Among the 13 DHA vs. control diet samples exposed to HDE, six genes were significantly up-regulated (*BCL3*, *CFB*, *ITGAX*, *LILRB3*, *MARCO*, and *TGFBI*) while *STAT5B* was down-regulated (Figure 6B). Three of these differentially expressed genes (*BCL3*, *LILRB3*, and MARCO) had counts below the 82-count threshold for all the saline-related samples, indicating minimal transcriptional expression under baseline conditions. As a result, these three genes were only assessed in the expression analysis of the DHA-vs.-control-diet, exposed-to-HDE sample set.

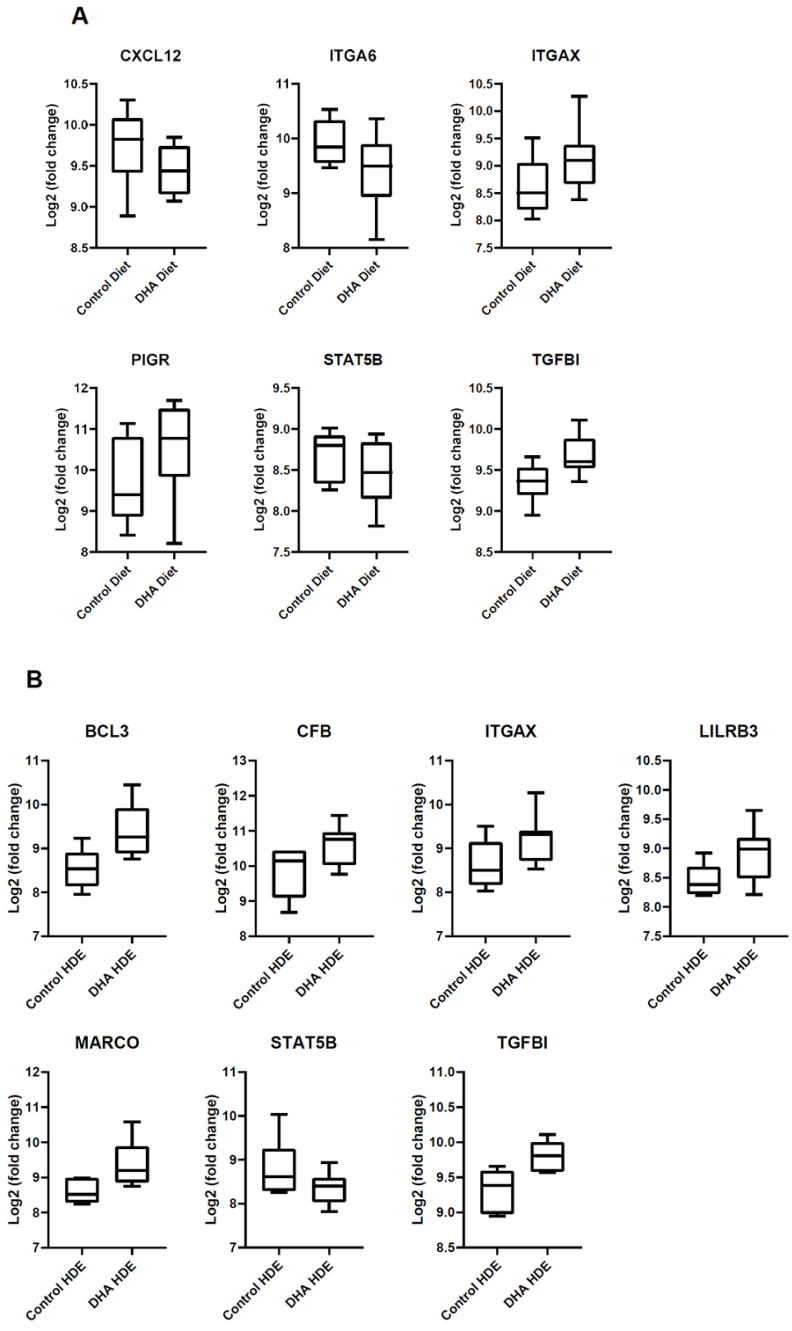

Figure 6. Box plots representing statistically significant ($p \leq 0.05$) alterations in gene expression in HDE- or saline-challenged mice fed a high-DHA diet or control diet containing no DHA. Normalized Log2 values were exported from nSolver and plotted. (A) List of 6 genes that were significantly altered among all 20 DHA vs. control diet samples. (B) The 7 differentially regulated genes within the 13 DHA vs. control diet samples exposed to HDE.

The z-scores produced from the gene expression data were plotted and analyzed by two-way ANOVA to identify significant pathway alterations between the diet and exposure experimental groups for genes related to immunological pathways. For genes related to the inflammatory response, the immune response, the innate immune response, cytokine activity, the defense response, and cytokine- and chemokine-mediated signaling pathways, HDE exposure was associated with a significant up-regulation of genes related to these responses when compared to saline exposure (Figure 7 and Figure 8). A brief examination of the sole effect of HDE vs. saline for additional altered pathways revealed significant changes in the activation of pathways relating to the cell surface, receptor activity, extracellular region, plasma membrane, and signal transduction.

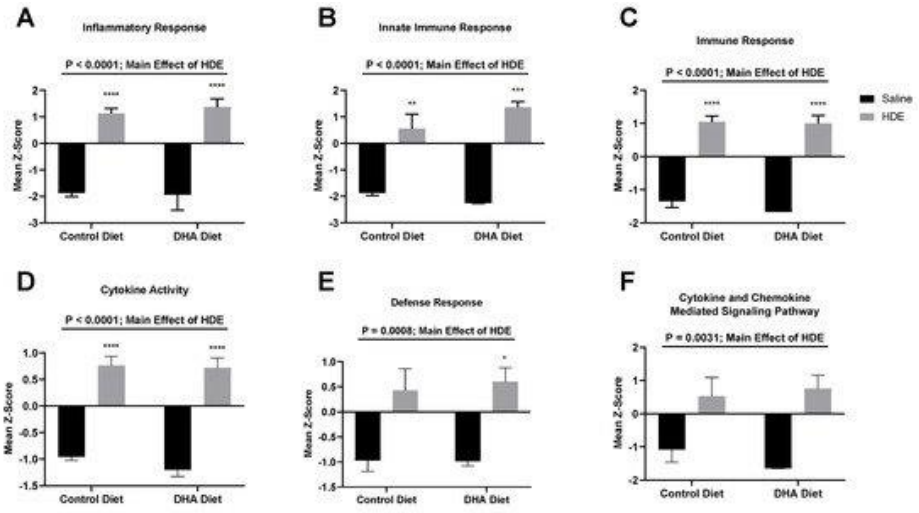

Figure 7. Expression changes in significantly altered pathways among all 20 DHA- vs. control-diet-fed mice. nSolver Advanced Analysis was performed to assess significant changes among pathway z-scores for various immunological pathways including inflammatory response (A); innate immune response (B); immune response (C); cytokine activity (D); defense response (E); and cytokine and chemokine-mediated signaling pathway (F). A major effect for HDE vs. saline exposure is indicated by the top significance bars and p-values. The * symbol above the HDE bars represents $p < 0.05$ versus all saline-treated conditions; ** $p < 0.01$; *** $p < 0.001$; **** $p < 0.0001$.

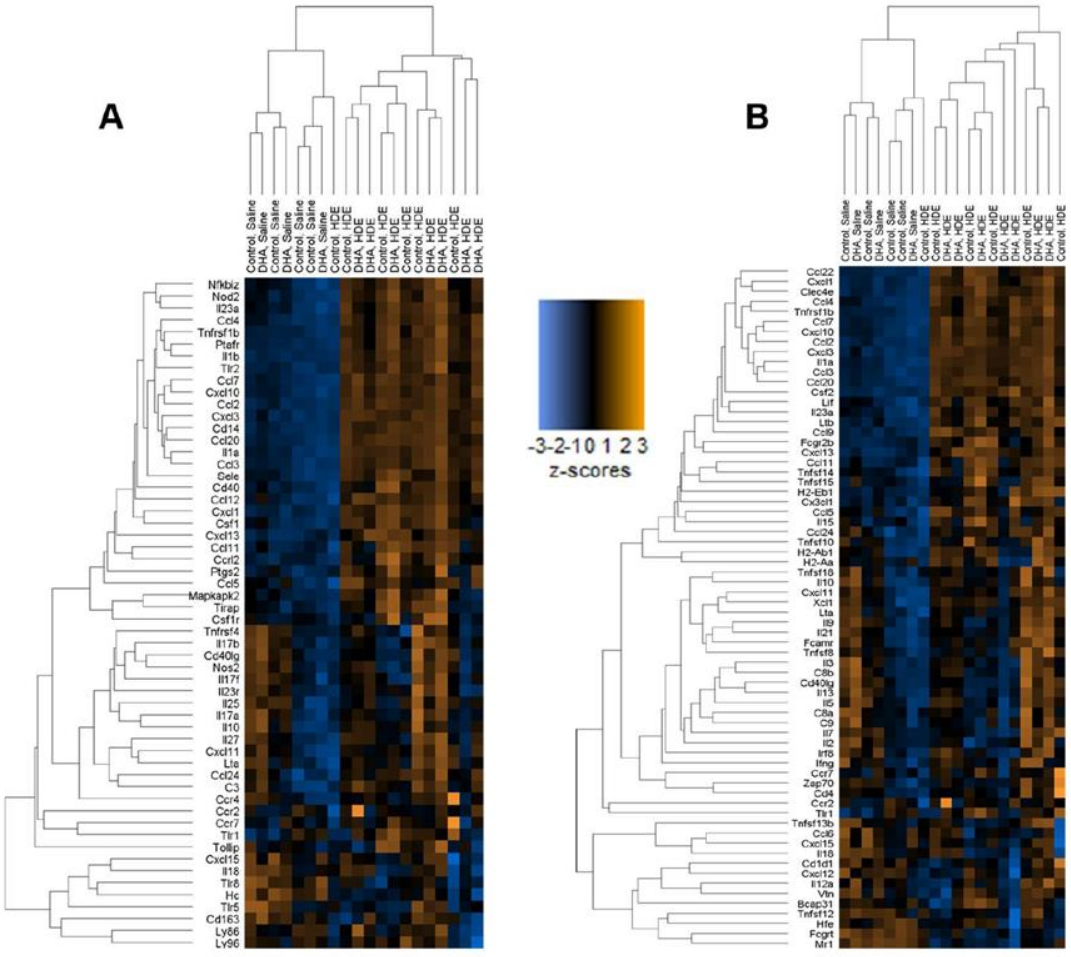

Figure 8. Hierarchal clustering shown by heat maps related to inflammation for all 20 normalized samples. (A) Heat map showing clustering of genes related to the inflammatory response. (B) Immune response heat map showing altered genes among all 20 samples.

4. Discussion

Acute and chronic dust exposure can lead to a variety of lung inflammatory diseases among exposed individuals, especially agricultural workers [1,2,3,36]. The use of omega-3 PUFAs and their SPM metabolites as a therapeutic approach to reduce dust-induced lung inflammation shows promise in reducing the lung's inflammatory response to environmental dust exposure [18,30,35]. We have previously shown that a single HDE exposure stimulates a strong inflammatory response that includes the release of pro-inflammatory cytokines and an increased neutrophil influx in the BALF of exposed mice [31]. In this study, we supplemented a standard mouse diet with DHA to assess the impact of a high-omega-3-PUFA diet as a preventative approach to mitigate the risk of inadvertent exposure by altering the lung inflammatory response. Through these investigations, we found that pretreating mice with a DHA-rich diet led to significant changes in the lung's inflammatory response to acute dust exposure. Unlike control-diet-fed mice, we identified that DHA-diet-fed mice exhibited a significant increase in BALF macrophages following HDE challenge (Figure 2C) along with a significant increase in BALF SPM RvD1 (Figure 4A). Furthermore, we identified alterations to AREG and MPO release in control-diet-fed versus DHA-diet-fed animals exposed to HDE, and significant alterations in numerous immune-associated genes. Together, these data indicate that a high-DHA diet leads to significant alterations in the lung's immune response to acute agricultural dust exposure, warranting its continued exploration as a potential modifier of the pathological inflammation experienced by individuals living or working in agricultural settings.

An omega-6 fatty acid to omega-3 fatty acid ratio of ~ 1:1 is thought to be associated with protective health effects by promoting the resolution of inflammation [17,23]. The dietary consumption of supplements high in omega-3 PUFAs such as fish oil has been shown to be effective in reducing the risk of cardiovascular and lung diseases [37,38,39]. In this study, mice fed a DHA-rich diet had a roughly three times lower omega-6 to omega-3 PUFA ratio than those on a control diet, suggesting that the employment of a high-DHA diet effectively increases the overall blood levels of omega-3 PUFAs. A lower dietary intake of omega-3 PUFAs in conjunction with the high degree of dust exposure agricultural workers experience can amplify their risk of developing acute/chronic lung diseases. A recent investigation identified an omega-6 PUFA/omega-3 PUFA ratio of over 50:1 in a cohort of COPD patients with agricultural work histories, highlighting the opportunity for impact in this population [40]. It is worth noting that even in our control-diet-fed mice, we identified an omega-6/omega-3 PUFA ratio of approximately 6.8:1, which is substantially lower than the typical Western diet ratio [17], suggesting more pronounced responses might have been identified in a dietary supplementation scheme yielding a higher omega-6/omega-3 PUFA ratio in control-diet-fed mice. In addition, while we identified significant elevations in the DHA-derived RvD1 in our DHA-diet-fed mice, a limitation to our studies is that we did not assess omega-6-PUFA-derived mediators. Doing so would have allowed for a more complete assessment of the ramifications of

decreasing the omega-6 fatty acid to omega-3 fatty acid ratio for modifying bioactive lipid generation.

Macrophages are known mediators of both inflammation and resolution/repair, and are both responsive to SPM and also generators of SPM during an inflammatory response in the lung [41,42]. In our previous 7-day DHA oral supplementation study, we found no statistical differences for macrophage influx or SPM production in the lungs of DHA-treated mice compared to the controls following HDE exposure [29]. We did, however, see that DHA reduced HDE-elicited responses in the immortalized monocyte cell line THP-1 [29]. The increased macrophage influx into the lungs along with the significant interaction between diet and dust exposure that we identified in these current investigations is unique to this dietary intervention method and suggests that a high-DHA diet may alter macrophage influx or activation kinetics, possibly in part through the increased generation of the SPM RvD1. RvD1 is a member of the resolvins family of SPMs that are produced during the resolution phase of inflammation [43,44], and RvD1 has been previously shown to regulate airway inflammation by reducing pro-inflammatory cytokine production and inducing an M2-like macrophage polarization phenotype [27,43,44,45,46]. Our 5 h model of acute dust exposure has been shown to induce an M1-type macrophage phenotype in challenged mice [47], while our NanoString gene expression analyses suggest a potential M2-like polarization of the immune response (e.g., increased Marco expression). Considered together with our findings of increased blood DHA

levels, elevated BALF RvD1, and increased macrophage influx, these outcomes suggest that the DHA diet is inducing alterations in the kinetics of the inflammatory cascade, possibly promoting the inflammation-resolution response. However, a limitation of our current study is the lack of characterization of the lung macrophage subsets for activation/polarization profiles.

Interestingly, we also identified alterations in neutrophil activities when comparing control-diet-fed with DHA-diet-fed animals. Here, we saw a trend towards reduced neutrophil influx in DHA-diet-fed mice versus control-diet-fed mice exposed to HDE that did not reach statistical significance ($p = 0.070$) yet found enhanced levels of MPO in the BALF of DHA-diet-fed mice and similar levels of NET formation. These data imply that the entering neutrophils may have enhanced antimicrobial activity (based on increased MPO release) in the setting of a high-DHA diet or that infiltrating neutrophils were more quickly subsiding or being efferocytosed by our five-hour timepoint. Together, these findings warrant future studies aimed at identifying the inflammation resolution kinetics following acute HDE exposure, including how PUFAs alter these kinetics, particularly in neutrophils and macrophages.

The gene expression analysis performed in this study details some of the effects a DHA-rich diet can have on immune-associated networks. We found that the main driver for the activation of the lung immune response was the HDE exposure itself, as opposed to dietary intervention (Figure 7). The top 20 significantly altered genes for HDE vs. saline exposure were input into the

STRING database and produced a significant interaction ($p < 1.0 \times 10-16$). Pathway analysis using nSolver and the STRING database showed that most of these 20 genes are involved in a variety of biological processes including cell surface receptor signaling and signal transduction. Among the 20 DHA vs. control diet samples, *ITGAX*, *PIGR*, and *TGFBI* were up-regulated while *CXCL12*, *ITGA6*, and *STAT5B* were down-regulated (Figure 6A). Assessment of the 13 DHA vs. control diet samples with exposure to HDE identified six genes that were significantly upregulated (*BCL3*, *CFB*, *ITGAX*, *LILRB3*, *MARCO*, and *TGFBI*), while only *STAT5B* was down-regulated (Figure 6B). A list of all relevant genes and their expression/fold changes are presented for DHA-related samples and all other sample groups in Table 3 and Table 4, respectively. The genes listed in Table 4 are expressed among all the analysis sets, whereas *BCL3*, *LILRB3*, and *MARCO* are unique to the DHA-vs.-control-diet-with-HDE analysis (Table 3) because the threshold counts for these three genes were < 82 counts for the saline-related samples.

Table 3. Fold regulation of expressed genes in DHA-related samples.

Gene Symbol	Fold Change In Each Data Set	
	DHA vs. Control Diet	*DHA vs. Control Diet, Exposed to HDE*
BCL3	[b] Below Threshold	↑ 2.24
CFB	[a] ↑ 1.48	↑ 1.57
CXCL12	↓ 1.41	[a] ↓ 1.37
ITGA6	↓ 1.52	[a] ↓ 1.40
ITGAX	↑ 1.31	↑ 1.47
LILRB3	[b] Below Threshold	↑ 1.59
MARCO	[b] Below Threshold	↑ 2.07
PIGR	↑ 1.44	[a] ↑ 1.57
STAT5B	↓ 1.45	↓ 1.61
TGFBI	↑ 1.2	↑ 1.31

[a]Denotes expression values were not significant ($p > 0.05$). b Denotes expression was below threshold (< 82 counts); could not assess.

Table 4. Fold regulation of expressed genes in diet/exposure groups compared to control diet + saline exposure group.

Gene Symbol	Fold Change/Regulation		
	Control Diet + HDE	*DHA Diet + Saline*	*DHA Diet + HDE*
CFB	↑ 3.66	[a] ↑ 1.32	↑ 5.77
CXCL12	[a] ↓ 1.35	[a] ↓ 1.47	↓ 1.83
ITGA6	[a] ↓ 1.37	[a] ↓ 1.74	↓ 1.93
ITGAX	[a] ↑ 1.01	[a] ↑ 1.07	↑ 1.47
PIGR	↑ 2.89	[a] ↑ 1.21	↑ 4.54
STAT5B	[a] ↑ 1.03	[a] ↓ 1.20	↓ 1.56
TGFBI	[a] ↓ 1.08	[a] ↑ 1.02	[a] ↑ 1.06

[a]Denotes expression values were not significant ($p > 0.05$).

Transforming growth factor-β-induced (TGFBI) is a negative regulator of TLR signaling [48,49], and the increased expression of *TGFBI* has been shown to aid in wound healing and increase macrophage endocytosis [50,51]. Integrin α6

(ITGA6) is expressed in the epithelia and forms a complex with either β1 or β4 integrins to function as a receptor for laminin, a basement membrane protein [52]. Additionally, studies have shown that during epithelial injury, the expression of the integrin α6β4 complex increases, suggesting that the decreased expression of *ITGA6* we identified could be due to DHA altering dust-induced inflammation and lung injury [52,53]. Prior research has shown that organic dusts from swine facilities induce CD11c+ macrophages, which can mitigate inflammatory responses in the lung [54,55]. The expression of *ITGAX* (the gene encoding CD11c) in both DHA-diet sample sets suggests that in the setting of a high DHA diet, alveolar macrophages may be playing a role in altering the inflammatory response. This outcome corresponds to the increased BALF macrophages of HDE-treated mice fed a DHA-rich diet and collectively suggests that the resulting increased omega-3 PUFAs may alter the recruitment and/or activation of infiltrating and resident macrophages in the lung following a single dust exposure. In addition to our findings of elevated BALF macrophage levels and increased CD11c transcripts in the lungs of DHA-diet-fed mice challenged with HDE, we also identified significant alterations in *MARCO* (macrophage receptor with collagenous structure). *MARCO* is known to play a role in M2-like macrophage polarization to aid in host pathogen defense with additional known roles in inflammation resolution and repair processes [56,57]. In conjunction with our findings of increased RvD1 levels, our finding of the increased expression of *MARCO* in our DHA-diet-fed mice further supports the effectiveness of a high-

DHA diet in promoting a pro-resolution/repair response following inflammatory insult in the lung. Leukocyte Immunoglobulin Like Receptor B3 (LILRB3) also codes for an anti-inflammatory protein expressed on monocytes, dendritic cells, and granulocytes; has been suggested to inhibit stimulated inflammatory responses; and is similarly elevated in DHA-related samples [58,59,60]. Furthermore, we see increased expression of Polymeric Immunoglobulin Receptor (PIGR) in our DHA-diet samples; *PIGR* serves as a transporter of IgA across mucosal epithelial cells to help reduce the inflammation stimulated by foreign pathogens [61,62]. The increased expression of this receptor has been shown to occur following the release of the pro-inflammatory cytokines TNF-α and IFN-γ that are produced in response to viral or bacterial infection [61,62]. As previously reported, lipopolysaccharide (LPS) exists within the dusts from swine confinement facilities and contributes to the inflammatory response seen in this exposure model [9,12]. The inhibition of LPS-induced TNF-α expression in macrophages has been shown to be mediated by IL-10, the expression of which is promoted by *BCL3* (B-Cell Leukemia/Lymphoma) [63]. The expression of *BCL3* in our DHA-diet samples is supported by BCL3′s ability to promote the downstream inhibition of the LPS-stimulated TNF-α expression in macrophages.

Prior research has shown that elevated levels of complement factor B (CFB) are associated with inflammation and airway hyperresponsiveness [64]. The up-regulation of *CFB* was only seen in our DHA-diet samples that were exposed to HDE. Since we only see increased expression of *CFB* in the DHA samples with

HDE exposure, it could be suggested that in addition to altering the effects of HDE-induced inflammation, DHA also strengthens overall host immunity to bacterial/viral challenge. In this case, DHA would be functioning to promote systemic immunity to foreign pathogens—a hypothesis that is also supported by the increased levels of MPO release in the DHA-diet- versus control-diet-fed mice treated with HDE. In addition to the various receptors and ECM-related genes differentially expressed in DHA-related samples, we see significant alterations in different cytokine- and chemokine-related genes. The pro-inflammatory chemokine ligand 12 (CXCL12) binds to *CXCR4* and has previously been shown to recruit numerous cell types such as lymphocytes, monocytes, and eosinophils into the lung airway fluid (BALF) of asthma patients [65]. The decreased expression of *CXCL12* in the DHA- vs. control-diet analysis set suggests that a high-DHA diet modulates the expression of pro-inflammatory responses at the transcriptomic level. Similarly, *STAT5B* has been shown to be activated by IL-5 and GM-CSF activation; *STAT5B* recruits eosinophils into the airways and causes a downstream allergic response [66,67,68]. The down-regulation of *STAT5B* in both DHA-diet-related analysis sets demonstrates the impact of omega-3 PUFAs in reducing the HDE-stimulated inflammatory response.

5. References

1. Kirkhorn, S.R.; Garry, V.F. Agricultural lung diseases. *Environ. Health Perspect.* **2000**, *108* (Suppl 4), 705–712, doi:10.1289/ehp.00108s4705.

2. Langley, R.L. Consequences of respiratory exposures in the farm environment. *N. C. Med. J.* **2011**, *72*, 477–480.

3. Respiratory Health Hazards in Agriculture. *Am. J. Respir. Crit. Care Med.* **1998**, *158*, S1–S76, doi:10.1164/ajrccm.158.supplement_1.rccm1585s1.

4. Von Essen, S.; Donham, K. Illness and injury in animal confinement workers. *Occup. Med.* **1999**, *14*, 337–350.

5. Bongers, P.; Houthuijs, D.; Remijn, B.; Brouwer, R.; Biersteker, K. Lung function and respiratory symptoms in pig farmers. *Br. J. Ind. Med.* **1987**, *44*, 819–823, doi:10.1136/oem.44.12.819.

6. Eduard, W.; Pearce, N.; Douwes, J. Chronic bronchitis, COPD, and lung function in farmers: The role of biological agents. *Chest* **2009**, *136*, 716–725, doi:10.1378/chest.08-2192.

7. Von Essen, S.; Romberger, D. The respiratory inflammatory response to the swine confinement building environment: The adaptation to respiratory exposures in the chronically exposed worker. *J. Agric. Saf. Health* **2003**, *9*, 185–196, doi:10.13031/2013.13684.

8. Szczyrek, M.; Krawczyk, P.; Milanowski, J.; Jastrzebska, I.; Zwolak, A.; Daniluk, J. Chronic obstructive pulmonary disease in farmers and agricultural workers—An overview. *Ann. Agric. Environ. Med.* **2011**, *18*, 310–313.

9. Boissy, R.J.; Romberger, D.J.; Roughead, W.A.; Weissenburger-Moser, L.; Poole, J.A.; LeVan, T.D. Shotgun pyrosequencing metagenomic analyses of dusts from swine confinement and grain facilities. *PLoS ONE* **2014**, *9*, e95578, doi:10.1371/journal.pone.0095578.

10. Romberger, D.J.; Heires, A.J.; Nordgren, T.M.; Souder, C.P.; West, W.; Liu, X.-D.; Poole, J.A.; Toews, M.L.; Wyatt, T.A. Proteases in agricultural dust induce lung inflammation through PAR-1 and PAR-2 activation. *Am. J. Physiol. Lung Cell. Mol. Physiol.* **2015**, *309*, L388–L399, doi:10.1152/ajplung.00025.2015.

11. Wang, Z.; Larsson, K.; Palmberg, L.; Malmberg, P.; Larsson, P.; Larsson, L. Inhalation of swine dust induces cytokine release in the upper and lower airways. *Eur. Respir. J.* **1997**, *10*, 381–387, doi:10.1183/09031936.97.10020381.

12. Romberger, D.J.; Bodlak, V.; Essen, S.G.V.; Mathisen, T.; Wyatt, T.A. Hog barn dust extract stimulates IL-8 and IL-6 release in human bronchial epithelial cells via PKC activation. *J. Appl. Physiol.* **2002**, *93*, 289–296, doi:10.1152/japplphysiol.00815.2001.

13. Mitchell, D.C.; Schenker, M.B. Protection against breathing dust: Behavior over time in Californian farmers. *J. Agric. Saf. Health* **2008**, *14*, 189–203, doi:10.13031/2013.24350.

14. Schenker, M.B.; Orenstein, M.R.; Samuels, S.J. Use of protective equipment among California farmers. *Am. J. Ind. Med.* **2002**, *42*, 455–464, doi:10.1002/ajim.10134.

15. Moldoveanu, B.; Otmishi, P.; Jani, P.; Walker, J.; Sarmiento, X.; Guardiola, J.; Saad, M.; Yu, J. Inflammatory mechanisms in the lung. *J. Inflamm. Res.* **2009**, *2*, 1–11.

16. Sansbury, B.E.; Spite, M. Resolution of Acute Inflammation and the Role of Resolvins in Immunity, Thrombosis, and Vascular Biology. *Circ. Res.* **2016**, *119*, 113–130, doi:10.1161/CIRCRESAHA.116.307308.

17. Simopoulos, A.P. The importance of the ratio of omega-6/omega-3 essential fatty acids. *Biomed. Pharm.* **2002**, *56*, 365–379, doi:10.1016/s0753-3322(02)00253-6.

18. Giudetti, A.M.; Cagnazzo, R. Beneficial effects of n-3 PUFA on chronic airway inflammatory diseases. *Prostaglandins Other Lipid Mediat.* **2012**, *99*, 57–67, doi:10.1016/j.prostaglandins.2012.09.006.

19. Levy, B.D.; Clish, C.B.; Schmidt, B.; Gronert, K.; Serhan, C.N. Lipid mediator class switching during acute inflammation: Signals in resolution. *Nat. Immunol.* **2001**, *2*, 612–619, doi:10.1038/89759.

20. Patterson, E.; Wall, R.; Fitzgerald, G.; Ross, R.; Stanton, C. Health implications of high dietary omega-6 polyunsaturated fatty acids. *J. Nutr. Metab.* **2012**, *2012*, 539426.

21. Serhan, C.N.; Chiang, N.; Van Dyke, T.E. Resolving inflammation: Dual anti-inflammatory and pro-resolution lipid mediators. *Nat. Rev. Immunol.* **2008**, *8*, 349–361, doi:10.1038/nri2294.

22. Serhan, C.N.; Savill, J. Resolution of inflammation: The beginning programs the end. *Nat. Immunol.* **2005**, *6*, 1191–1197, doi:10.1038/ni1276.

23. Bannenberg, G.L. Therapeutic applicability of anti-inflammatory and proresolving polyunsaturated fatty acid-derived lipid mediators. *Sci. World J.* **2010**, *10*, 676–712, doi:10.1100/tsw.2010.57.

24. Serhan, C.N.; Dalli, J.; Karamnov, S.; Choi, A.; Park, C.-K.; Xu, Z.-Z.; Ji, R.-R.; Zhu, M.; Petasis, N.A. Macrophage proresolving mediator maresin 1 stimulates tissue regeneration and controls pain. *FASEB J.* **2012**, *26*, 1755–1765, doi:10.1096/fj.11-201442.

25. Wang, W.; Zhu, J.; Lyu, F.; Panigrahy, D.; Ferrara, K.W.; Hammock, B.; Zhang, G. ω-3 Polyunsaturated fatty acids-derived lipid metabolites on angiogenesis, inflammation and cancer. *Prostaglandins Other Lipid Mediat.* **2014**, *113–115*, 13–20, doi:10.1016/j.prostaglandins.2014.07.002.

26. Duvall, M.G.; Levy, B.D. DHA- and EPA-derived resolvins, protectins, and maresins in airway inflammation. *Eur. J. Pharmacol.* **2016**, *785*, 144–155, doi:10.1016/j.ejphar.2015.11.001.

27. Hsiao, H.-M.; Sapinoro, R.E.; Thatcher, T.H.; Croasdell, A.; Levy, E.P.; Fulton, R.A.; Olsen, K.C.; Pollock, S.J.; Serhan, C.N.; Phipps, R.P., et al. A novel anti-inflammatory and pro-resolving role for resolvin D1 in acute cigarette smoke-induced lung inflammation. *PLoS ONE* **2013**, *8*, e58258, doi:10.1371/journal.pone.0058258.

28. Serhan, C.N. Novel Lipid Mediators and Resolution Mechanisms in Acute Inflammation: To Resolve or Not? *Am. J. Pathol.* **2010**, *177*, 1576–1591, doi:10.2353/ajpath.2010.100322.

29. Nordgren, T.M.; Friemel, T.D.; Heires, A.J.; Poole, J.A.; Wyatt, T.A.; Romberger, D.J. The Omega-3 Fatty Acid Docosahexaenoic Acid Attenuates Organic Dust-Induced Airway Inflammation. *Nutrients* **2014**, *6*, 5434–5452.

30. Nordgren, T.M.; Heires, A.J.; Bailey, K.L.; Katafiasz, D.M.; Toews, M.L.; Wichman, C.S.; Romberger, D.J. Docosahexaenoic acid enhances amphiregulin-mediated bronchial epithelial cell repair processes following organic dust exposure. *Am. J. Physiol. Lung Cell. Mol. Physiol.* **2018**, *314*, L421–l431, doi:10.1152/ajplung.00273.2017.

31. Poole, J.A.; Wyatt, T.A.; Oldenburg, P.J.; Elliott, M.K.; West, W.W.; Sisson, J.H.; Von Essen, S.G.; Romberger, D.J. Intranasal organic dust exposure-induced airway adaptation response marked by persistent lung inflammation and pathology in mice. *Am. J. Physiol. Lung Cell. Mol. Physiol.* **2009**, *296*, L1085–L1095, doi:10.1152/ajplung.90622.2008.

32. Poole, J.A.; Romberger, D.J. Immunological and inflammatory responses to organic dust in agriculture. *Curr. Opin. Allergy Clin. Immunol.* **2012**, *12*, 126–132, doi:10.1097/ACI.0b013e3283511d0e.

33. Perez, S.E.; Berg, B.M.; Moore, K.A.; He, B.; Counts, S.E.; Fritz, J.J.; Hu, Y.S.; Lazarov, O.; Lah, J.J.; Mufson, E.J. DHA diet reduces AD pathology in young APPswe/PS1 Delta E9 transgenic mice: Possible gender effects. *J. Neurosci. Res.* **2010**, *88*, 1026–1040, doi:10.1002/jnr.22266.

34. Vargas, A.; Boivin, R.; Cano, P.; Murcia, Y.; Bazin, I.; Lavoie, J.-P. Neutrophil extracellular traps are downregulated by glucocorticosteroids in lungs in an equine model of asthma. *Respir. Res.* **2017**, *18*, 207, doi:10.1186/s12931-017-0689-4.

35. Nordgren, T.M.; Bauer, C.D.; Heires, A.J.; Poole, J.A.; Wyatt, T.A.; West, W.W.; Romberger, D.J. Maresin-1 reduces airway inflammation associated with acute and repetitive exposures to organic dust. *Transl. Res.* **2015**, *166*, 57–69, doi:10.1016/j.trsl.2015.01.001.

36. Linaker, C.; Smedley, J. Respiratory illness in agricultural workers. *Occup. Med.* **2002**, *52*, 451–459, doi:10.1093/occmed/52.8.451.

37. Kromhout, D.; Bosschieter, E.B.; Coulander, C.D.L. The Inverse Relation between Fish Consumption and 20-Year Mortality from Coronary Heart Disease. *N. Engl. J. Med.* **1985**, *312*, 1205–1209, doi:10.1056/NEJM198505093121901.

38. Kromhout, D.; Feskens, E.J.M.; Bowles, C.H. The Protective Effect of a Small Amount of Fish on Coronary Heart Disease Mortality in an Elderly Population. *Int. J. Epidemiol.* **1995**, *24*, 340–345, doi:10.1093/ije/24.2.340.

39. Marik, P.E.; Varon, J. Omega-3 dietary supplements and the risk of cardiovascular events: A systematic review. *Clin. Cardiol.* **2009**, *32*, 365–372, doi:10.1002/clc.20604.

40. Hanson, C.; Lyden, E.; Weissenburger-Moser, L.; Furtado, J.; Hinds, J.; LeVan, T. Serum Level of Nutritional Antioxidants are Decreased in Veteran Smokers with COPD. *Mil. Veterans Health* **2016**, in press.

41. Chazaud, B. Macrophages: Supportive cells for tissue repair and regeneration. *Immunobiology* **2014**, *219*, 172–178, doi:10.1016/j.imbio.2013.09.001.

42. Oishi, Y.; Manabe, I. Macrophages in inflammation, repair and regeneration. *Int. Immunol.* **2018**, *30*, 511–528, doi:10.1093/intimm/dxy054.

43. Levy, B. Resolvin D1 and Resolvin E1 Promote the Resolution of Allergic Airway Inflammation via Shared and Distinct Molecular Counter-Regulatory Pathways. *Front. Immunol.* **2012**, *3*, doi:10.3389/fimmu.2012.00390.

44. Serhan, C.N.; Hong, S.; Gronert, K.; Colgan, S.P.; Devchand, P.R.; Mirick, G.; Moussignac, R.-L. Resolvins : A Family of Bioactive Products of Omega-3 Fatty Acid Transformation Circuits Initiated by Aspirin Treatment that Counter Proinflammation Signals. *J. Exp. Med.* **2002**, *196*, 1025–1037, doi:10.1084/jem.20020760.

45. Liao, Z.; Dong, J.; Wu, W.; Yang, T.; Wang, T.; Guo, L.; Chen, L.; Xu, D.; Wen, F. Resolvin D1 attenuates inflammation in lipopolysaccharide-induced acute lung injury through a process involving the PPARγ/NF-κB pathway. *Respir. Res.* **2012**, *13*, 110, doi:10.1186/1465-9921-13-110.

46. Uddin, M.; Levy, B.D. Resolvins: Natural agonists for resolution of pulmonary inflammation. *Prog. Lipid Res.* **2011**, *50*, 75–88, doi:10.1016/j.plipres.2010.09.002.

47. Nordgren, T.M.; Heires, A.J.; Zempleni, J.; Swanson, B.J.; Wichman, C.; Romberger, D.J. Bovine milk-derived extracellular vesicles enhance inflammation and promote M1 polarization following agricultural dust exposure in mice. *J. Nutr. Biochem.* **2019**, *64*, 110–120, doi:10.1016/j.jnutbio.2018.10.017.

48. Nummela, P.; Lammi, J.; Soikkeli, J.; Saksela, O.; Laakkonen, P.; Hölttä, E. Transforming Growth Factor Beta-Induced (TGFBI) Is an Anti-Adhesive Protein Regulating the Invasive Growth of Melanoma Cells. *Am. J. Pathol.* **2012**, *180*, 1663–1674, doi:10.1016/j.ajpath.2011.12.035.

49. Thapa, N.; Lee, B.-H.; Kim, I.-S. TGFBIp/βig-h3 protein: A versatile matrix molecule induced by TGF-β. *Int. J. Biochem. Cell Biol.* **2007**, *39*, 2183–2194, doi:10.1016/j.biocel.2007.06.004.

50. Cao, W.; Tan, P.; Lee, C.H.; Zhang, H.; Lu, J. A transforming growth factor–β–induced protein stimulates endocytosis and is up-regulated in immature dendritic cells. *Blood* **2006**, *107*, 2777–2785, doi:10.1182/blood-2005-05-1803.

51. Rawe, I.M.; Zhan, Q.; Burrows, R.; Bennett, K.; Cintron, C. Beta-ig. Molecular cloning and in situ hybridization in corneal tissues. *Investig. Ophthalmol. Vis. Sci.* **1997**, *38*, 893–900.

52. Chapman, H.A.; Li, X.; Alexander, J.P.; Brumwell, A.; Lorizio, W.; Tan, K.; Sonnenberg, A.; Wei, Y.; Vu, T.H. Integrin α6β4 identifies an adult distal lung epithelial population with regenerative potential in mice. *J. Clin. Investig.* **2011**, *121*, 2855–2862, doi:10.1172/JCI57673.

53. Sheppard, D. Functions of Pulmonary Epithelial Integrins: From Development to Disease. *Physiol. Rev.* **2003**, *83*, 673–686, doi:10.1152/physrev.00033.2002.

54. Guth, A.M.; Janssen, W.J.; Bosio, C.M.; Crouch, E.C.; Henson, P.M.; Dow, S.W. Lung environment determines unique phenotype of alveolar macrophages. *Am. J. Physiol. Lung Cell. Mol. Physiol.* **2009**, *296*, L936–L946, doi:10.1152/ajplung.90625.2008.

55. Poole, J.A.; Gleason, A.M.; Bauer, C.; West, W.W.; Alexis, N.; van Rooijen, N.; Reynolds, S.J.; Romberger, D.J.; Kielian, T.L. CD11c(+)/CD11b(+) cells are critical for organic dust-elicited murine lung inflammation. *Am. J. Respir. Cell Mol. Biol.* **2012**, *47*, 652–659, doi:10.1165/rcmb.2012-0095OC.

56. Murthy, S.; Larson-Casey, J.L.; Ryan, A.J.; He, C.; Kobzik, L.; Carter, A.B. Alternative activation of macrophages and pulmonary fibrosis are modulated by scavenger receptor, macrophage receptor with collagenous structure. *FASEB J.* **2015**, *29*, 3527–3536, doi:10.1096/fj.15-271304.

57. Zhang, L.; Nie, L.; Cai, S.-Y.; Chen, J.; Chen, J. Role of a macrophage receptor with collagenous structure (MARCO) in regulating monocyte/macrophage functions in ayu, Plecoglossus altivelis. *Fish Shellfish Immunol.* **2018**, *74*, 141–151, doi:10.1016/j.fsi.2017.12.059.

58. An, H.; Chandra, V.; Piraino, B.; Borges, L.; Geczy, C.; McNeil, H.P.; Bryant, K.; Tedla, N. Soluble LILRA3, a potential natural antiinflammatory protein, is increased in patients with rheumatoid arthritis and is tightly regulated by interleukin 10, tumor necrosis factor-alpha, and interferon-gamma. *J. Rheumatol.* **2010**, *37*, 1596–1606, doi:10.3899/jrheum.091119.

59. Hirayasu, K.; Arase, H. Functional and genetic diversity of leukocyte immunoglobulin-like receptor and implication for disease associations. *J. Hum. Genet.* **2015**, *60*, 703–708, doi:10.1038/jhg.2015.64.

60. Kang, X.; Kim, J.; Deng, M.; John, S.; Chen, H.; Wu, G.; Phan, H.; Zhang, C.C. Inhibitory leukocyte immunoglobulin-like receptors: Immune checkpoint proteins and tumor sustaining factors. *Cell Cycle* **2016**, *15*, 25–40, doi:10.1080/15384101.2015.1121324.

61. Kaetzel, C.S. The polymeric immunoglobulin receptor: Bridging innate and adaptive immune responses at mucosal surfaces. *Immunol. Rev.* **2005**, *206*, 83–99, doi:10.1111/j.0105-2896.2005.00278.x.

62. Kaetzel, C.S. Cooperativity among secretory IgA, the polymeric immunoglobulin receptor, and the gut microbiota promotes host–microbial mutualism. *Immunol. Lett.* **2014**, *162*, 10–21, doi:10.1016/j.imlet.2014.05.008.

63. Kreisel, D.; Sugimoto, S.; Tietjens, J.; Zhu, J.; Yamamoto, S.; Krupnick, A.S.; Carmody, R.J.; Gelman, A.E. Bcl3 prevents acute inflammatory lung injury in mice by restraining emergency granulopoiesis. *J. Clin. Investig.* **2011**, *121*, 265–276, doi:10.1172/JCI42596.

64. Taube, C.; Thurman, J.M.; Takeda, K.; Joetham, A.; Miyahara, N.; Carroll, M.C.; Dakhama, A.; Giclas, P.C.; Holers, V.M.; Gelfand, E.W. Factor B of the alternative complement pathway regulates development of airway hyperresponsiveness and inflammation. *Proc. Natl. Acad. Sci. USA* **2006**, *103*, 8084, doi:10.1073/pnas.0602357103.

65. Negrete-García, M.C.; Velazquez, J.R.; Popoca-Coyotl, A.; Montes-Vizuet, A.R.; Juárez-Carvajal, E.; Teran, L.M. Chemokine (C-X-C Motif) Ligand 12/Stromal Cell-Derived Factor-1 Is Associated With Leukocyte Recruitment in Asthma. *Chest* **2010**, *138*, 100–106, doi:10.1378/chest.09-2104.

66. Caldenhoven, E.; van Dijk, T.B.; Tijmensen, A.; Raaijmakers, J.A.M.; Lammers, J.-W.J.; Koenderman, L.; de Groot, R.P. Differential Activation of Functionally Distinct STAT5 Proteins by IL-5 and GM-CSF During Eosinophil and Neutrophil Differentiation from Human CD34+ Hematopoietic Stem Cells. *Stem Cells* **1998**, *16*, 397–403, doi:10.1002/stem.160397.

67. Kagami, S.-I.; Nakajima, H.; Kumano, K.; Suzuki, K.; Suto, A.; Imada, K.; Davey, H.W.; Saito, Y.; Takatsu, K.; Leonard, W.J.; et al. Both Stat5a and Stat5b are required for antigen-induced eosinophil and T-cell recruitment into the tissue. *Blood* **2000**, *95*, 1370–1377, doi:10.1182/blood.V95.4.1370.004k29_1370_1377.

68. Stout, B.A.; Bates, M.E.; Liu, L.Y.; Farrington, N.N.; Bertics, P.J. IL-5 and Granulocyte-Macrophage Colony-Stimulating Factor Activate STAT3 and STAT5 and Promote Pim-1 and Cyclin D3 Protein Expression in Human Eosinophils. *J. Immunol.* **2004**, *173*, 6409, doi:10.4049/jimmunol.173.10.6409.

Chapter 2

Aspirin-triggered Resolvin D1 Reduces Chronic Dust-induced Lung Pathology Without Altering Susceptibility to Dust-enhanced Carcinogenesis

Edward C. Dominguez, Rattapol Phandthong, Matthew Nguyen, Arzu Ulu, Stephanie Guardado, Stefanie Sveiven, Prue Talbot, and Tara M. Nordgren

Submitted to *Cancers* for review, 2022

Abstract: Lung cancer is the leading cause of cancer-related deaths worldwide with increased risk being associated with unresolved or chronic inflammation. Agricultural and livestock workers endure significant exposures to agricultural dusts on a routine basis; however, the chronic inflammatory and carcinogenic effects of these dust exposures is unclear. We have developed a chronic dust exposure model of lung carcinogenesis in which mice were intranasally challenged three times a week for 24 weeks, using an aqueous dust extract (HDE) made from dust collected in swine confinement facilities. We also treated mice with the omega-3-fatty acid lipid mediator, aspirin-triggered resolvin D1 (AT-RvD1) to provide a novel therapeutic strategy for mitigating the inflammatory and carcinogenic effects of HDE. Exposure to HDE resulted in significant immune cell influx into the lungs, enhanced lung tumorigenesis, severe tissue pathogenesis, and a pro-inflammatory and carcinogenic gene signature, relative to saline-exposed mice. AT-RvD1 treatment mitigated the dust-induced inflammatory response but did not protect against HDE+NNK-enhanced tumorigenesis. Our data suggest chronic HDE exposure induces a significant inflammatory and pro-carcinogenic response, whereas treatment with AT-RvD1 dampens the inflammatory responses, providing a strong argument for the therapeutic use of AT-RvD1 to mitigate chronic inflammation.

1. Introduction

Chronic, unresolved inflammation can lead to an increased risk for the development of chronic lung diseases including fibrosis, COPD, and cancer [1,2]. Exposure to organic dusts, including those from animal confinement facilities, have been shown to elicit potent lung inflammatory responses in exposed individuals, which are attributed to proteases, fungal and bacterial components, such as lipopolysaccharides (LPS) or endotoxin, that exist within these dusts [3-5]. The current literature reports conflicting epidemiological studies examining the association between LPS and cancer, with some studies citing an enhancement effect on tumorigenesis whereas others report a protective effect against tumorigenesis [6-9]. Acute and repetitive exposure to organic dusts, specifically extracts from swine confinement facilities (HDE), have been shown to induce a potent inflammatory response that includes increased immune cell influx in the lung, secretion of pro-inflammatory cytokines, and inflammatory lung tissue pathology [10,11]. Despite these findings, the chronic effects of these dusts, including the carcinogenic properties, have yet to be fully investigated. Agricultural and farm workers endure exposure to organic dusts on an everyday basis, and as such, face increased risk for the development of chronic lung disease [12-15]. Current preventative measures including the use of masks and respirators are available for these occupational groups; however, use of these personal protective equipment by these communities is not common [16-18]. Moreover, there is a need for innovative and effective therapeutic strategies to mitigate or inhibit dust-induced inflammation.

The resolution of inflammation is a key step in the immunoregulatory process to ensure our bodies avoid unresolved inflammation following acute or chronic injury [19,20]. One such way our bodies support this mechanism, is through the metabolism of polyunsaturated fatty acids (PUFAs) including the omega-6 PUFA arachidonic acid (AA), and omega-3 PUFAs docosahexaenoic acid (DHA) and eicosapentaenoic acid (EPA). During the initial inflammatory response, AA is enzymatically activated by cyclooxygenase (COX-1 and COX-2) and 5-lipoxygenase (5-LOX) into the pro-inflammatory eicosanoids, prostaglandins, thromboxanes, and leukotrienes [21,22]. During inflammation resolution, there is a lipid mediator class switching mechanism and AA becomes activated by 12-LOX and begins to produce lipoxins, which are a group of specialized pro-resolving mediators (SPMs) that function as biological anti-inflammatory substrates to resolve inflammation cascades and promote a return to tissue homeostasis [23,24]. In addition to lipoxin production, EPA and DHA undergo enzymatic activation by LOX, COX, and cytochrome P450 into SPMs including the maresins, protectins, and resolvins [25-27]. SPMs promote the resolution of inflammation by reducing neutrophil influx, increase macrophage recruitment and efferocytosis, and repairing tissue damage at the site of inflammation [19,26,28].

Resolvin D1 and its synthetic epimer, aspirin-triggered resolvin D1 (AT-RvD1), are SPMs that have been shown in the literature to possess anti-inflammatory and an-ti-tumorigenic attributes [28-30]. Previous studies have identified that dietary supple-mentation with fish oil or omega-3 PUFAs, as well as treatment using SPMs, effectively dampen lung inflammatory responses, and in some studies inhibits tumorigenesis [28,31-

33]. We have previously reported that the use of a DHA-rich diet significantly increases RvD1 levels in the lungs of HDE-exposed mice, however use of this SPM or its epimer as a therapeutic strategy for alleviating agricultural organic dust-induced inflammation have yet to be examined [31]. To build upon our previous investigations and assess the carcinogenic effects of HDE, as well as provide a therapeutic strategy for combatting HDE-induced chronic inflammation, we established a chronic dust exposure mouse model of lung carcinogenesis. A/J mice were exposed to HDE for 24 weeks while receiving a weekly i.v. treatment of AT-RvD1. Upon completion of the exposures, we assessed lung tumor burden, tissue histopathology, pathway and gene-expression alterations, and screened for biomarkers related to carcinogenesis and metastasis using the A549 lung adenocarcinoma cell line. Overall, these studies demonstrate the chronic lung inflammatory and carcinogenic properties associated with agricultural organic dust exposure and highlight the use of AT-RvD1 treatment as an effective therapeutic strategy for alleviating dust-induced inflammation.

2. Materials and Methods

2.1. Chemicals & Reagents

4-(Methylnitrosamino)-1-(3-pyridyl)-1-butanone (NNK) was purchased from Sigma Aldrich (St. Louis, MO). 17(R)-Resolvin D1 (AT-RvD1) was purchased from Cayman Chemicals (Ann Arbor, MI, USA). Interleukin-6 (IL-6), interleukin-10 (IL-10), and transforming growth factor beta-1 (TGFβ-1) Duoset ELISA kits were purchased from R&D Systems (Minneapolis, MN, USA).

2.2. Preparation of Hog Dust Extract

Agricultural organic dusts collected from swine confinement facilities were collected and prepared into aqueous extracts (HDE) as previously described [10,31]. In brief, settled dusts were collected off surfaces 1 m off the ground within indoor swine confinement facilities. These dusts were suspended in Hank's Balanced Salt Solution at a 100 mg/mL concentration. The aqueous mixture was then centrifuged and sterile filtered at 0.22 μm to form a 100% HDE extract (vol/vol) and stored in −20°C for later use. Using sterile phosphate-buffered saline (PBS), the 100% HDE was diluted to 12.5% HDE for all animal studies, and diluted to 1%, 2.5%, and 5% concentrations in cell culture medium for all cell-culture-related experiments. Characterization of the bacterial components of these dusts have been previously documented [3].

2.3. Animal Housing & Care

Male and female A/J mice 8-12 weeks of age were received from The Jackson Laboratory (Bar Harbor, ME, USA) and housed in micro-isolator cages (five per cage) at the University of California, Riverside animal barrier facilities. Mice were allowed unrestricted access to food and water, monitored for any behavioral or physiological changes, and weighed weekly (see Figure. S1 for weights at initial and final exposures). All experiments and procedures were approved by the University of California River-side Institutional Animal Care and Use Committee.

2.4. Chronic Dust Exposure Model

This study utilized a newly optimized mouse model of chronic lung disease using long-term exposure to HDE, which was adapted from prior acute and repetitive murine dust exposure models [11,34,35]. We used a total of 20 A/J mice for the preliminary study with 10 of them being HDE-treated and the other 10 saline-treated. Each mouse was lightly anesthetized by isoflurane inhalation prior to receiving a single intranasal challenge of either 50 uL of 12.5% HDE or 1x PBS, thrice weekly for 24 consecutive weeks. To study the tumorigenic potential of the dust in a chronic exposure setting, we used the tobacco-specific carcinogen NNK to induce lung tumorigenesis in the mice. At the start of week 4, we administered a one-time intraperitoneal injection (i.p.) of 100 mg/kg NNK, which has been well-established to generate lung adenomas in A/J mice 21 weeks post-injection [36,37]. Of the 20 exposed mice, 5 HDE-exposed and 5 saline-exposed were administered an i.p injection of NNK while the other 5 from each

respective group received 1x PBS via i.p injection as the control. Concluding the 24 weeks of HDE-exposure, mice were euthanized, blood was collected, and bronchoalveolar lavage fluid (BALF) retrieval was performed using three 1 mL washes with sterile saline. Each BALF wash was centrifuged, and the first aliquot was saved for cytokine analyses, while the pelleted cells from the second and third wash were combined with the first wash pellets and used to obtain total and differential immune cell counts (see Figure S2 for immune cell differential example). Counts were determined microscopically on cyto-centrifuge slides stained with Diff-Quik (Siemens, Newark, DE). Murine cytokine levels were measured using the cell-free BALF from the first PBS wash using mouse-specific ELISA kits. We examined the levels of IL-6, IL-10, and TGFβ-1 using commercially available kits (Duoset ELISA development kits, R&D Systems). Tumors were counted and excised from the left lungs following collection and half of the left lung was then stored in RNA later (Thermo Fisher, Waltham, MA, USA) for gene expression analyses while the other half was flash frozen in liquid nitrogen and stored at -80°C for oxylipin analysis (see Figure S3 for representative images of left and right lungs with tumors). Right lungs were inflated in formalin overnight at 25 cm pressure, and visible tumors were counted the next day to achieve total lung tumor counts per mouse.

2.5. Lung Histopathology Scoring

Fixed lungs were paraffin embedded and sectioned at 5 µm in preparation for subsequent staining and histological assessment. Slides were stained with hematoxylin and eosin (H&E; VWR, Radnor, PA) to visualize tumor and inflammatory pathology

such as lymphoid aggregate counts, bronchial and vascular inflammation, and alveolar inflammation (see Figure. S4 for bronchial/vascular inflammation and goblet cell hyperplasia lung tissue histology). To assess fibrotic changes within the lung tissues, we stained slides with Masson's Trichrome (IHC World, LLC., Ellicott City, MD). Goblet cell hyperplasia was determined via Alcian blue staining (IHC World, LLC., Ellicott City, MD). Each of these pathological outcomes were determined by blindly scoring each slide and collecting five images taken at either 10x or 20x objective, of each sample that were then assigned an individual score based on disease severity using an Echo Revolve brightfield micro-scope (San Diego, CA, USA). To assess bronchial/vascular inflammation, alveolar inflammation, and goblet cell hyperplasia, we assigned each image a number on a scale of 0 to 5 with 0 depicting no pathology and 5 representing severe pathology. Bronchial and vascular inflammation scoring criteria were determined by increased inflammation and cellularity around the lung airways and vasculature, as well as airway closure due to significant inflammation. Severe alveolar inflammation pathology was depicted by increased cellularity and reduced open area within the alveoli. Our criteria for goblet cell hyperplasia were based on how impacted the major airways were with goblet cells, with a score of 5 representing an airway fully encapsulated with goblet cells. The five images were then averaged to determine the final representative score for that respective sample. Lymphoid aggregate scoring was performed by counting the total number of lymphoid aggregates (assessed at 4x and 10x) and assigning a score of 0-5 based on the number of aggregates formed with 0 being no aggregates and 5 being twenty or more. We defined a lymphoid aggregate as a collection of thirty or more

closely packed lymphocytes. To assess changes in tissue fibrosis we employed the use of the Ashcroft's score which has been well established [38,39]. Ki-67 (1:200; #12202; Cell Signaling Technologies, MA, USA) staining to assess cell proliferation was achieved through immunohistochemistry as recommended by cell-signaling procedures (see Figure S5 for representative images of lung adenomas and lymphoid aggregates expression Ki-67).

2.6. AT-RvD1 Treatment Study

We have previously identified that mice fed a DHA-rich diet for 4 weeks prior to receiving a single intranasal dust challenge exhibited significantly elevated levels of the SPM, resolvin D1 (RvD1), compared to dust-exposed mice administered a control diet containing no DHA [31]. To build upon our previous findings, we opted to utilize a synthetic epimer of RvD1, AT-RvD1, as a therapeutic strategy to dampen the lung inflammatory and carcinogenic outcomes identified in the HDE-exposed mice from our 24-week exposure preliminary study. AT-RvD1 carries the same anti-inflammatory and pro-resolving properties as RvD1 but has a one-log order of increased potency and is much more resistant to rapid inactivation by eicosanoid oxido-reductase (EOR), which allows it to have a longer bioactive repair process [22,40]. We utilized the same 24-week exposure model as mentioned previously; however, this time incorporated a once weekly treatment of 500 ng AT-RvD1 administered by intravenous tail injection (i.v.) beginning the start of week 4 and ending on week 24. The AT-RvD1 was prepared into 500 ng/100 µL solution using a 100 ng/µL stock solution purchased from Cayman Chemicals (Ann

Arbor, MI, USA). The control mice received 5 µL of ethanol in 95 µL of sterile saline. The dosing and frequency of administration were adapted from previous studies [29,30,41]. Other than treatment with AT-RvD1, all animal handling procedures, dosing strategies, and major outcomes were the same in this study as the initial chronic exposure study mentioned previously, thus all data presented here will be the combination of both experimental studies. These studies were performed using male and female A/J mice which comprised 8 experimental groups: saline only, n=10; HDE only, n=10; saline+NNK, n=9; HDE+NNK, n=9; saline+AT-RvD1, n=8; HDE+AT-RvD1, n=6; saline+NNK+AT-RvD1, n=7; and HDE+NNK+AT-RvD1, n=6.

2.7. Oxylipin Analysis

Frozen left lung tissues were thawed and weighed, then 10 µL of antioxidant solution (0.2 mg/mL of Butylated hydroxytoluene (BHT) and Ethylenediaminetetraacetic acid (EDTA), 10 µL of internal standard mix, and 400 µL of ice-cold methanol containing 0.1 % of acetic acid, were added onto the tissue samples in preparation of oxylipin analysis, as previously reported [42]. In brief, tissues were homogenized then centrifuged to retrieve the supernatant while the remaining pellets were washed with 100 µL of ice-cold methanol with 0.1 % of acetic acid and 0.1% of BHT and centrifuged. The supernatants of each sample were diluted with 2 mL of H2O and loaded onto Oasis-HLB cartridges (Waters Corp., Milford, MA, USA) to be processed via solid-phase extraction (SPE). The cartridges (30 mg/30 µm) were washed with ethyl acetate (1 mL), methanol (2 × 1 mL), and 95:5 v/v water/methanol with 0.1% acetic acid (1 mL). The extracted

supernatant was loaded on the cartridge and washed twice with 20% methanol. The cartridges were dried under vacuum and analytes were eluted from SPE cartridges into tubes with 250 μL of methanol followed by 1 mL of ethyl acetate into 2 mL tubes containing 6 μL of 30% glycerol in MeOH as a trap solution. The eluted fraction was dried under nitrogen and the residues reconstitute in 70 μL of methanol containing 20 nM 1-cyclohexyluriedo-3-dodecanoic acid (CUDA). Samples were vortexed for 5 min, then transferred to autosampler vials and stored at -20 °C until analysis. Following SPE, targeted oxylipin estimation was performed using a QQQ XEVO TQ-XS (Waters Corp., Milford, MA, USA) at the UC Riverside Metabolomics Core. The liquid chromatography–mass spectrometry (LC-MS) autosampler was maintained at 4 °C prior to analysis. For oxylipins analysis, injection volume of 3 μL of the extract was used. The separation was performed on the Ascentis Express column (2.1×150 mm, 2.7 μm particles; Sigma-Aldrich Supelco, St. Louis, MO, USA). The flow rate was maintained at 0.35 mL/min at 40 °C. Solvent A consisted of water with 0.1% acetic acid while solvent B was comprised of 90:10 v/v acetonitrile/isopropanol. The gradient separation method was used as follows: 26 min (0–3.5 min from 15 % B to 33 % B; 3.5–5.5 min B to 38 %, 5–7 min to 42 % B; 7–9 min to 48 % B; 9–15 min to 65 % B; 15–17 min to 75 % B; 17–18.5 min to 85% B; 18.5–19.5 min to 95 % B; from 19.5 to 21 min to 15 % B, 21–26 min 15 % B).. The MS data was acquired on multiple reaction monitoring (MRM) mode. The electrospray ionization was performed in negative ion mode. The source and desolvation temperatures were maintained at 150° C and 500° C, respectively. Desolvation gas was set to 1000 L/hr and cone gas to 150 L/hr and the collision gas was set to 0.15 mL/min.

All gases used were nitrogen other than the collision gas which was argon. The capillary voltage was 1 kV. Samples were normalized for relative abundance against the internal standards while normalization for absolute quantification was performed in relation to the mg of lung tissue used from each sample. Data processing (peak integration) was performed with Skyline software (Herndon, VA, USA).

2.8. NanoString Gene Expression Analyses

Of the 65 total mice used in these studies, 24 left lung tissues were randomly selected among the saline-only, HDE-only, saline+NNK, and HDE+NNK-exposed groups, for transcript and pathway gene expression analyses using the NanoString platform. Left lung tissues were homogenized and RNA was extracted using the PureLink RNA Mini Kit (Invitrogen, Carlsbad, California, USA) and sample quality was quantified using the NanoDrop ND-100 (NanoDrop Technologies, Inc, Wilmington, DE, USA) and an Agilent 2100 Bioanalyzer (UC Riverside Core Facilities, Agilent Technologies, Santa Clara, CA, USA). We utilized the mouse PanCancer Immune Profiling Panel (NanoString Technologies, Seattle, WA, USA) codeset which is a pre-designed panel containing 770 target genes related to immune response and carcinogenesis. Sample preparation was performed by mixing 50 ng of total RNA with the codeset and reporter probes and hybridizing the mixture for 16 hrs to form the desired target-probe complex. The hybridized complex was then plated and run on a nCounter Sprint profiler to image and quantify the data. Following sample processing, the data were downloaded and analyzed using the nSolver software (version 4.0, NanoString

Technologies, Seattle, WA, USA). Manual normalization of the expression data was performed using the geometric mean of the housekeeping genes EEF1G, OAZ1, RPL19, and SDHA. Proceeding sample normalization, 21 of the 24 samples passed the normalization parameters and were deemed viable for subsequent analyses. The samples breakdown are as follows: 6 sa-line-only, 4 HDE-only, 6 saline+NNK, and 5 HDE+NNK. Protein-protein interactions of differentially expressed genes were examined using the STRING database. Raw NanoString data are deposited at in the GEO database [link provided upon publication].

2.9. Culturing of A549 lung cells

Human lung adenocarcinoma-derived A549 (CCL-185) cells (ATCC, Manassas, VA USA) were grown on non-coated T-75 flasks and cultured using ATCC F-12 K medium with 10% fetal bovine serum and 1% penicillin-streptomycin in 5% CO2 at 37 °C. Cells were grown until at least 75% confluency, then passaged using TrypLE Express (Thermo Fisher, Waltham, MA, USA). For all HDE exposure studies, cells were seeded then treated 24 hrs later with either 0%, 1%, 2.5%, or 5% (vol/vol) HDE for 48 hrs. All preventative studies required cells be pre-treated for 1 hr using 1 ng/mL, 10 ng/mL, 20 ng/mL or 100 ng/mL of AT-RvD1 24 hrs after seeding, then immediately treated with 5% HDE for 48 hrs. Dosing strategies for all HDE and AT-RvD1 experiments were determined based on investigations from previous in vitro investigations [43-45].

2.10. Western Blotting

Cell lysates were harvested from A549 cells, and proteins were resolved by SDS-PAGE and electro transferred to PVDF membranes where primary antibodies against E-cadherin (1:2000; #610181, BD Biosciences, USA), N-cadherin (1:1000; #610921, BD Biosciences, USA), and vimentin (1:500; sc-6260, Santa Cruz Biotechnology, USA) were used. Corresponding secondary horseradish peroxidase-conjugated antibodies (1:2000; Santa Cruz Biotechnology, USA) were used to detect primary antibodies on the membrane. Membranes were developed using BioRad Clarity Western ECL Substrate reagent in BioRad ChemiDoc imaging system (BioRad, Carlbad CA, USA). Protein levels were quantified by densitometry using Fiji open-source software (Image J version 1.52p).

2.11. Bioinformatics Data Processing and Analyses

A549 cells underwent live cell imaging using a BioStation CT incubator (Nikon Instruments, Tokyo, Japan) for 48 hrs after being treated with HDE. We used CL-Quant (DR Vision, Seattle, WA) and CellProfiler (open-source) software, to process BioStation captured images, and MATLAB (MathWorks Natick, MA, USA) machine learning algorithm to classify cell morphology [44,46]. The time-lapse images were captured in phase contrast every 15 minutes for 48 hrs. Time-lapse images were imported into CL-Quant to segment individual cells and to process phase contrast images into binary images of cells' silhouette. Following segmentation, binary images were imported into CellProfiler which assigned object numbers to each cell and extracted morphological

features from these cells. We imported these data into MATLAB and used 11 morphological features (area, major axis length, minor axis length, maximum radius, median radius, perimeter, and numbers of nearby cells) to developed machine learning library consisted of 300 total sampled cells. The machine learning algorithm used the training library to automatically categorize cells into cobblestone (standard A549 morphology) or elongated (mesenchymal-shaped). This library allows for a non-biased determination of cellular morphology with 97% accuracy in detection of each of the morphology classes. Total number of cells in each image was used to normalize the two categories. All data presented underwent automatic morphology classification using a combination of these softwares.

2.12. Statistical Analyses

All statistical analyses and graphing were performed using GraphPad Prism Software (Version 9.3.1; San Diego, CA, USA). Data are reported as the mean ± standard error of the mean for all graphs and figures. All statistical calculations performed for animal data are depicted using either two- or three-way ANOVA with Tukey's post-hoc test for multiple comparisons between the groups. Significance for all reported data was set at $p \leq 0.05$. On all appropriate graphs, the # symbol is used to indicate significant differences in post-hoc comparisons between the AT-RvD1 and non-AT-RvD1-treated groups. The * symbol is used to indicate significant post-hoc differences between saline and HDE-exposed mice within each respective NNK-exposed group. All data presented underwent a Grubb's outlier test to exclude statistical outliers. Western blot data are

presented in relation to the 0% HDE-control group and t-tests using hypothetical value of 1 were used to measure significant fold change relative to normalized 0% HDE-control group. Cell morphology changes are analyzed with one-way ANOVA with Dunnett's post-hoc test. Manual sample QC and normalization for the NanoString gene expression panels was accomplished by eliminating gene probes with less than 87 counts from the data set. The threshold count was determined through background subtraction (mean +/− two standard deviations of negative controls) to screen for bio-logical or technical variation within the sample sets without bias. All differentially ex-pressed genes were assessed using raw p-values. Subsequent clustering figures were produced using nCounter Analysis and Advanced Analysis packages in nSolver 4.0 (NanoString Technologies, Seattle, WA, USA).

3. Results

3.1. AT-RvD1 Reduces Cellular Recruitment Into the Airways of Dust-Exposed Mice

Our previous single and repetitive (15 instillations over 3 weeks) HDE-exposure studies have shown that HDE exposure elicits a significant increase in total and immune cell recruitment into the airways of mice [32,34]. No study has yet investigated the chronic impact of agricultural dust exposure in mice and thus, this study sought to address that gap in knowledge by examining the effects of 24 weeks of HDE exposure. Moreover, we have previously identified that both the supplemented use of a DHA-rich diet or administration of omega-3 derived SPMs to mice, dampened the dust-induced lung inflammatory response within both our single and repetitive dust exposure mouse models [31,32,34,47]. To build on our previous investigations, we opted to administer 500 ng via tail i.v. of the SPM AT-RvD1 once weekly for 21 weeks as a therapeutic strategy to mitigate lung inflammation and carcinogenesis associated with 24 weeks of HDE exposure in A/J mice (Figure 1).

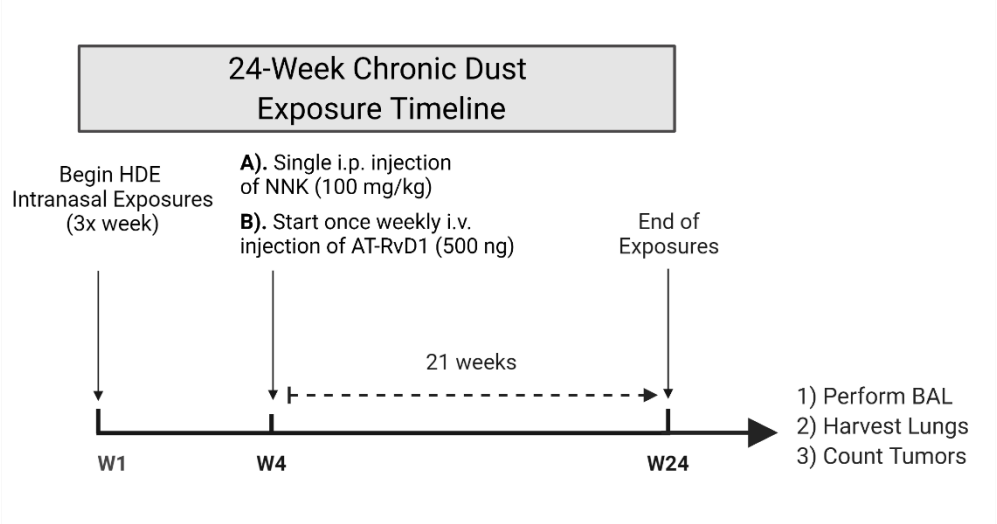

Figure 1. Schematic of our chronic dust exposure mouse model and dosing timeline. Male and female A/J mice received 24 weeks of intranasal challenges of 12.5% HDE, a single i.p. injection of 100 mg/kg NNK to induce tumorigenesis, and a once weekly tail i.v. of 500 ng AT-RvD1 for 21 weeks.

We found that chronic HDE exposure, independent of NNK administration, had a significant ($p < 0.0001$) effect on total cell influx into the lung airways of mice (Figure 2A). This effect of HDE was also seen with macrophage (Figure 2B), neutrophil (Figure 2C), lymphocyte (Figure 2D), and eosinophil (Figure 2E) recruitment into the lung airways. We also saw a significant main effect of AT-RvD1 treatment within neutrophil (Figure 2C; $p < 0.0001$), lymphocyte (Figure 2D; $p = 0.008$), and eosinophil (Figure 2E; $p = 0.0002$) immune cells in the BALF. Interestingly, HDE-exposed mice treated with AT-RvD1 had significantly reduced levels of neutrophils in the BALF compared to HDE only (Figure 2C; $p = 0.0003$) and HDE+NNK-exposed mice (Figure 2C; $p < 0.0001$). Further assessment identified significant reductions of lymphocyte recruitment in HDE+NNK+AT-RvD1-exposed mice (Figure 2D; $p = 0.007$), compared to HDE+NNK-exposed mice. We also identified significant reductions in eosinophil cell influx into the

lungs of HDE+AT-RvD1-exposed (Figure 2E; p = 0.01) and HDE+NNK+AT-RvD1-exposed mice (Figure 2E; p = 0.002), compared to their HDE-counterparts.

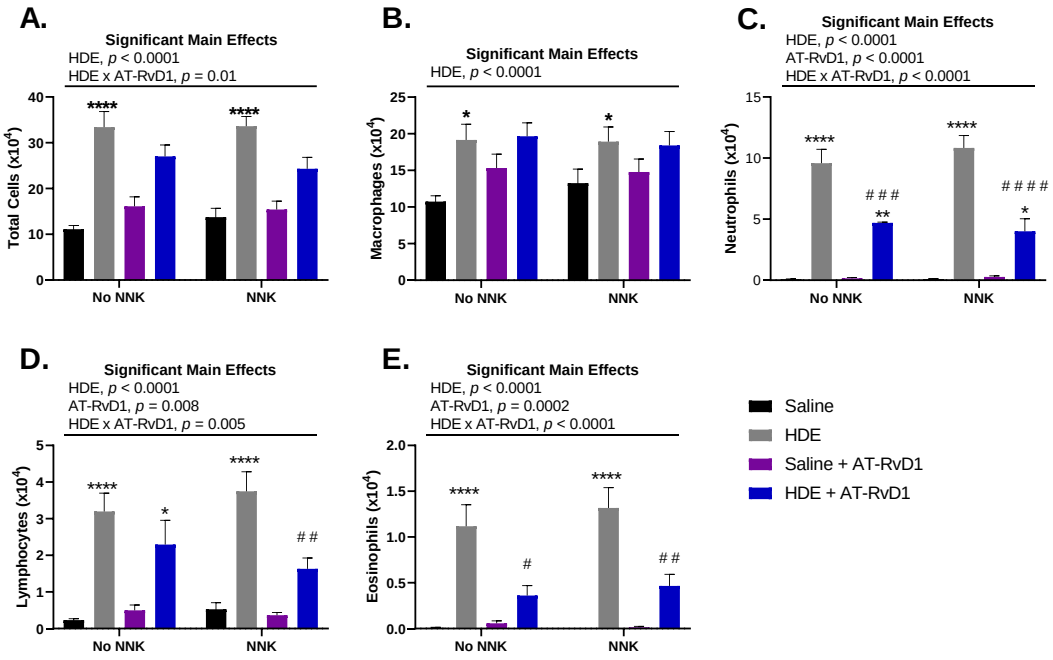

Figure 2. Total and immune cell counts in A/J mice following chronic HDE exposure and AT-RvD1 treatment. Following 24 weeks of HDE exposure, mice were euthanized and bronchoalveolar lavage fluid was collected and assessed for total (A) macrophage (B), neutrophil (C), lymphocyte (D), and eosinophil (E) cell influx into the lung airways of the mice. Main significant effects and interactions are presented above each graph as depicted from three-way ANOVA analysis. The * symbol above the HDE bars represents the statistical post-hoc comparisons between the HDE- and saline-treated conditions within each respective NNK-administration groups; (* $p < 0.05$; ** $p < 0.01$; **** $p < 0.0001$). Post-hoc comparisons between HDE+AT-RvD1-exposed mice and their non-AT-RvD1 treated counterparts are depicted by the # symbol above each HDE+AT-RvD1 (control and NNK) bar; (# $p < 0.05$; ## $p < 0.01$; ### $p < 0.001$; #### $p < 0.0001$).

HDE exposure has been well characterized to elicit a potent pro-inflammatory response that includes the secretion of pro-inflammatory cytokines into the lung air-ways of exposed mice [4,48]. Alternatively, omega-3 fatty acids and their respective SPMs are known to be anti-inflammatory and thus drive an increased release of related anti-

inflammatory and pro-resolving cytokines [49-51]. We observed a significant main effect of HDE for the secretion the pro-inflammatory cytokine IL-6 (Figure 3A; p = 0.01), anti-inflammatory cytokine IL-10 (Figure 3B; p = 0.01), and pro-EMT cytokine TGFβ-1 (Figure 3C; p = 0.001), in the BALF of exposed mice. We found a significant main effect of AT-RvD1 treatment and increased levels of BALF IL-10 (Figure 3C; p = 0.05) detected in exposed mice. Post-hoc comparisons within TGFβ-1 BALF levels identified a significant increase in the HDE-exposed mice compared to the saline control mice (Figure 3B; p = 0.001).

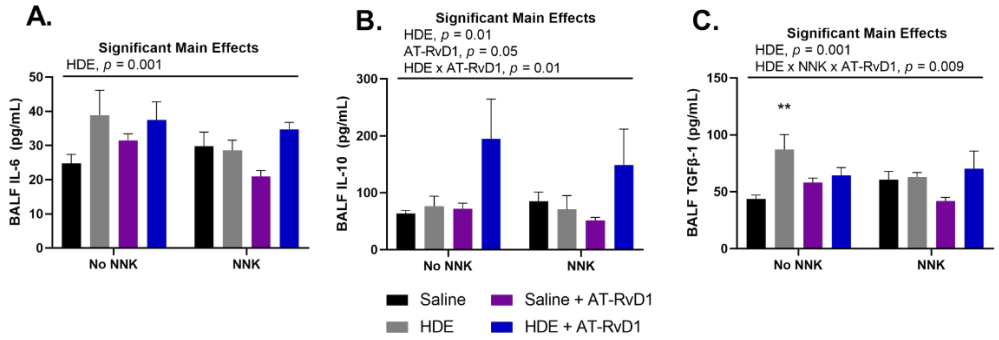

Figure 3. Effects of chronic HDE exposure and AT-RvD1 treatment on BALF cytokine levels after 24 weeks. Bronchoalveolar lavage was performed at the end of the 24 weeks and the fluid was collected to assess cytokine levels as described in the methods. For IL-6 (A), IL-10 (B), and TGFβ-1 (C); n = 5-10 for saline only; n = 7-8 for HDE only; n = 6-7 for saline+NNK; n = 6-9 for HDE+NNK; n = 5-8 for saline+AT-RvD1; n = 5 for HDE+AT-RvD1; n = 5-6 for saline+NNK+AT-RvD1; n = 4-5 for HDE+NNK+AT-RvD1. Main significant effects and interactions from three-way ANOVA analysis are shown above each graph. The * symbol above the HDE bar represents the statistical post-hoc comparison to the saline control group; (** p < 0.01).

3.2. Fatty Acid Levels in Murine Lung Tissues

Left lung tissues were harvested and used for oxylipin analysis using a pre-designed panel of fatty acids and oxylipins, such as eicosanoids and SPMs. Lung tissue samples were processed using Triple Quadrupole LC-MS following 24-weeks of

exposure to HDE. Samples were normalized to relative and absolute quantification using the Skyline data processing software (Herndon, VA, USA). All oxylipins presented in Figure 4 had a significant main effect of HDE ($p < 0.05$) for relative abundance in the lung tissues, while prostaglandin D2 (PGD2) and resolvin E1 (RvE1) also had a main effect of NNK (Figure 4B; $p = 0.02$ and Figure 4H; $p = 0.006$), respectively. There was a significant main effect of AT-RvD1 for relative abundance of prostaglandin F1 alpha (PGF1a; Figure 4C; $p = 0.009$), prostaglandin F2 alpha (PGF2a; Figure 4D; $p = 0.02$), and RvE1 (Figure 4H; $p = 0.004$) in the lungs of exposed mice. Levels of PGD2 were significantly elevated in HDE ($p < 0.0001$) and HDE+AT-RvD1 ($p = 0.0005$) samples, compared to the saline control. We also identified a significant increase in PGD2 levels in HDE+AT-RvD1 exposed mice ($p = 0.006$) versus the saline+AT-RvD1-exposed group, Figure 4A. Relative abundance of prostaglandin E2 (PGE2) was significantly greater in HDE ($p = 0.0002$) and HDE+NNK ($p = 0.03$)-exposed mice, compared to their respective saline controls, Figure 4B. Post-hoc comparisons did identify a significant increase in PGE2 levels within the HDE+AT-RvD1-exposed mice when compared to saline-exposed ($p = 0.003$) and saline+AT-RvD1-exposed ($p = 0.02$), Figure 4B. Thromboxane B2 (TXB2) was elevated in HDE ($p = 0.0007$) and HDE+NNK ($p = 0.008$), compared to their respective saline controls, Figure 4E. We also saw an increase in TXB2 among HDE+AT-RvD1 ($p = 0.01$) versus saline-exposed samples, Figure 4E. The SPM, resolvin E1 (RvE1) was significantly elevated in HDE+AT-RvD1 compared to all other experimental groups, Figure 4H. NNK-exposed mice had reduced abundance of these oxylipins compared to those not administered NNK, however this trend was not

significant. Levels of PGD2, PGE2, PGF2a, TXB2, and LXA4 were all above the limit of detection when normalized for absolute quantification in mg of tissue.

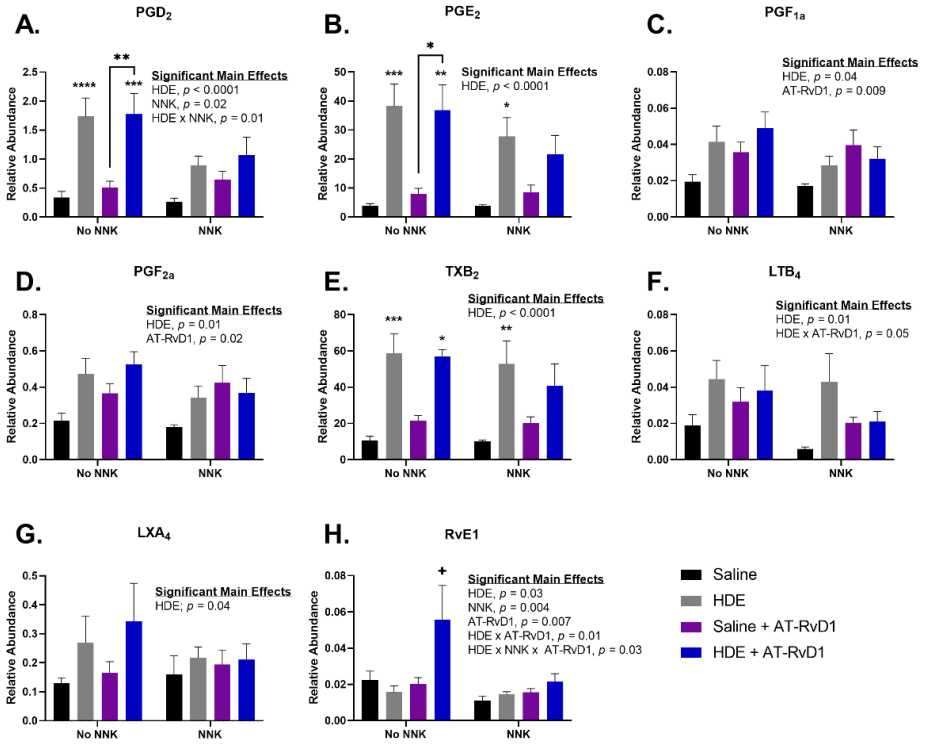

Figure 4. Pro-inflammatory eicosanoid and pro-resolving SPM levels in mice lung tissues following 24 weeks of HDE exposure. Oxylipin analysis was performed to assess the relative abundance of fatty acids and their bioactive mediators in murine lung tissue after chronic dust exposure. Three-way ANOVA with Tukey's post-hoc comparisons were performed to examine statistical changes between the experimental groups. Significant main effects and interactions of HDE, NNK, and AT-RvD1 are shown above each oxylipin. The * above the HDE samples represents significance compared to the saline-control in the respective NNK-group; (* $p < 0.05$; ** $p < 0.01$; *** $p < 0.001$; **** $p < 0.0001$). The + symbol above the HDE+AT-RvD1 bar depicts all post-hoc comparisons are significant between each other experimental group; ($p < 0.05$).

3.3. Chronic Dust Exposure Enhances Lung Tumorigenesis in Mice

Male and female A/J mice ages 8-12 weeks of age were intranasally challenged with 50 µL of 12.5% HDE three times a week for 24 weeks. To induce lung tumorigenesis, we performed a one-time 100 mg/kg i.p. injection of the tobacco-derived

carcinogen, NNK, at the start of week 4. Treatment was performed using a once-weekly 500 ng tail vein injection of AT-RvD1 beginning at the start of week 4 and extending until the end of the 24 weeks of HDE exposure. At the conclusion of the 24 weeks, mice were euthanized, and total tumor counts were assessed by combining counts from each lung. Tumors were determined to be lung adenomas through histopathological assessment. Tumor incidence and mean counts for each experimental group can be seen on Table 1. **Table 1.** Lung Tumor Incidence and Multiplicity in A/J Mice Treated with NNK, Swine Dust Extract, and AT-RvD1.

Experimental Group	**% Of Mice with Lung Tumor [a]**	**Lung Tumor/ mouse $\pm$ SE [a]**	**Confidence Interval (95%)**
Saline Only	0	0	(0.00 – 0.00)
Saline + AT-RvD1	0	0	(0.00 – 0.00)
HDE Only	20	0.20 $\pm$ 0.13	(0.00 – 0.50)
HDE + AT-RvD1	0	0	(0.00 – 0.00)
Saline + NNK	100	2.38 $\pm$ 0.46	(1.29 – 3.46)
Saline + NNK + AT-RvD1	100	3.57 $\pm$ 0.57	(2.17 – 4.97)
HDE + NNK	100	5.33 $\pm$ 1.18	(2.62 – 8.054)
HDE + NNK + AT-RvD1	100	6.33 $\pm$ 1.15	(3.39 – 9.28)

[a]Assessed through macroscopic and microscopic examination for lung adenomas.

We identified two main significant effects for tumor formation including main effects of NNK ($p < 0.0001$) and HDE ($p = 0.001$), Figure 5. There was also a significant interaction for lung tumor formation between HDE and NNK ($p = 0.003$). Mice exposed to HDE+NNK, had significantly elevated tumors ($p = 0.02$) compared to the saline+NNK control for tumorigenesis. HDE+NNK-exposed mice treated with AT-RvD1, had significantly greater lung tumors ($p = 0.002$), compared to the baseline saline+NNK-

exposed mice. HDE-exposed mice had significantly less tumors than HDE+NNK ($p < 0.0001$), saline+NNK+AT-RvD1 ($p = 0.005$), and HDE+NNK+AT-RvD1 ($p < 0.0001$)-exposed mice. There was no significance between HDE and saline+NNK-exposed mice.

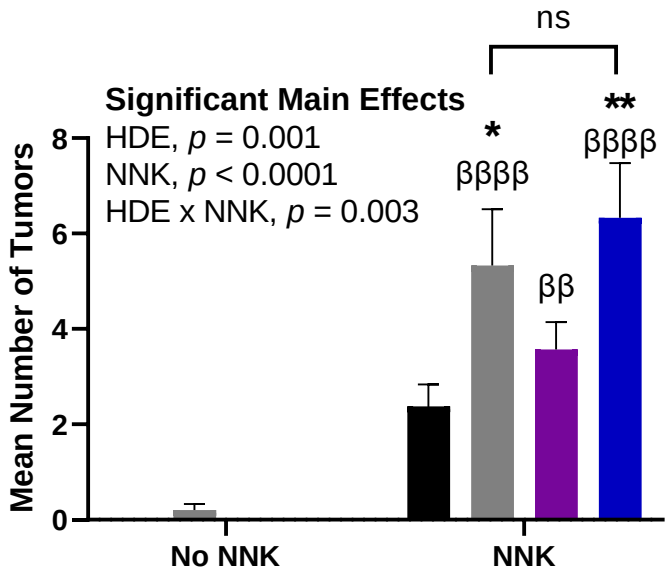

Figure 5. Mean lung tumor counts in mice following 24 weeks of chronic dust exposure. Right and left murine lung tissues were assessed for lung tumors following mouse euthanasia. The β symbol above each NNK sample bar represents statistical significance versus the HDE-only exposed mice (ββ $p < 0.01$; ββββ $p < 0.0001$). The * symbol above each of the bars represents statistical significance in relation to the NNK+saline-exposed control group; (* $p < 0.05$; ** $p < 0.01$).

3.4. AT-RvD1 Alters Dust-induced Lung Histopathology Outcomes

Blinded scoring was performed to evaluate the lung tissues for histopathological outcomes including lymphoid aggregates, bronchial and vascular inflammation, goblet cell hyperplasia, alveolar inflammation, and tissue fibrosis (Figure 6). We observed a significant main effect of HDE exposure ($p < 0.0001$) for each of these outcomes of interest, and a main effect of AT-RvD1 treatment for alveolar inflammation (Figure

6E,G; $p < 0.0001$) and tissue fibrosis (Figure 6F,H; $p = 0.0004$), with each parameter exhibiting significant upregulation in HDE exposed mice vs. saline-treated mice ($p < 0.05$ for all features). Alveolar cell hyperplasia (Figure 6E,G) was significantly elevated within HDE-exposed ($p = 0.01$) and HDE+NNK-exposed ($p < 0.0001$), compared to their respective saline conditions. In HDE+NNK-exposed mice treated with AT-RvD1, alveolar hyperplasia was significantly worse (Figure 6E,G; $p = 0.03$) compared to saline+NNK-exposed mice treated with AT-RvD1. We did identify that HDE+NNK-exposed mice had significantly greater ($p = 0.03$) alveolar inflammation and cellularity compared to the HDE-only condition. HDE-exposed mice treated with AT-RvD1 did experience reduced inflammation and cellular influx in the alveolar space compared to the non-AT-RvD1 treated mice, with significance being greater in NNK-treated ($p = 0.0005$) than non NNK-treated groups ($p = 0.01$). Severe tissue fibrosis (Figure 6F,H) was observed in HDE-exposed mice compared to the saline conditions within the no NNK ($p = 0.002$) and NNK-treated conditions ($p = 0.003$). Increased fibrotic changes were also identified in HDE+NNK+AT-RvD1-exposed mice versus the saline+NNK+AT-RvD1-group (Figure 6F,H; $p = 0.008$). Ki-67 IHC staining showed expression within lymphoid aggregates of HDE-exposed mice and within lung adenomas of NNK-administered mice, Figure S5.

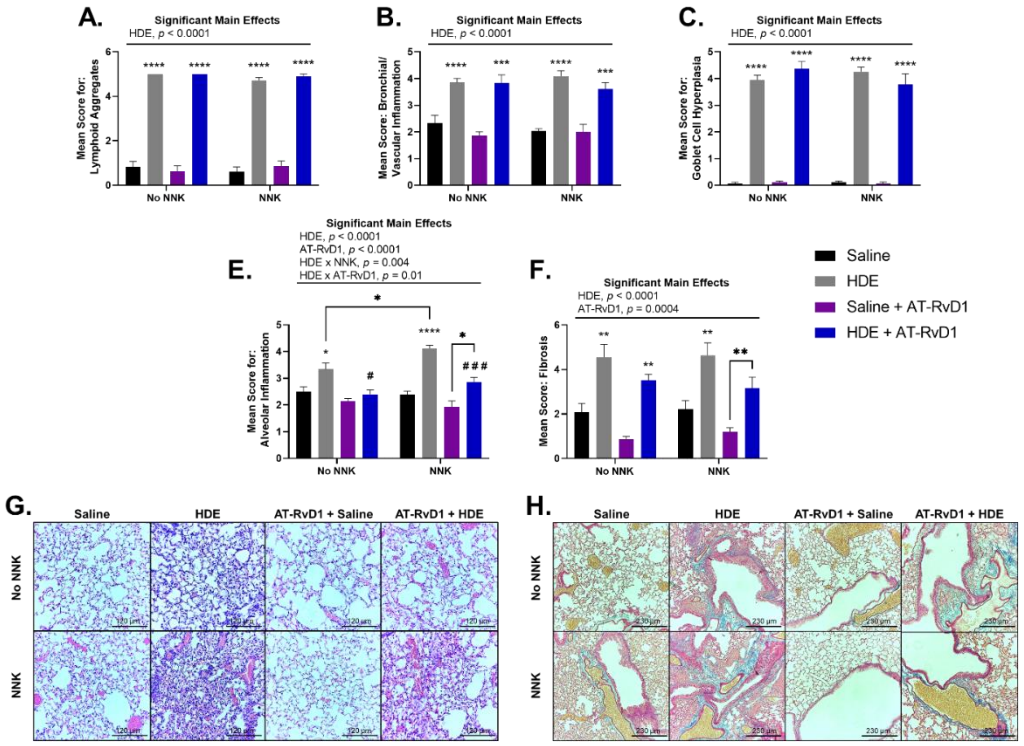

Figure 6. Murine lung tissue histopathology and scoring following chronic HDE exposure and AT-RvD1 treatment. Left lung tissues of mice were sectioned and blindly scored for tissue pathogenesis including (A) lymphoid aggregates (B) bronchial/vascular inflammation (C) goblet cell hyperplasia (D) alveolar inflammation (E) fibrosis. Lung tissues were stained with H&E to visualize (G) alveolar inflammation (imaged at 20x) and Masson's Trichrome for (H) tissue fibrosis (imaged at 10x). Significant main effects and interactions of HDE, NNK, and AT-RvD1 are shown above each histological scoring parameter. The * symbol above each of the HDE bars represents statistical significance in relation to their respective saline-exposed group; (* $p < 0.05$; ** $p < 0.01$; *** $p < 0.001$; **** $p < 0.0001$). Post-hoc comparisons between HDE+AT-RvD1-exposed mice and their non-AT-RvD1 treated counterparts are depicted by the # symbol above each HDE+AT-RvD1 bar; (# $p < 0.05$; ### $p < 0.001$). Direct post-hoc comparisons between HDE and saline AT-RvD1-treated mice are represented by the * symbol and lines connecting those graphs.

3.5. HDE Drives Increased Inflammation- and Cancer-related Gene Expression

Transcript and pathway-level gene expression changes were assessed in the lungs of HDE- versus saline-exposed mice using the NanoString mouse PanCancer Immune

Profiling Panel. We performed an advanced analysis of the 21-sample data set including 6 saline-only, 4 HDE-only, 6 saline+NNK, and 5 HDE+NNK-exposed samples, using the nSolver software. Following sample normalization, we performed a principal component analysis (Figure 7A) which showed a clear separation of HDE and saline samples, as well as clustering being driven by HDE exposure, not NNK. Furthermore, the advanced analysis identified 129 differentially expressed ($p < 0.05$) genes between the HDE vs. saline samples sets (Figure 7B), and 3 differentially expressed genes between the HDE vs. HDE+NNK-exposed mice, Figure 7C.

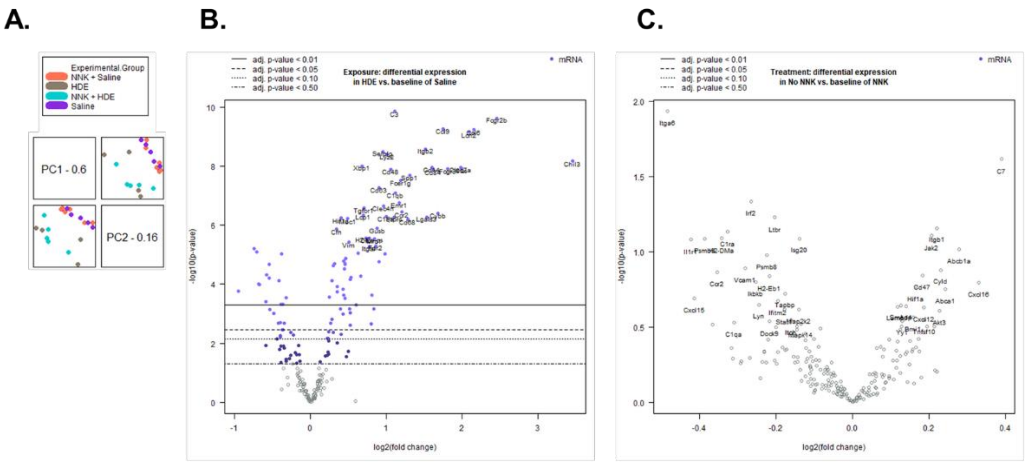

Figure 7. Sample clustering and differential gene expression are driven by HDE exposure. (A) Principal component analysis shows a separation of sample association is determined by dust, not NNK exposure. (B) Volcano plot of differentially expressed genes between HDE- and saline-exposed mice following 24 weeks of exposure (C) Volcano plot of differentially expressed genes between HDE- and HDE+NNK-exposed mice following 24 weeks of HDE exposure.

Using the STRING database, we input the 129 differentially expressed genes and identified significant protein-protein interactions ($p < 1.0e-16$) for these genes. In-depth investigations into the interactions of these 129 differentially expressed genes were

performed, and we identified sub-sets of these genes related to immune cell interactions, with an emphasis on macrophage functions (Table 2) and cancer progression (Table 3).

Table 2. Dust-induced Differentially Expressed Genes ($p < 0.05$) Related to Immune Cell Interactions.

Gene Symbol	Fold Change (HDE vs. Saline)
CCL6	4.43 ↑
CCL9	3.37 ↑
CCR2	2.30 ↑
CD14	3.03 ↑
CD68	2.44 ↑
CD84	3.08 ↑
CHIL3	10.9 ↑
CLEC7a	3.95 ↑
CSF1R	1.23 ↑
CXCR4	1.18 ↑
FPR2	1.81 ↑
IL13Ra1	1.35 ↑
JAK2	1.21 ↑
LCN2	4.26 ↑
MRC1	1.79 ↑
STAT1	1.25 ↓
TLR4	1.35 ↑

Table 3. Differential Expression of Cancer Progression Related Genes ($p < 0.05$) in HDE-exposed Mice.

Gene Symbol	Fold Change (HDE vs. Saline)
CD274	1.87 ↑
CD9	1.14 ↑
CDH1	1.12 ↓
FN1	1.44 ↑
KDR	1.63 ↓
LAMP1	1.24 ↑
MUC1	1.40 ↑
TGFB1	1.38 ↑
TGFBR1	1.63 ↑
VEGFA	1.68 ↓
VIM	1.42 ↑

Table 4. Differential Expression of Genes ($p < 0.05$) in HDE vs. HDE+NNK-exposed Mice.

Gene Symbol	Fold Change (HDE vs. HDE+NNK)
C7	1.40 ↓
ITGA6	1.31 ↑
IRF2	1.20 ↓

The advanced analysis generated z-scores produced from the HDE vs. saline gene expression data that we then plotted and analyzed by two-way ANOVA to assess for significant pathway changes. Genes related to inflammation, cancer progression, innate immunity, adaptive immunity, and macrophage cell function pathways (Figures 8A-D,F), all generated a mean z-score that was associated with a significant up-regulation driven by HDE-exposure, but not NNK administration. Conversely, genes associated with cell adhesion (Figure 8E) showed a significant reduction ($p < 0.001$) in expression within the HDE-exposed group compared to the saline control group. Further examination of genes

specifically related to cancer progression (Figure 9) showed increased expression changes and clustering being driven by HDE samples, independent of NNK.

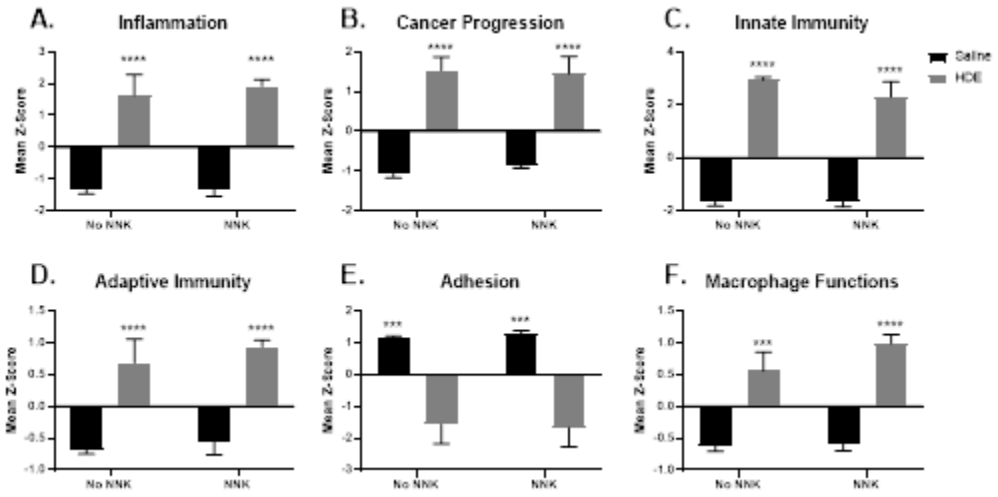

Figure 8. Significantly altered pathway expression changes among the 21 HDE and saline- exposed mouse lungs. NanoString Advanced Analysis was performed and the z-scores for each sample pertaining to generalized cancer and immunological-related pathways were assessed including: (A) inflammation (B) cancer progression (C) innate immunity (D) adaptive immunity (E) adhesion (F) Macrophage cell functions. The * symbol above the HDE bars represents significance against all saline-treated conditions within each respective NNK-group; (*** $p < 0.001$; **** $p < 0.0001$).

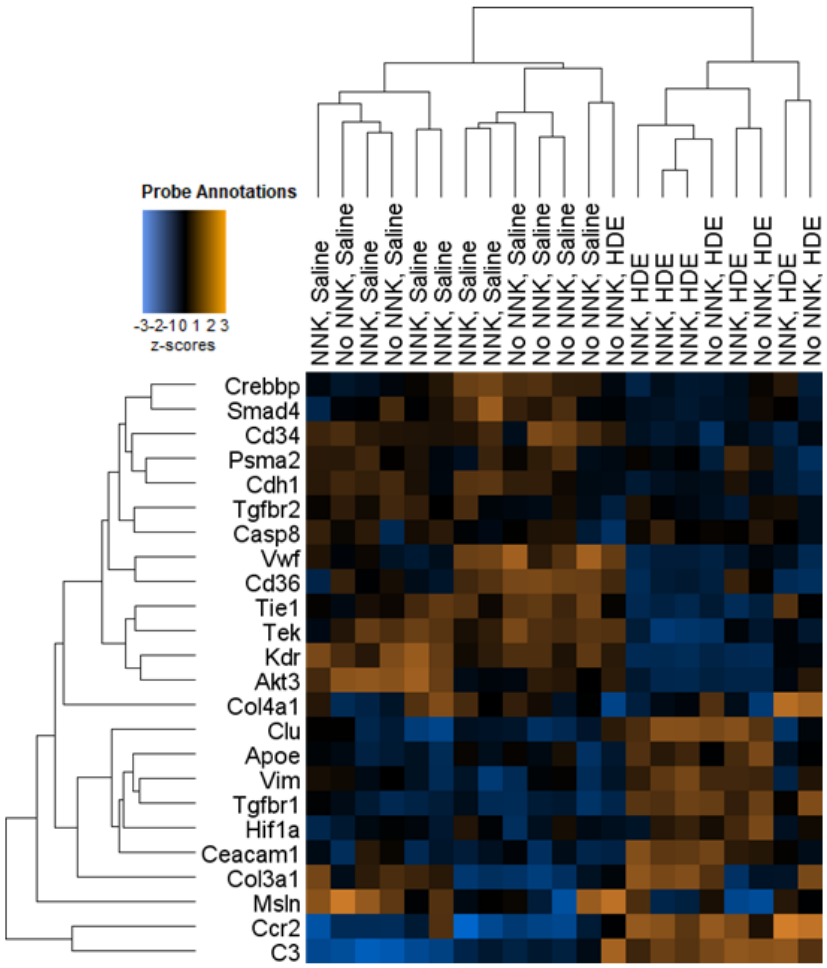

Figure 9. Heat map showing hierarchal clustering of cancer progression-related genes and expression changes for the 21 HDE and saline murine lung samples used in NanoString analysis.

3.6. Agricultural Dust Exposure Induces EMT in Human Lung Adenocarcinoma Cells

The results from our chronic in vivo studies suggested that dust exposure enhances lung tumorigenesis with alterations in several genes associated with epithelial to mesenchymal transition (EMT; e.g. *CHD1*, *FN1*, *TGFB1*, *VIM*). To confirm these

findings, we next assessed the pro-carcinogenic EMT potential of the dust using human lung adenocarcinoma cells (A549). We used a Biostation CT Incubator (Nikon Instruments, Tokyo, Japan) to capture time-lapse images of A549 cells treated with 0% (control), 1%, 2.5%, or 5% HDE over 48 hrs. Time-lapse images were captured in phase contrast and imported into CL-Quant software (DR Vision, Seattle, WA) to segment individual cells and convert the phase contrast image into binary images, which were imported into CellProfiler software to extract morphological features of each segmented cell. The morphological data were imported into MATLAB software (MathWorks Natick, MA, USA) equipped with a custom machine learning algorithm to classify cells based on their morphological data [44,46]. Data processing using these bioinformatic softwares identified differences in cell morphology following treatment, including cells appearing cobblestone (standard A549 morphology) or elongated (mesenchymal-like). Cells treated with 5% HDE had significantly ($p = 0.02$) greater number of elongated cell populations, and significantly fewer number of cobblestone cells ($p = 0.02$) compared to the 0% control-group, Figure 10.

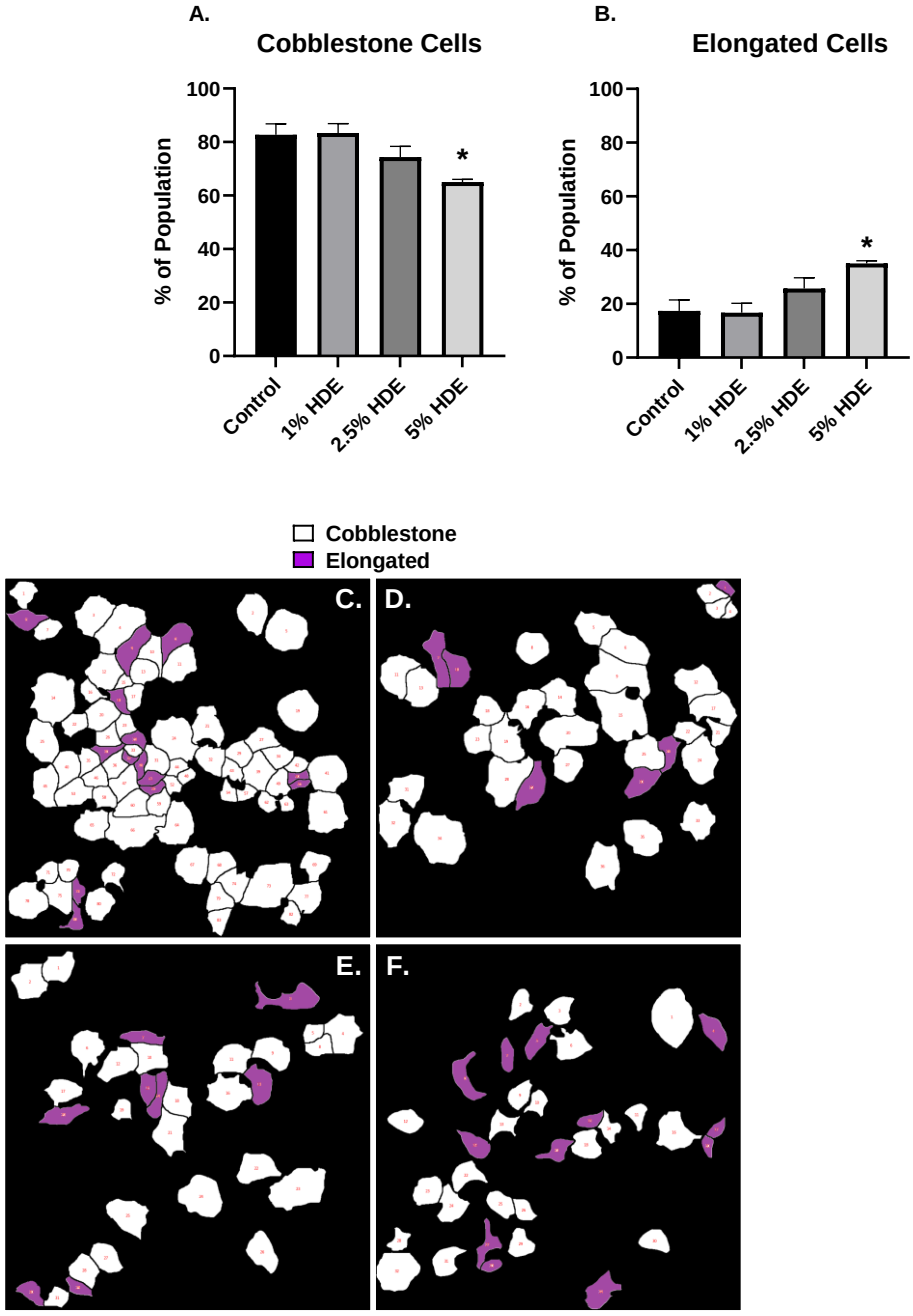

Figure 10. A549 cell morphological changes 48 hrs after treatment with HDE. One-way ANOVA was performed to assess significance for cobblestone (A) or elongated (B) cell morphology counts following 48 hrs of treatment with HDE. Changes in cell phenotype was determined using bioinformatic image processing software in A549 cells treated with either the 0% HDE- control group (C), 1% HDE (D), 2.5% HDE (E), or 5% HDE (F); (* $p < 0.05$).

To build upon our in vivo findings identifying significant gene expression changes of *CDH1* (E-cadherin), *VIM* (vimentin), *TGFβ1*, and *TGFβR1* in dust-exposed mice compared to the control-exposed (Table 3), we assessed levels of EMT biomarkers via Western blotting in A549 cells. Furthermore, to complement our findings of altered inflammation and HDE-enhanced carcinogenesis via AT-RvD1 treatment in vivo, we assessed the impact of AT-RvD1 treatment on the EMT-associated changes identified in HDE-treated human adenocarcinoma lung cells (A549 cells). Evaluation of the carcinogenic effects of HDE was performed by treating A549 cells with 0%, 1%, 2.5%, or 5% HDE for 48 hrs, while assessment of AT-RvD1 was performed by pre-treating cells with 1 ng/mL, 10 ng/mL, 20 ng/mL, or 100 ng/mL of AT-RvD1 for 1 hr prior to exposing cells with 5% HDE for 48 hrs. Western blotting was performed to evaluate protein levels of vimentin, and the tight-junction proteins E-cadherin and N-cadherin. Through these investigations, we detected a significant reduction in E-cadherin (Figure 11A,D) within the 2.5% HDE ($p = 0.01$), 5% HDE-treated group ($p = 0.009$), and 20 ng/mL AT-RvD1-treated cells ($p = 0.004$), compared to the 0% HDE control group. Expression of N-cadherin (Figure 11B,E) was significantly increased compared to the 0% control within the 5% HDE ($p = 0.02$) and 1 ng/mL AT-RvD1-treated cells ($p = 0.04$), with the 20 ng/mL and 100 ng/mL missing significance ($p = 0.09$ for both). Changes in the mesenchymal cell marker vimentin (Figure 11C,E) was seen within the 2.5% HDE ($p = 0.03$), 5% HDE-treated group ($p = 0.04$), 1 ng/mL AT-RvD1-treated group ($p = 0.03$), and 100 ng/mL AT-RvD1-treated cells ($p = 0.01$, compared to the 0% HDE control

group. There were no significant differences for the 5% HDE treated cells versus the 5% HDE+AT-RvD1 treated cells, regardless of the dose of AT-RvD1.

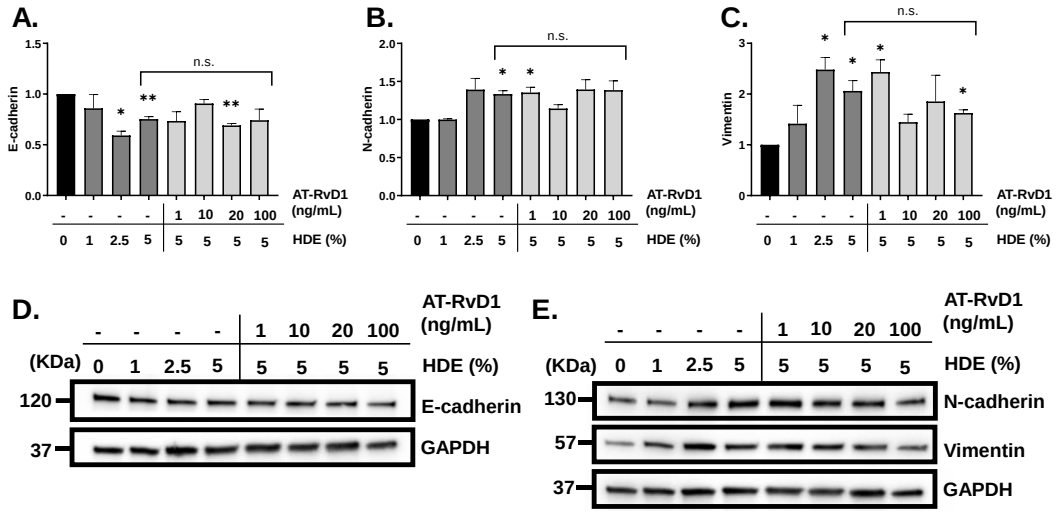

Figure 11. Changes in protein expression of the tight junction proteins E-cadherin (120 KDa) and N-cadherin (130 KDa), and mesenchymal cell marker vimentin (57 KDa). A549 cells were treated for 48 hrs with (A) 0% HDE; (B) 1% HDE; (C) 2.5% HDE; (D) 5% HDE; (E) 1 ng/mL AT-RvD1; (F) 10 ng/mL AT-RvD1; (G) 20 ng/mL AT-RvD1; (H) 100 ng/mL AT-RvD1. One-sample t-tests were performed relative to the 0% HDE control groups; (* $p < 0.05$; ** $p < 0.01$).

4. Discussion

The lung inflammatory and immunomodulatory effects of acute and repetitive dust exposure have been previously studied; however, the carcinogenic and chronic inflammatory damage caused by dust particulates are unclear [35,52,53]. To examine the reported anti-inflammatory and anti-tumorigenic properties of AT-RvD1, we utilized this SPM in a mouse model of chronic (24-week) dust exposure. Here, we identified a significant HDE-induced inflammation including macrophage, neutrophil, lymphocyte, and eosinophil cell influx into the lungs of HDE-exposed mice compared to the saline controls, while AT-RvD1 treatment significantly reduced immune cell recruitment. Significantly higher levels of the pro-resolving SPM RvE1 as well as anti-inflammatory cytokine IL-10 were detected in HDE+AT-RvD1-exposed mouse lungs which could be contributing factors to the reduced inflammation identified in AT-RvD1-treated mice. These observations demonstrate the potential harm chronic HDE exposure may cause, as well as the therapeutic benefits of AT-RvD1 treatment, which dampen inflammation caused by HDE.

Our NanoString differential expression assessment identified increased expression changes in the chemokine receptor *CXCR4* among the HDE-exposed mice. *CXCR4* is one of the most abundant chemokine receptors expressed on murine and human fibrocytes and plays a major role in the recruitment of fibrocytes to the lungs in both species [56-58]. This finding suggests chronic HDE exposure is directly correlated with in-creased tissue damage and as such, recruitment of fibrocytes to the lungs during fibrotic disease

progression. In HDE-exposed mice we identified increased expression of *MUC1* (mucin-1), which is associated with over-production of mucin and is a hallmark of goblet cell hyperplasia, supporting the histopathology identified in the HDE-exposed lungs [59]. Treatment with AT-RvD1 significantly reduced alveolar inflammation and cellularity in both NNK and no NNK+HDE-exposed mice. The anti-inflammatory properties of AT-RvD1 were also observed in the fibrotic lung tissue of HDE-only ex-posed mice Treatment with AT-RvD1 alleviated the lung inflammatory responses induced by chronic dust exposure, however, it's role in mitigating the lung tumorigenic response from chronic HDE exposure was of interest. Within our HDE are lipopolysaccharides (LPS), which comprise the gram-negative bacteria, endotoxin, and have been argued in the literature to possess both protective or enhancement effects for lung tumorigenesis [6,7,60,61]. Epidemiological studies have identified an inverse association with reduced lung cancer risk and long-term exposure to endotoxin in work environments such as dairy, cattle, poultry, and swine farms [8,62]. Specifically, these studies found an inverse association with endotoxin exposure and risk of developing lung adenocarcinoma, which is the most prominent form of non-small cell lung cancers [62,63]. Conversely, other studies assessing population risk for lung cancer have reported that exposure to occupational organic dusts, which contain endotoxins, are associated with increased risk of lung carcinogenesis in exposed individuals [9].

Following 24 weeks of HDE exposure, we determined NNK-treated mice that were exposed to HDE did see significantly increased lung tumor development compared to the saline+NNK control group, indicating that HDE exposure provided an

enhancement effect in a chronic setting. Interestingly, HDE+NNK-exposed mice that were treated with AT-RvD1 did not exhibit altered tumor counts compared to the HDE+NNK group. These findings differed from a recent study identifying AT-RvD1 reduces tumor growth in the lungs of $Kras^{G12D}$ mice, which may suggest this change could be model specific [64]. The pro-inflammatory eicosanoids PGD2, PGE2, and TXB2 increase vasodilation and vascular permeability, which may not only cause increased recruitment of neutrophils and monocytes to the site of inflammation but also allow for the tumor to have the oxygen and nutrients needed to grow and survive [65,66]. PGE2 is an immunomodulatory agent and has been shown in the literature to suppress apoptosis and cytotoxicity of NK cells, which may also facilitate a stronger tumor microenvironment [65,67].

We propose that AT-RvD1 was ineffective at reducing HDE+NNK-enhanced tumorigenesis due to activation of a repair process promoting a M2 or tumor-associated macrophage (TAM) phenotype in the lungs of these mice. SPMs, including AT-RvD1, assist in wound-repair, tissue regeneration, and promote of the resolution of inflammation via binding to surface receptors on structural and immune cells [19,24,68]. Many of these SPMs, such as RvE1 and LXA4, exhibit anti-inflammatory properties that are facilitated by the clearance of neutrophils via macrophage efferocytosis, M2 macrophage polarization, and release of anti-inflammatory and tissue-repair cytokines [23,69]. Although alternatively activated M2 macrophages are considered anti-inflammatory phagocytes, many reports have suggested that these tissue-repairing immune cells can also lead to tissue over-remodeling, resulting in disease pathogenesis such as fibrosis,

although we did not see enhanced fibrosis in the AT-RvD1-treated mice [70-72]. This can be further supported by the elevation of BALF IL-10 levels in HDE+AT-RvD1-treated mice, an anti-inflammatory cytokine that has been shown to induce M2 polarization [73-75]. Transcript level expression of formyl peptide receptor 2 (*FPR2*), the main re-ceptor in mice for RvD1, AT-RvD1, and LXA4 was identified in our dust-exposed mice. Expression of this receptor could provide evidence for the how HDE+AT-RvD1-treatment mediated its protective effects in dust-exposed animals [76,77]. Moreover, PGE2 also modulates polarization of TAM's towards a more M2 phenotype which would increase the secretion of growth factors and promote tumor cell proliferation [65,67]. Pathway analysis showed significant increases in expression changes related to macrophage functions in the HDE-exposed mice versus the saline controls, with increased expression changes in receptors and chemokines relating to macrophage recruitment, including *MRC1* (mannose receptor C, type 1), *CSF1R* (colony stimulating factor 1 receptor), and *CCR2* (C-C motif chemokine receptor 2). Several studies have showed that increased *CCR2* expression in tandem with elevated IL-10 expression is correlated with elevated M2 macrophage activity, further suggesting that HDE+AT-RvD1 exposure promotes M2 macrophage recruitment to the site of inflammation [72,78]. Additionally, within dust-exposed mice we identified increased ex-pression changes in *CHIL3* (chitinase-like protein 3; 10.9-fold increase in HDE vs. saline-treated mice) which encodes the protein Ym1, a well-known marker for M2 macrophages [79]. In one of our recent studies examining the effects of a DHA-rich diet prior to administering 3 weeks of repetitive HDE-exposures in mice, we identified HDE-exposed

mice fed a DHA-rich diet displayed significantly elevated Ym1+ macro-phage expression in the lungs of exposed mice, further supporting the current findings [32].

EMT is a hallmark of cancer metastasis [1,80,81]. In our assessment of gene expression changes among HDE-exposed mice we identified markers of EMT (Table 3), including reduced expression of the tight junction protein *CADH1* (E-cadherin), increased expression of the mesenchymal cell markers *VIM* (vimentin), *FN1* (fibronectin), growth factor *TGFB1* (transforming growth factor beta 1), and *TGFBR1* (TGFβ-1 receptor) [1,80-83]. We also identified reduced pathway expression for genes related to adhesion, which can be supported by the down regulation of *CDH1* seen within HDE-exposed mice in Figure 8. We identified significantly elevated levels of TGFβ-1 in the BALF of HDE-exposed mice as well, which may provide additional evidence for an overactive repair process or serve as evidence for the promotion of EMT, as TGFβ-1 has been well-established as an inducer of EMT in various models of carcinogenesis [45,81]. To complement these observations, we further examined the carcinogenic effects of HDE exposure within human lung adenocarcinoma cells. Since the tumors formed in the NNK-administered mice were pathologically characterized as lung adenomas, we opted to use the A549 cell line to confirm the transformative effects of HDE-exposure within the tumor microenvironment. HDE-treated cells showed EMT-associated changes (Figure 10). These expression changes support the visual non-transformed to elongated or mesenchymal-like phenotypic changes identified in HDE-treated cells, compared to the non-treated, a characteristic of tumor metastasis [1,80,82]. Although AT-RvD1 is better known to have a direct effect on immune cells rather than tumor cells, we utilized AT-

RvD1 to identify if pre-treatment of A549 adenocarcinoma cells with AT-RvD1 would dampen or mitigate the HDE-induced EMT response identified in these cells. Several investigations have identified that SPMs can be produced by and act on non-immune cell populations, thus providing rationale for its investigation in our study [43,44,84]. Furthermore, there are multiple documented effects of AT-RvD1 on EMT processes, including in the A549 cell line [44,84].

The in vitro data presented here accompany our findings that chronic HDE exposure enhances lung tumorigenesis by suggesting that individuals with lung cancer that endure long-term exposure to agricultural organic dust, may be at increased risk of cancer metastasis. The increase in EMT-biomarkers between both our in vivo and in vitro studies provide evidence that exposure to these dusts rather enhance lung tumorigenesis and promote a metastatic tumor environment. Our results more closely align with the literature that propose LPS enhances lung carcinogenesis, rather than protects against it.

5. References

1. Hanahan, D.; Weinberg, Robert A. Hallmarks of Cancer: The Next Generation. Cell 2011, 144, 646-674, doi:10.1016/j.cell.2011.02.013.

2. Raposo, T.P.; Beirão, B.C.B.; Pang, L.Y.; Queiroga, F.L.; Argyle, D.J. Inflammation and cancer: Till death tears them apart. The Veterinary Journal 2015, 205, 161-174, doi:https://doi.org/10.1016/j.tvjl.2015.04.015.

3. Boissy, R.J.; Romberger, D.J.; Roughead, W.A.; Weissenburger-Moser, L.; Poole, J.A.; LeVan, T.D. Shotgun pyrosequencing metagenomic analyses of dusts from swine confinement and grain facilities. PLoS One 2014, 9, e95578-e95578, doi:10.1371/journal.pone.0095578.

4. Romberger, D.J.; Bodlak, V.; Essen, S.G.V.; Mathisen, T.; Wyatt, T.A. Hog barn dust extract stimulates IL-8 and IL-6 release in human bronchial epithelial cells via PKC activation. Journal of Applied Physiology 2002, 93, 289-296, doi:10.1152/japplphysiol.00815.2001.

5. Romberger, D.J.; Heires, A.J.; Nordgren, T.M.; Souder, C.P.; West, W.; Liu, X.-d.; Poole, J.A.; Toews, M.L.; Wyatt, T.A. Proteases in agricultural dust induce lung inflammation through PAR-1 and PAR-2 activation. American journal of physiology. Lung cellular and molecular physiology 2015, 309, L388-L399, doi:10.1152/ajplung.00025.2015.

6. Liebers, V.; Brüning, T.; Raulf-Heimsoth, M. Occupational endotoxin-exposure and possible health effects on humans (review). American Journal of Industrial Medicine 2006, 49, 474-491, doi:https://doi.org/10.1002/ajim.20310.

7. Lundin, J.I.; Checkoway, H. Endotoxin and cancer. Environ Health Perspect 2009, 117, 1344-1350, doi:10.1289/ehp.0800439.

8. Mastrangelo, G.; Marzia, V.; Marcer, G. Reduced lung cancer mortality in dairy farmers: Is endotoxin exposure the key factor? American Journal of Industrial Medicine 1996, 30, 601-609, doi:10.1002/(SICI)1097-0274(199611)30:5<601::AID-AJIM8>3.0.CO;2-V.

9. Peters, S.; Kromhout, H.; Olsson, A.C.; Wichmann, H.-E.; Brüske, I.; Consonni, D.; Landi, M.T.; Caporaso, N.; Siemiatycki, J.; Richiardi, L., et al. Occupational exposure to organic dust increases lung cancer risk in the general population. Thorax 2012, 67, 111-116, doi:10.1136/thoraxjnl-2011-200716.

10. Nordgren, T.M.; Heires, A.J.; Bailey, K.L.; Katafiasz, D.M.; Toews, M.L.; Wichman, C.S.; Romberger, D.J. Docosahexaenoic acid enhances amphiregulin-mediated

bronchial epithelial cell repair processes following organic dust exposure. Am J Physiol Lung Cell Mol Physiol 2018, 314, L421-l431, doi:10.1152/ajplung.00273.2017.

11. Poole, J.A.; Wyatt, T.A.; Oldenburg, P.J.; Elliott, M.K.; West, W.W.; Sisson, J.H.; Von Essen, S.G.; Romberger, D.J. Intranasal organic dust exposure-induced airway adaptation response marked by persistent lung inflammation and pathology in mice. Am J Physiol Lung Cell Mol Physiol 2009, 296, L1085-1095, doi:10.1152/ajplung.90622.2008.

12. Salerno, C.; Sacco, S.; Panella, M.; Berchialla, P.; Vanhaecht, K.; Palin, L.A. Cancer risk among farmers in the Province of Vercelli (Italy) from 2002 to 2005: an ecological study. Ann Ig 2014, 26, 255-263, doi:10.7416/ai.2014.1983.

13. Bailey, K.L.; Meza, J.L.; Smith, L.M.; Von Essen, S.G.; Romberger, D.J. Agricultural exposures in patients with COPD in health systems serving rural areas. J Agromedicine 2007, 12, 71-76, doi:10.1300/J096v12n02_10.

14. Guillien, A.; Puyraveau, M.; Soumagne, T.; Guillot, S.; Rannou, F.; Marquette, D.; Berger, P.; Jouneau, S.; Monnet, E.; Mauny, F., et al. Prevalence and risk factors for COPD in farmers: a cross-sectional controlled study. European Respiratory Journal 2016, 47, 95-103, doi:10.1183/13993003.00153-2015.

15. Nordgren, T.M.; Bailey, K.L. Pulmonary health effects of agriculture. Curr Opin Pulm Med 2016, 22, 144-149, doi:10.1097/MCP.0000000000000247.

16. Mitchell, D.C.; Schenker, M.B. Protection against breathing dust: behavior over time in Californian farmers. J Agric Saf Health 2008, 14, 189-203, doi:10.13031/2013.24350.

17. Schenker, M.B.; Orenstein, M.R.; Samuels, S.J. Use of protective equipment among California farmers. American Journal of Industrial Medicine 2002, 42, 455-464, doi:10.1002/ajim.10134.

18. Von Essen, S.; Fryzek, J.; Nowakowski, B.; Wampler, M. Respiratory symptoms and farming practices in farmers associated with an acute febrile illness after organic dust exposure. Chest 1999, 116, 1452-1458.

19. Levy, B.D.; Serhan, C.N. Resolution of acute inflammation in the lung. Annu Rev Physiol 2014, 76, 467-492, doi:10.1146/annurev-physiol-021113-170408.

20. Moldoveanu, B.; Otmishi, P.; Jani, P.; Walker, J.; Sarmiento, X.; Guardiola, J.; Saad, M.; Yu, J. Inflammatory mechanisms in the lung. J Inflamm Res 2009, 2, 1-11.

21. Serhan, C.N.; Savill, J. Resolution of inflammation: the beginning programs the end. Nature Immunology 2005, 6, 1191-1197, doi:10.1038/ni1276.

22. Serhan, C.N.; Chiang, N.; Van Dyke, T.E. Resolving inflammation: dual anti-inflammatory and pro-resolution lipid mediators. Nature Reviews Immunology 2008, 8, 349-361, doi:10.1038/nri2294.

23. Buckley, C.D.; Gilroy, D.W.; Serhan, C.N. Proresolving lipid mediators and mechanisms in the resolution of acute inflammation. Immunity 2014, 40, 315-327, doi:10.1016/j.immuni.2014.02.009.

24. Levy, B.D.; Clish, C.B.; Schmidt, B.; Gronert, K.; Serhan, C.N. Lipid mediator class switching during acute inflammation: signals in resolution. Nature Immunology 2001, 2, 612-619, doi:10.1038/89759.

25. Serhan, C.N. Pro-resolving lipid mediators are leads for resolution physiology. Nature 2014, 510, 92-101, doi:10.1038/nature13479.

26. Serhan, C.N.; Petasis, N.A. Resolvins and protectins in inflammation resolution. Chemical reviews 2011, 111, 5922-5943.

27. Serhan, C.N.; Yang, R.; Martinod, K.; Kasuga, K.; Pillai, P.S.; Porter, T.F.; Oh, S.F.; Spite, M. Maresins: novel macrophage mediators with potent antiinflammatory and proresolving actions. The Journal of experimental medicine 2009, 206, 15-23, doi:10.1084/jem.20081880.

28. Gilligan, M.M.; Gartung, A.; Sulciner, M.L.; Norris, P.C.; Sukhatme, V.P.; Bielenberg, D.R.; Huang, S.; Kieran, M.W.; Serhan, C.N.; Panigrahy, D. Aspirin-triggered proresolving mediators stimulate resolution in cancer. Proceedings of the National Academy of Sciences 2019, 116, 6292-6297, doi:10.1073/pnas.1804000116.

29. Hsiao, H.-M.; Thatcher, T.H.; Colas, R.A.; Serhan, C.N.; Phipps, R.P.; Sime, P.J. Resolvin D1 Reduces Emphysema and Chronic Inflammation. The American journal of pathology 2015, 185, 3189-3201, doi:10.1016/j.ajpath.2015.08.008.

30. Posso, S.V.; Quesnot, N.; Moraes, J.A.; Brito-Gitirana, L.; Kennedy-Feitosa, E.; Barroso, M.V.; Porto, L.C.; Lanzetti, M.; Valença, S.S. AT-RVD1 repairs mouse lung after cigarette smoke-induced emphysema via downregulation of oxidative stress by NRF2/KEAP1 pathway. International Immunopharmacology 2018, 56, 330-338, doi:https://doi.org/10.1016/j.intimp.2018.01.045.

31. Dominguez, E.C.; Heires, A.J.; Pavlik, J.; Larsen, T.D.; Guardado, S.; Sisson, J.H.; Baack, M.L.; Romberger, D.J.; Nordgren, T.M. A High Docosahexaenoic Acid Diet Alters the Lung Inflammatory Response to Acute Dust Exposure. Nutrients 2020, 12, 2334.

32. Ulu, A.; Burr, A.; Heires, A.J.; Pavlik, J.; Larsen, T.; Perez, P.A.; Bravo, C.; DiPatrizio, N.V.; Baack, M.; Romberger, D.J., et al. A high docosahexaenoic acid diet alters lung inflammation and recovery following repetitive exposure to aqueous organic dust extracts. The Journal of Nutritional Biochemistry 2021, 97, 108797, doi:https://doi.org/10.1016/j.jnutbio.2021.108797.

33. Mernitz, H.; Lian, F.; Smith, D.E.; Meydani, S.N.; Wang, X.-D. Fish Oil Supplementation Inhibits NNK-Induced Lung Carcinogenesis in the A/J Mouse. Nutrition and Cancer 2009, 61, 663-669, doi:10.1080/01635580902825589.

34. Nordgren, T.M.; Bauer, C.D.; Heires, A.J.; Poole, J.A.; Wyatt, T.A.; West, W.W.; Romberger, D.J. Maresin-1 reduces airway inflammation associated with acute and repetitive exposures to organic dust. Translational Research 2015, 166, 57-69, doi:https://doi.org/10.1016/j.trsl.2015.01.001.

35. Poole, J.A.; Alexis, N.E.; Parks, C.; MacInnes, A.K.; Gentry-Nielsen, M.J.; Fey, P.D.; Larsson, L.; Allen-Gipson, D.; Von Essen, S.G.; Romberger, D.J. Repetitive organic dust exposure in vitro impairs macrophage differentiation and function. J Allergy Clin Immunol 2008, 122, 375-382, 382.e371-374, doi:10.1016/j.jaci.2008.05.023.

36. Hecht, S.S. Biochemistry, Biology, and Carcinogenicity of Tobacco-Specific N-Nitrosamines. Chemical Research in Toxicology 1998, 11, 559-603, doi:10.1021/tx980005y.

37. Hecht, S.S.; Chen, C.-h.B.; Hirota, N.; Ornaf, R.M.; Tso, T.C.; Hoffmann, D. Tobacco-Specific Nitrosamines: Formation From Nicotine In Vitro and During Tobacco Curing and Carcinogenicity in Strain A Mice23. JNCI: Journal of the National Cancer Institute 1978, 60, 819-824, doi:10.1093/jnci/60.4.819.

38. Ashcroft, T.; Simpson, J.M.; Timbrell, V. Simple method of estimating severity of pulmonary fibrosis on a numerical scale. J Clin Pathol 1988, 41, 467-470, doi:10.1136/jcp.41.4.467.

39. Hübner, R.-H.; Gitter, W.; Eddine El Mokhtari, N.; Mathiak, M.; Both, M.; Bolte, H.; Freitag-Wolf, S.; Bewig, B. Standardized quantification of pulmonary fibrosis in histological samples. BioTechniques 2008, 44, 507-517, doi:10.2144/000112729.

40. Sun, Y.-P.; Oh, S.F.; Uddin, J.; Yang, R.; Gotlinger, K.; Campbell, E.; Colgan, S.P.; Petasis, N.A.; Serhan, C.N. Resolvin D1 and its aspirin-triggered 17R epimer stereochemical assignments, anti-inflammatory properties, and enzymatic inactivation. Journal of Biological Chemistry 2007, 282, 9323-9334.

41. Hsiao, H.-M.; Sapinoro, R.E.; Thatcher, T.H.; Croasdell, A.; Levy, E.P.; Fulton, R.A.; Olsen, K.C.; Pollock, S.J.; Serhan, C.N.; Phipps, R.P., et al. A novel anti-

inflammatory and pro-resolving role for resolvin D1 in acute cigarette smoke-induced lung inflammation. PLoS One 2013, 8, e58258-e58258, doi:10.1371/journal.pone.0058258.

42. Strassburg, K.; Huijbrechts, A.M.L.; Kortekaas, K.A.; Lindeman, J.H.; Pedersen, T.L.; Dane, A.; Berger, R.; Brenkman, A.; Hankemeier, T.; van Duynhoven, J., et al. Quantitative profiling of oxylipins through comprehensive LC-MS/MS analysis: application in cardiac surgery. Anal Bioanal Chem 2012, 404, 1413-1426, doi:10.1007/s00216-012-6226-x.

43. Nordgren, T.M.; Heires, A.J.; Wyatt, T.A.; Poole, J.A.; LeVan, T.D.; Cerutis, D.R.; Romberger, D.J. Maresin-1 reduces the pro-inflammatory response of bronchial epithelial cells to organic dust. Respir Res 2013, 14, 51, doi:10.1186/1465-9921-14-51.

44. Zahedi, A.; Phandthong, R.; Chaili, A.; Remark, G.; Talbot, P. Epithelial-to-mesenchymal transition of A549 lung cancer cells exposed to electronic cigarettes. Lung Cancer 2018, 122, 224-233, doi:10.1016/j.lungcan.2018.06.010.

45. Liu, Y.; Yuan, X.; Li, W.; Cao, Q.; Shu, Y. Aspirin-triggered resolvin D1 inhibits TGF-β1-induced EMT through the inhibition of the mTOR pathway by reducing the expression of PKM2 and is closely linked to oxidative stress. International journal of molecular medicine 2016, 38, 1235-1242.

46. Carpenter, A.E.; Jones, T.R.; Lamprecht, M.R.; Clarke, C.; Kang, I.H.; Friman, O.; Guertin, D.A.; Chang, J.H.; Lindquist, R.A.; Moffat, J., et al. CellProfiler: image analysis software for identifying and quantifying cell phenotypes. Genome Biology 2006, 7, R100, doi:10.1186/gb-2006-7-10-r100.

47. Nordgren, T.M.; Friemel, T.D.; Heires, A.J.; Poole, J.A.; Wyatt, T.A.; Romberger, D.J. The Omega-3 Fatty Acid Docosahexaenoic Acid Attenuates Organic Dust-Induced Airway Inflammation. Nutrients 2014, 6, 5434-5452.

48. Bailey, K.L.; Poole, J.A.; Mathisen, T.L.; Wyatt, T.A.; Von Essen, S.G.; Romberger, D.J. Toll-like receptor 2 is upregulated by hog confinement dust in an IL-6-dependent manner in the airway epithelium. Am J Physiol Lung Cell Mol Physiol 2008, 294, L1049-1054, doi:10.1152/ajplung.00526.2007.

49. Tanaka, T.; Narazaki, M.; Kishimoto, T. IL-6 in inflammation, immunity, and disease. Cold Spring Harb Perspect Biol 2014, 6, a016295-a016295, doi:10.1101/cshperspect.a016295.

50. Iyer, S.S.; Cheng, G. Role of interleukin 10 transcriptional regulation in inflammation and autoimmune disease. Crit Rev Immunol 2012, 32, 23-63, doi:10.1615/critrevimmunol.v32.i1.30.

51. Ramirez, H.; Patel, S.B.; Pastar, I. The role of TGFβ signaling in wound epithelialization. Advances in wound care 2014, 3, 482-491.

52. Linaker, C.; Smedley, J. Respiratory illness in agricultural workers. Occupational Medicine 2002, 52, 451-459, doi:10.1093/occmed/52.8.451.

53. Von Essen, S.; Romberger, D. The respiratory inflammatory response to the swine confinement building environment: the adaptation to respiratory exposures in the chronically exposed worker. J Agric Saf Health 2003, 9, 185-196, doi:10.13031/2013.13684.

54. Crooks, S.W.; Stockley, R.A. Leukotriene B4. The International Journal of Biochemistry & Cell Biology 1998, 30, 173-178, doi:https://doi.org/10.1016/S1357-2725(97)00123-4.

55. Krishnamoorthy, S.; Recchiuti, A.; Chiang, N.; Fredman, G.; Serhan, C.N. Resolvin D1 receptor stereoselectivity and regulation of inflammation and proresolving microRNAs. The American journal of pathology 2012, 180, 2018-2027, doi:10.1016/j.ajpath.2012.01.028.

56. Mehrad, B.; Burdick, M.D.; Strieter, R.M. Fibrocyte CXCR4 regulation as a therapeutic target in pulmonary fibrosis. The international journal of biochemistry & cell biology 2009, 41, 1708-1718, doi:10.1016/j.biocel.2009.02.020.

57. Phillips, R.J.; Burdick, M.D.; Hong, K.; Lutz, M.A.; Murray, L.A.; Xue, Y.Y.; Belperio, J.A.; Keane, M.P.; Strieter, R.M. Circulating fibrocytes traffic to the lungs in response to CXCL12 and mediate fibrosis. J Clin Invest 2004, 114, 438-446, doi:10.1172/jci20997.

58. Strieter, R.M.; Keeley, E.C.; Hughes, M.A.; Burdick, M.D.; Mehrad, B. The role of circulating mesenchymal progenitor cells (fibrocytes) in the pathogenesis of pulmonary fibrosis. Journal of leukocyte biology 2009, 86, 1111-1118.

59. Kato, K.; Chang, E.H.; Chen, Y.; Lu, W.; Kim, M.M.; Niihori, M.; Hecker, L.; Kim, K.C. MUC1 contributes to goblet cell metaplasia and MUC5AC expression in response to cigarette smoke in vivo. American journal of physiology. Lung cellular and molecular physiology 2020, 319, L82-L90, doi:10.1152/ajplung.00049.2019.

60. Lange, J.H. Reduced cancer rates in agricultural workers: a benefit of environmental and occupational endotoxin exposure. Medical Hypotheses 2000, 55, 383-385, doi:https://doi.org/10.1054/mehy.2000.1072.

61. Liebers, V.; Raulf-Heimsoth, M.; Bruning, T. Health effects due to endotoxin inhalation (review). Arch Toxicol 2008, 82, 203-210, doi:10.1007/s00204-008-0290-1.

62. Ben Khedher, S.; Neri, M.; Guida, F.; Matrat, M.; Cenée, S.; Sanchez, M.; Menvielle, G.; Molinié, F.; Luce, D.; Stücker, I. Occupational exposure to endotoxins and lung cancer risk: results of the ICARE Study. Occupational and Environmental Medicine 2017, 74, 667, doi:10.1136/oemed-2016-104117.

63. Torre, L.A.; Siegel, R.L.; Jemal, A. Lung Cancer Statistics. In Lung Cancer and Personalized Medicine: Current Knowledge and Therapies, Ahmad, A., Gadgeel, S., Eds. Springer International Publishing: Cham, 2016; 10.1007/978-3-319-24223-1_1pp. 1-19.

64. Vannitamby, A.; Saad, M.I.; Aloe, C.; Wang, H.; Kumar, B.; Vlahos, R.; Selemidis, S.; Irving, L.; Steinfort, D.; Jenkins, B.J., et al. Aspirin-Triggered Resolvin D1 Reduces Proliferation and the Neutrophil to Lymphocyte Ratio in a Mutant KRAS-Driven Lung Adenocarcinoma Model. Cancers (Basel) 2021, 13, 3224, doi:10.3390/cancers13133224.

65. Finetti, F.; Travelli, C.; Ercoli, J.; Colombo, G.; Buoso, E.; Trabalzini, L. Prostaglandin E2 and Cancer: Insight into Tumor Progression and Immunity. Biology (Basel) 2020, 9, 434, doi:10.3390/biology9120434.

66. Wang, D.; DuBois, R.N. Eicosanoids and cancer. Nature Reviews Cancer 2010, 10, 181-193, doi:10.1038/nrc2809.

67. Nakanishi, M.; Rosenberg, D.W. Multifaceted roles of PGE2 in inflammation and cancer. Semin Immunopathol 2013, 35, 123-137, doi:10.1007/s00281-012-0342-8.

68. Levy, B. Resolvin D1 and Resolvin E1 Promote the Resolution of Allergic Airway Inflammation via Shared and Distinct Molecular Counter-Regulatory Pathways. Front Immunol 2012, 3, doi:10.3389/fimmu.2012.00390.

69. Serhan, C.N.; Krishnamoorthy, S.; Recchiuti, A.; Chiang, N. Novel anti-inflammatory--pro-resolving mediators and their receptors. Curr Top Med Chem 2011, 11, 629-647, doi:10.2174/1568026611109060629.

70. Mantovani, A.; Biswas, S.K.; Galdiero, M.R.; Sica, A.; Locati, M. Macrophage plasticity and polarization in tissue repair and remodelling. J Pathol 2013, 229, 176-185, doi:https://doi.org/10.1002/path.4133.

71. Murthy, S.; Larson-Casey, J.L.; Ryan, A.J.; He, C.; Kobzik, L.; Carter, A.B. Alternative activation of macrophages and pulmonary fibrosis are modulated by scavenger receptor, macrophage receptor with collagenous structure. The FASEB Journal 2015, 29, 3527-3536, doi:https://doi.org/10.1096/fj.15-271304.

72. Sun, L.; Louie, M.C.; Vannella, K.M.; Wilke, C.A.; LeVine, A.M.; Moore, B.B.; Shanley, T.P. New concepts of IL-10-induced lung fibrosis: fibrocyte recruitment and M2

activation in a CCL2/CCR2 axis. American journal of physiology. Lung cellular and molecular physiology 2011, 300, L341-L353, doi:10.1152/ajplung.00122.2010.

73. Saraiva, M.; O'Garra, A. The regulation of IL-10 production by immune cells. Nat Rev Immunol 2010, 10, 170-181, doi:10.1038/nri2711.

74. Makita, N.; Hizukuri, Y.; Yamashiro, K.; Murakawa, M.; Hayashi, Y. IL-10 enhances the phenotype of M2 macrophages induced by IL-4 and confers the ability to increase eosinophil migration. International Immunology 2014, 27, 131-141, doi:10.1093/intimm/dxu090.

75. Moore, B.B.; Kolodsick, J.E.; Thannickal, V.J.; Cooke, K.; Moore, T.A.; Hogaboam, C.; Wilke, C.A.; Toews, G.B. CCR2-mediated recruitment of fibrocytes to the alveolar space after fibrotic injury. The American journal of pathology 2005, 166, 675-684.

76. He, H.-Q.; Ye, R.D. The Formyl Peptide Receptors: Diversity of Ligands and Mechanism for Recognition. Molecules 2017, 22, 455, doi:10.3390/molecules22030455.

77. Pirault, J.; Bäck, M. Lipoxin and Resolvin Receptors Transducing the Resolution of Inflammation in Cardiovascular Disease. Frontiers in Pharmacology 2018, 9, doi:10.3389/fphar.2018.01273.

78. Hao, Q.; Vadgama, J.V.; Wang, P. CCL2/CCR2 signaling in cancer pathogenesis. Cell Commun Signal 2020, 18, 82-82, doi:10.1186/s12964-020-00589-8.

79. Yu, T.; Gan, S.; Zhu, Q.; Dai, D.; Li, N.; Wang, H.; Chen, X.; Hou, D.; Wang, Y.; Pan, Q., et al. Modulation of M2 macrophage polarization by the crosstalk between Stat6 and Trim24. Nature Communications 2019, 10, 4353, doi:10.1038/s41467-019-12384-2.

80. Hanahan, D.; Weinberg, R.A. The Hallmarks of Cancer. Cell 2000, 100, 57-70, doi:10.1016/S0092-8674(00)81683-9.

81. Brabletz, T.; Kalluri, R.; Nieto, M.A.; Weinberg, R.A. EMT in cancer. Nature Reviews Cancer 2018, 18, 128-134, doi:10.1038/nrc.2017.118.

82. Loh, C.-Y.; Chai, J.Y.; Tang, T.F.; Wong, W.F.; Sethi, G.; Shanmugam, M.K.; Chong, P.P.; Looi, C.Y. The E-Cadherin and N-Cadherin Switch in Epithelial-to-Mesenchymal Transition: Signaling, Therapeutic Implications, and Challenges. Cells 2019, 8, 1118, doi:10.3390/cells8101118.

83. Li, B.; Shen, W.; Peng, H.; Li, Y.; Chen, F.; Zheng, L.; Xu, J.; Jia, L. Fibronectin 1 promotes melanoma proliferation and metastasis by inhibiting apoptosis and regulating EMT. Onco Targets Ther 2019, 12, 3207-3221, doi:10.2147/OTT.S195703.

84. Lee, H.J.; Park, M.K.; Lee, E.J.; Lee, C.H. Resolvin D1 inhibits TGF-β1-induced epithelial mesenchymal transition of A549 lung cancer cells via lipoxin A4 receptor/formyl peptide receptor 2 and GPR32. Int J Biochem Cell Biol 2013, 45, 2801-2807, doi:10.1016/j.biocel.2013.09.018.

Conclusions

Chapter 1

In conclusion, a high-DHA diet significantly alters the lung's inflammatory response to acute agricultural dust exposure, likely by increasing omega-3 PUFAs, which serve as substrates for SPM generation to modify the inflammatory response stimulated by HDE exposure. Evidence in support of this hypothesis includes the elevated blood levels of omega-3 PUFAs, increased macrophage influx into the lung, increased BALF RvD1, and altered gene expression signature associated with macrophage activities in DHA-diet-fed mice exposed to dust compared to mice fed a diet without DHA. These findings warrant future studies to ascertain the potential preventative or therapeutic roles for omega-3 PUFAs in reducing the lung's inflammatory response to particulate matter exposures such as those experienced in agricultural settings

Chapter 2

Chronic exposure to dust from swine confinement facilities induced severe lung inflammatory and carcinogenic responses, including fibrosis, enhanced tumorigenesis, and EMT. The anti-inflammatory effects of AT-RvD1 were evidenced by reduced influx of neutrophil, lymphocyte, and eosinophils within the BALF of dust-exposed mice, increased RvE1 levels, and decreased alveolar inflammation in the lung tissues of mice. Despite the therapeutic effects of AT-RvD1 presented in these studies, treatment with this SPM reduced inflammation and promoted a repair process in dust-exposed mice, which

did not protect against HDE+NNK-enhanced lung tumorigenesis. We propose this response is due to an increase in M2 or tumor-associated macrophage populations in the lungs of HDE-exposed mice, which can be evidenced by the pathway and transcript alterations of prominent macrophage recruitment markers, as well as elevated IL-10 in the BALF of dust-exposed mice treated with AT-RvD1.

Our data provide a murine model that demonstrates the significant inflammatory and carcinogenic health implications that chronic agricultural dust exposure can have. The results from our studies give new insight to lung disease progression in farm workers who endure chronic exposure to agricultural organic dusts, including an increased risk for lung carcinogenesis. Furthermore, these studies propose an effective therapeutic strategy using AT-RvD1 treatment, for mitigating the negative health impacts of dust exposure among individuals in the livestock and farming industries.

Appendix

Chapter 1: SUPPLEMENTAL DATA

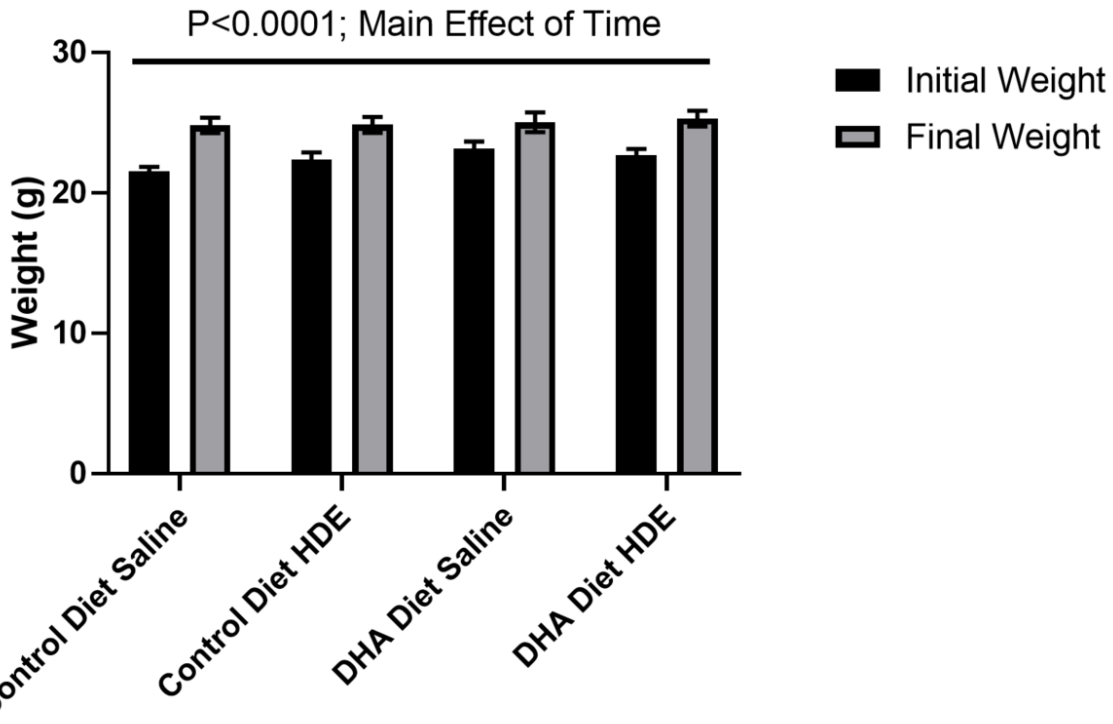

Supplemental Figure 1. Initial and Final weights of mice fed a control diet or high DHA diet for 4 weeks. A significant main effect of time was identified (P<0.0001), with mice in all experimental groups gaining weight over the 4-week period. There were no significant impacts of diet/HDE treatment on animal weights.

Chapter 2: Supplementary Data

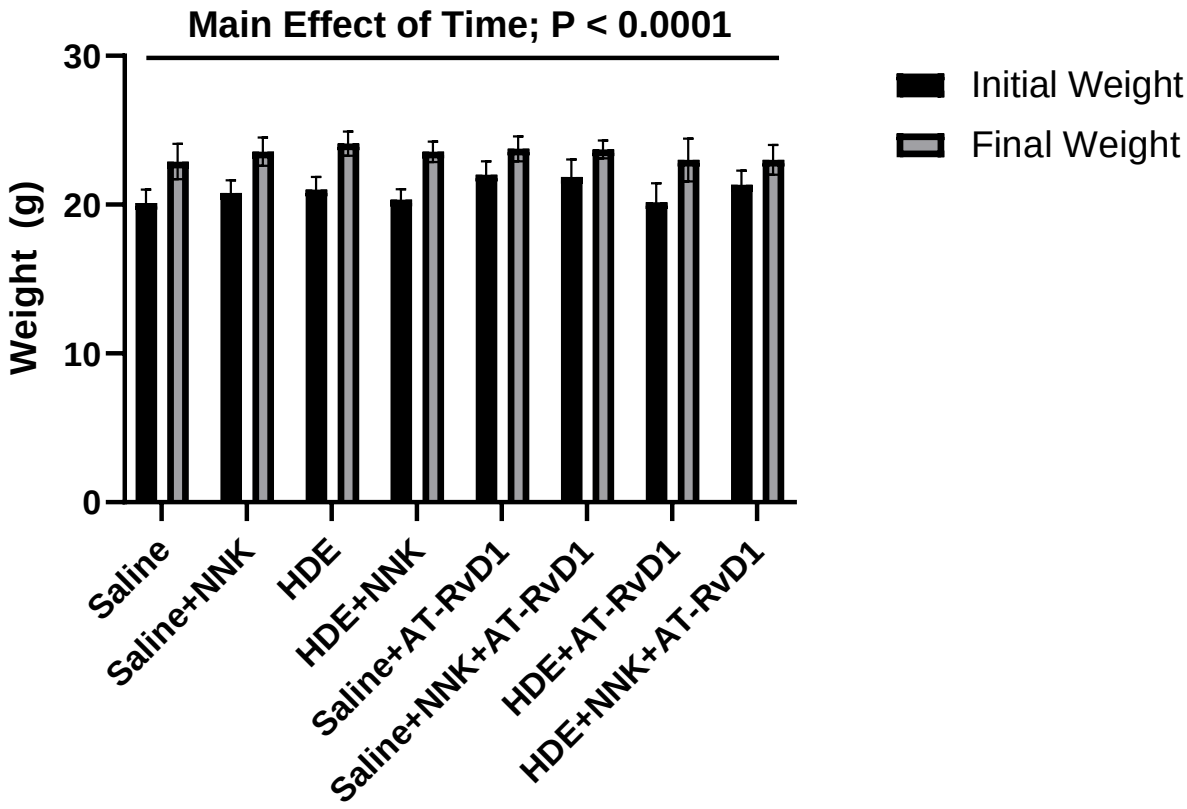

Figure S1. Mice initial and final weights following 24-weeks of chronic exposure. Two-way ANOVA identified a significant main effect of time ($p < 0.0001$) for weight gain in all experimental groups over the 24-week exposure period with HDE, NNK, or AT-RvD1 administration having no impact.

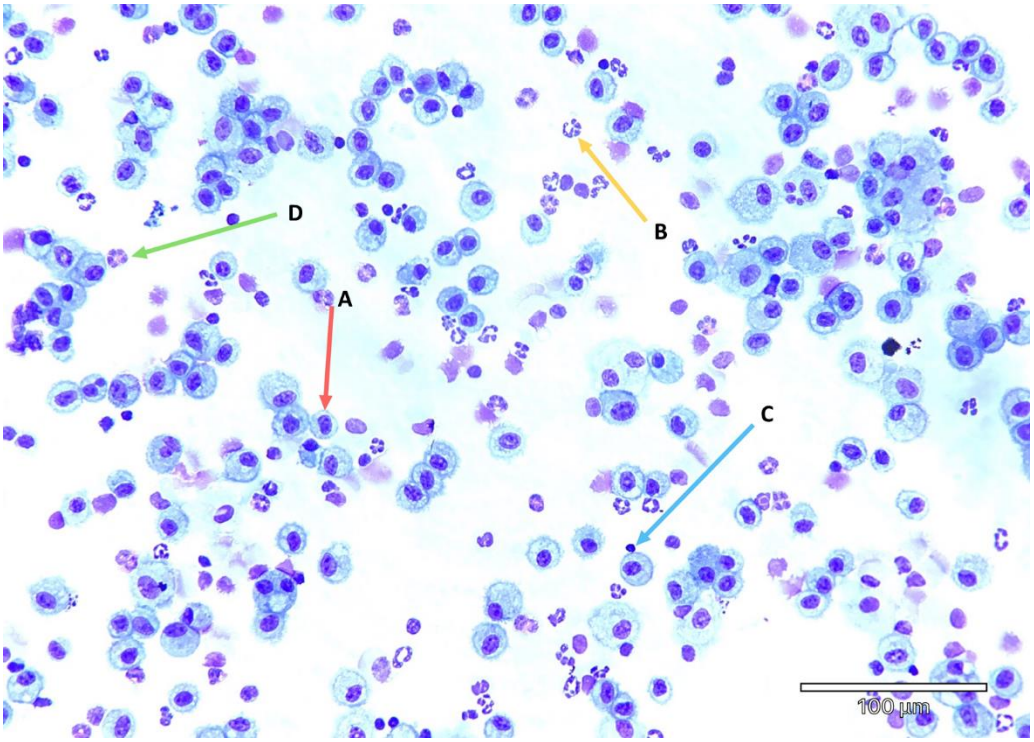

Figure S2. Representative image of BALF immune cell differential analyses. Differential analyses allowed for distinction of immune cells recruited including (A) macrophages, (B) neutrophils, (C) lymphocytes, (D) eosinophils.

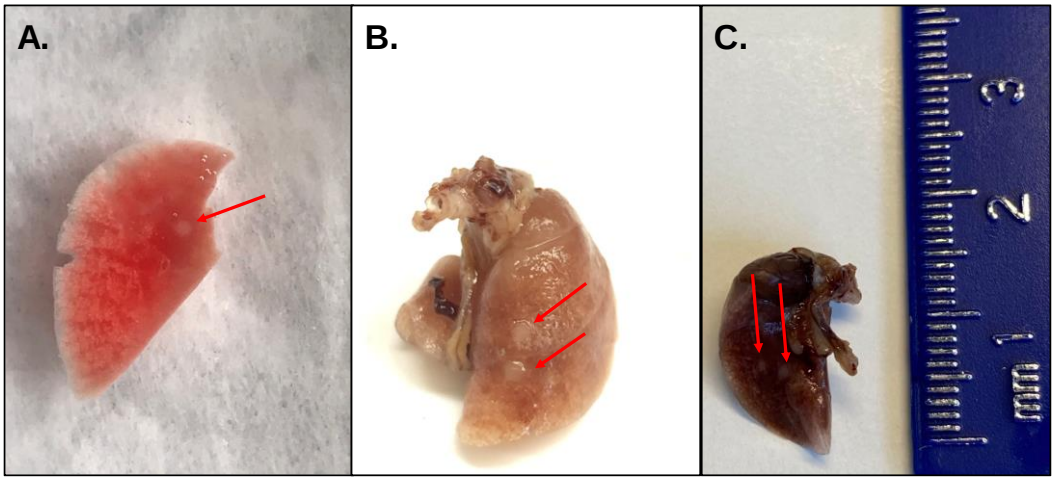

Figure S3. Images of left and right lung tissues with adenomas. (A) Left lung tissue from saline+NNK-exposed mouse that was used for NanoString analyses and oxylipin analysis (B-C) Right HDE+NNK-exposed mouse lung inflated with formalin and used for histopathological analyses. Red arrows point to lung adenomas on the lung tissues.

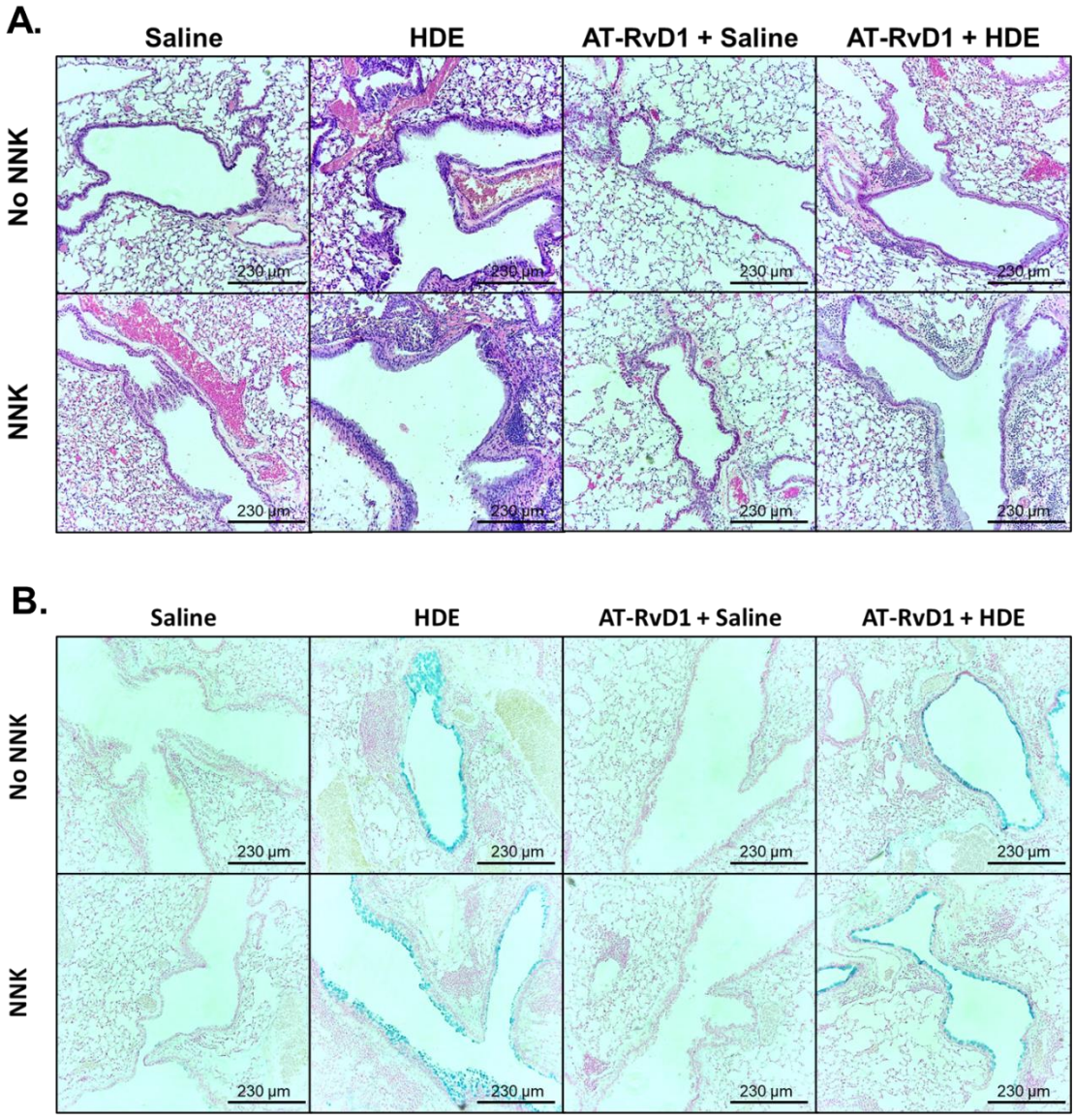

Figure S4. Murine lung tissue histopathology at the conclusion of 24-weeks of chronic HDE exposure. H&E staining was used to assess changes in (A) bronchial/vascular inflammation while Alcian Blue staining was used to assess (B) goblet cell hyperplasia. There was a significant ($p < 0.0001$) main effect of HDE for each of these pathological outcomes. All images were taken using a 10x objective.

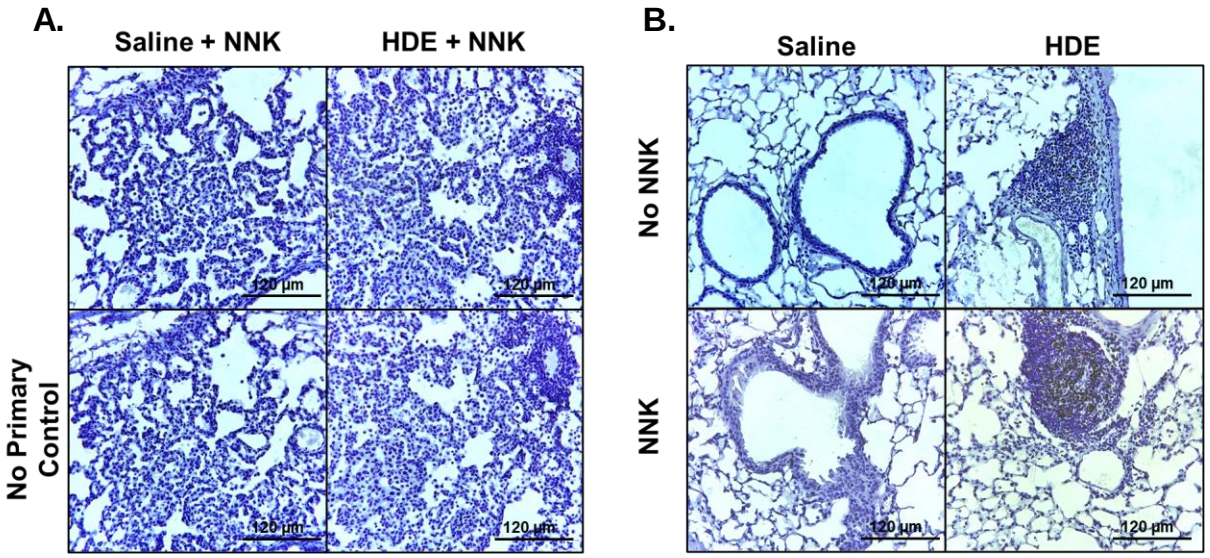

Figure S5. Ki-67 immunohistochemistry staining of FFPE lung tissues. Right lung tissues were formalin-fixed, and paraffin embedded and stained for the cell proliferation marker Ki-67. (A) Staining within lung adenomas of NNK-exposed mice showed Ki-67 expression. (B) Ki-67 expression was prominent in HDE lymphoid aggregates and along the bronchi/ bronchioles of exposed mice.